Understanding the Role and Regulation of PTEN in Adenovirus 5 Infection

Katie Louise Brighton

201004811

Submitted in fulfilment of the requirements of the degree of
Master of Science by Research

School of Molecular and Cellular Biology

University of Leeds, Leeds, LS2 9JT

June 2021

Declaration of Academic Integrity

Understanding the Role and Regulation of PTEN in Adenovirus 5 Infection

Katie Louise Brighton

Submitted in accordance with the requirements for the degree of Master of Science by Research

University of Leeds

School of Molecular and Cellular Biology

June 2021

The candidate confirms that the work submitted is their own and that appropriate credit has been given where reference has been made to the work of others.

Acknowledgements

I would like to give my thanks to my project supervisor, Professor Eric Blair, firstly for the opportunity to undertake a Masters by Research, and secondly for his invaluable support and guidance throughout this project, especially with help overcoming the challenges of working through a pandemic. I would also like to thank the other members of the Blair group, for their help around the lab, particularly in the first few months of this project. Thanks also go to Ruth Hughes and Sally Boxall for assisting with Flow Cytometry work.

Abstract

Cancer is caused by random, accumulated gene mutations (for example, to the tumour suppressor p53 and PTEN genes) that lead to dysregulated cell growth and proliferation and to invasion and metastasis. Current treatments include chemotherapy, radiotherapy and surgery, but these can be insufficient. Novel therapies are needed, including the designing of adenoviruses (Ads) to target and kill cancer cells.

Loss of the p53 gene product in cancer cells has been previously exploited to confer conditional replication of certain mutant Ads in cancer cells without affecting normal cells. p53 activates PTEN transcription and the PTEN protein is stabilised by p53. PTEN could present another promising target to enable cancer-cell specific targeting of Ad-based therapies.

Previous work in the Blair lab that led up to this project showed that both PTEN mRNA and protein were reduced by approx. 50% in Ad5-infected human cells. In this project, the activity of the PTEN promoter was analysed during Ad5 infection of cells in which the normal p53 genes were either present or absent (mediated by targeted deletion). Using dual luciferase assays that measure the activity of a transfected PTEN promoter, it was established that there was no significant difference in PTEN promoter activity between Ad5-infected or mock-infected cells and that the presence or absence of p53 did not affect PTEN promoter activity in Ad5-infected cells. This suggests that any reduction in PTEN mRNA that occurs during Ad5 infection is mediated at a post-transcriptional level. In addition, Ad5 was previously shown in the Blair lab to be restricted for growth in a glioblastoma cell line, U87MG, which is PTEN-null. Here, PTEN-expressing derivatives of U87MG were generated by retroviral transduction. These cell lines were characterised in preparation for detailed comparative studies on Ad5 replication and killing of isogenic PTEN-null and PTEN-positive cells.

Contents

1.1. Table of Figures

1.2. Table of Tables

1.3. Abbreviations

Abbreviation	Term
Ad	Adenovirus
ADP	Adenovirus death protein
AMPK	Adenosine monophosphate-activated protein kinase
ARV	Avian reovirus
BMI1	B cell-specific Moloney murine leukaemia virus integration site 1 protein
cAMP	Cyclic adenosine monophosphate
CAR	Coxsackie adenovirus receptor
CREB1	cAMP response binding element 1
CRM1	Chromosomal region maintenance 1
DNA	Deoxyribonucleic acid
EBV	Epstein-Barr virus
EGR1	Early growth receptor 1
FoxO	Forkhead transcription factor
GPCR	G-protein coupled receptor
GSK3	Glycogen synthase kinase 3
HCV	Hepatitis C virus
HDAC	Histone deacetylase
HES1	Hairy and enhancer of split 1
HPV	human papillomavirus
hTERT	Human telomerase reverse transcriptase
IKK	I kappa B kinase
lncRNA	long non-coding ribonucleic acid
MAGI2	Membrane associated guanylate kinase, WW And PDZ domain containing 2
MDM2	Mouse double minute two homologue
MHC	Major histocompatibility complex
miRNA	micro ribonucelic acid
MKK4	Mitogen kinase kinase 4
mTOR (C.)	Mammalian target of rapamycin (complex)
NEDD4	Neural precursor cell expressed developmentally down-regulated protein 4
NF-KB	nuclear factor kappa-light-chain-enhancer of activated B cells
PDK1	Protein dependent kinase 1
PI3K	Phosphoinositol-3-kinase
PIP2	Phosphatidylinositol (4,5) bisphosphate
PIP3	Phosphatidylinositol (3,4,5) trisphosphate
PKB/AKT	Protein kinase B
PKR	Protein kinase R
PML	Promyleocytic leukaemia protein

PPAR	Peroxisome proliferator-activated receptor
PTEN	Phosphatase and tensin homologue deleted on chromosome ten
PTP	Protein tyrosine phosphatase
Rb	Retinoblastoma protein
RBPJ	Recombining suppressor of hairless
RDG motif	Arginine-Glycine-Aspartate motif
RNA	Ribonucleic acid
RT-QPCR	Real time- quantitative polymerase chain reaction
SPRY	Protein sprout homolog
SV40	Simian virus 40
TGF	Transforming growth factor beta
TNF	Tumour necrosis factor
TRAIL	Tumour necrosis factor-related apoptosis-inducing ligand
TSP	Tumour suppressor protein
USP7	Ubiquitin-specific processing protease 7

2. Introduction

2.1. Subversion of host cell signalling pathways by viruses

Viruses are pathogens which must subvert the signalling pathways of the host cell to benefit their own replication. To enable viral replication, viral proteins target host proteins to alter the signalling pathways and inhibit the immune response. Of particular interest in this study is the interaction between viruses and tumour suppressor proteins and their pathways.

Tumour suppressor proteins (TSPs) are involved in regulating cell processes including induction of apoptosis, inhibition of cell growth and DNA damage repair. Loss of function of TSPs contributes to cancer progression[1]. There is also some debate as to whether some tumour suppressor proteins may also indirectly have anti-viral functions[2]. In targeting tumour suppressor proteins, viruses are able to overcome cell cycle control and DNA damage repair mechanisms to alter the host cellular environment and make it more conducive to viral replication.

In targeting tumour suppressor proteins, some viruses become mediators of oncogenesis. An example of this is high-risk human papillomavirus (HPV) types 16 and 18, which are associated with a large majority of human cervical cancers[3].

These oncoviruses are useful for studying the interactions between viral proteins and TSPs. Many oncoviruses functionally deactivate the TSP p53, which leads to deregulation of apoptotic, DNA stability and cell proliferation pathways[4]. P53 exerts its tumour suppressor function as a transcription factor of genes involved in both intrinsic and extrinsic pathways of apoptosis[5]. Different viruses have evolved different mechanisms to target p53, to prevent apoptosis and thus permit viral replication. For example, the Hepatitis B virus protein HBx directly binds to p53 to sequester it in the cytoplasm, inhibiting its nuclear function. Additionally, HBx causes the overexpression of lncRNA HUR1, which interacts with p53 to promote cell proliferation by inhibiting the transcriptional regulation of p21 and Bax[4].

The HPV oncoprotein E6 contributes to transformation of the host cell by complexing with a ubiquitin ligase, E6AP, which polyubiquitinates p53. This leads to the ubiquitin-proteasome mediated degradation of p53[4].

P53 is not the only tumour suppressor protein targeted during viral infection. pRb is a cell cycle control protein frequently targeted by DNA tumour viruses such as HPV,

SV40, and Adenoviruses[6]. To exert control of the cell cycle, pRb forms a complex with E2F family members, which initiate transcription when unbound. pRb also recruits chromatin remodelling factors including histone deacetylase 1 to repress E2F-dependent transcription[6]. During cell cycling, pRb is phosphorylated by cyclin-dependent kinases which releases E2F and activates transcription of S-phase genes, thus overcoming the G1 to S-phase checkpoint.

DNA tumour virus oncoproteins often contain an LxCxE motif, which is necessary for binding to the pocket region of pRb and other Rb family members, such as p105. The high-risk HPV oncoprotein E7 adopts this mechanism of pRb targeting, binding the hypophosphorylated form of pRb, preventing the formation of pRb-E2F complexes and enabling cell cycle progression to the S-phase[6].

Similarly, the Adenovirus E1A proteins also bind to the pocket region of pRb via an LxCxE motif, which displaces factors such as HDAC1 from pRb as well as inhibiting pRb-E2F complex formation[6]. E1A also recruits cellular histone acetyltransferase p300 into a complex with pRb, leading to acetylation of the pRb C-terminus. Acetylation of pRb results in increased interaction with the ubiquitin ligase MDM2, and subsequent ubiquitin-proteasome mediated degradation of pRb[6].

Adenoviruses also target p53 via the E1B-55K protein and E4ORF6 gene product. E1B-55K binds p53 near the N-terminus, and E4orf6 near the C-terminus, to prevent the transcriptional activity of the tumour suppressor. The E1B-55K/E4Orf6 binding is also responsible for the ubiquitin-proteasome mediated degradation of p53 by a Cullin-containing E3 ligase complex[7].

In addition to p53 and pRb, Adenovirus infection also modulates the tumour suppressor protein promyelocytic leukaemia protein (PML). PML regulates cell growth and apoptosis by numerous different mechanisms. PML is necessary for the activation of cyclin-dependent kinase inhibitor gene $p21^{WAF1/CIP1}$ by retinoic acid[8], and isoform PML-4 negatively effects the PI3K pathway by inhibiting mTOR and activating PTEN, as well as positively regulating the tumour suppressor p53 by promoting p53 acetylation and phosphorylation[9]. PML is also involved in regulating the localisation of the tumour suppressor PTEN by opposing the action of USP7, a deubiquitinylating enzyme that is associated with nuclear exclusion of PTEN[10]. PML function is frequently disrupted in virus infection, and in Ad infection, the PML bodies are reorganised from spherical to fibrous structures[11]. The E4orf3 gene product is

responsible for the structural change to the PML bodies, and E1A also co-localises to the PML bodies, through its LxCxE motif[12].

As adenovirus infection is reported to dysregulate p53, pRb and PML, it is possible that other tumour suppressor proteins may also be involved during infection. This project will focus on the role played by the tumour suppressor PTEN during Ad5 infection.

2.2. PTEN function

Phosphatase and tensin homologue deleted on chromosome 10 (PTEN) is a dual specificity protein and lipid phosphatase that primarily dephosphorylates phosphatidylinositol phosphates at the 3' position of the inositol ring[13]. It shows particular affinity for phosphatidylinositol-3,4,5-triphosphate (PIP3), and as such, acts as a negative regulator of phosphoinositol-3-kinase (PI3K), which phosphorylates phosphatidylinositol-4,5-bisphosphate to form PIP3[13] (Figure 1).

In acting as a negative regulator of PI3K activity, PTEN aids the fine-tuning of downstream PI3K signalling, which includes protein kinase B (PKB, also known as AKT) and phosphoinositide dependent kinase 1 (PDK1). Further downstream effectors of these pathways include the Forkhead (FoxO) transcription factors, the mammalian target of rapamycin (mTOR) complex 1, cyclin D1 and others involved in key cellular processes such as glycogen synthesis, cell cycling and survival[14]. AKT is a key regulator of cell survival and is implicated in anti-apoptotic responses. Activation of AKT occurs by dual phosphorylation at Thr308 and Ser473, which is performed by PDK1 in response to PI3K signalling via PIP3[14]. PI3K signalling is triggered in response to growth factors and cytokines, to G-protein coupled receptor (GPCR) activation and integrin signalling[15]. Aberrant signalling through this pathway has the potential to contribute to oncogenesis, and thus PTEN can be defined as a tumour suppressor protein.

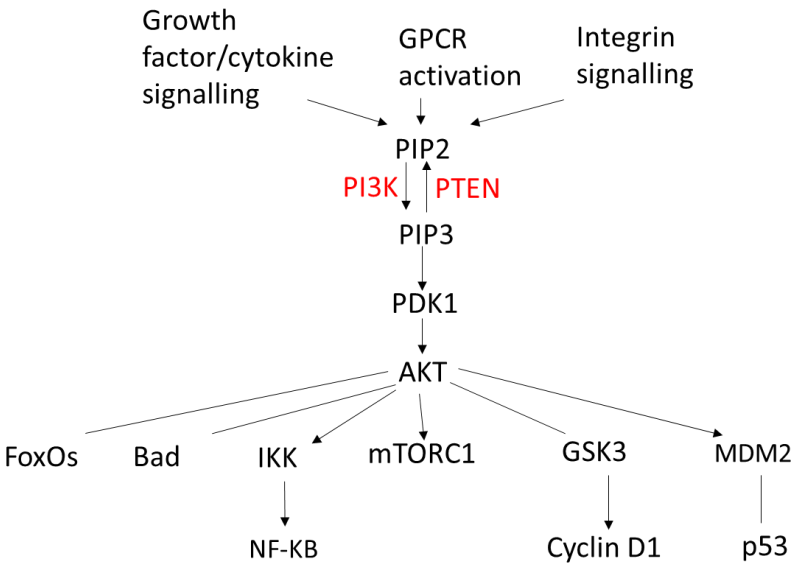

Figure 1. **The function of PTEN with reference to the AKT pathway.** Open connecting lines indicate inhibition or negative regulation, and arrows indicate activation or positive regulation. The inhibition of Bad and the FoxO transcription factors lead to the inhibition of apoptosis, as well as the activation of NF-κB transcription activity via IκB kinase (IKK). Inhibition of p53 via the activation of mouse double minute two homologue (MDM2) also suppresses apoptosis. Activation of cyclin D1 through glycogen synthase kinase 3 (GSK3) and the activation of mammalian target of rapamycin complex 1 (mTORC1) are involved in upregulating cell growth and proliferation genes.

Furthermore, individuals with germline PTEN-inactivating mutations present with tumour-susceptible phenotypes such as Cowden syndrome, Bannayan-Riley-Ruvalcaba syndrome and Proteus syndrome, which form a family of diseases known as PTEN hamartoma tumour syndromes. Clinically, PTEN hamartoma tumour syndromes are characterised by the elevated risk of forming benign or malignant tumours, especially in breast, endometrial and thyroid tissues[16 17]. This indicates a definitive role for PTEN as a tumour suppressor.

PTEN can localise to either the nucleus or the cytoplasm and has different roles depending on its localisation. For PTEN to perform the role of lipid phosphatase of PIP3, it must transiently interact with the plasma membrane. Nuclear PTEN regulates cell proliferation, transcription and genomic maintenance[18], and may even play a role in preventing double-stranded DNA breaks by inducing homologous recombination repair[19]. Cytoplasmic PTEN regulates inositol-3,4,5-trisphosphate receptors, which include those involved in calcium-mediated apoptosis and the transcriptional activation of the NF-κB pathway[18].

Moreover, PTEN is reported to have protein phosphatase activity in addition to its lipid phosphatase activity. Targets of PTEN protein phosphatase activity include focal adhesion kinase, cAMP-response binding element 1 (CREB1)[18] and cyclin D[20].

In addition, PTEN is also indicated in the stabilisation and transcriptional activity of p53, by direct association[20] and through its phosphatase activity. It has been noted that although PTEN and p53 are tumour suppressors that are both frequently mutated in cancers, mutations in both genes very rarely occur concomitantly[21]. Furthermore, in cells with low or null PTEN expression, cellular concentrations of p53 are also significantly decreased[22]. This may indicate that loss of PTEN might be sufficient to remove the selective pressure to reduce p53 expression during cancer progression. PTEN stabilises p53 in a phosphatase-dependent manner by negatively regulating the phosphorylation of the ubiquitin ligase MDM2 by AKT. By preventing MDM2 phosphorylation, the ubiquitination and subsequent degradation of p53 is also prevented[23]. Expression of a lipid-phosphatase inactive variant of PTEN also increases levels of p53, indicating that there is a phosphatase and MDM2 independent mechanism by which PTEN regulates p53, although this mechanism is yet to be elucidated[24]. It has also been found that PTEN and p53 are able to form a complex within the nucleus, further developing the PTEN-p53 network[25].

2.3. PTEN structure

The structure of PTEN consists of 2 major structural-functional elements, the N-terminal unit and the C-terminal unit. Within the N-terminal catalytic unit lies a PIP2 binding domain, and a protein tyrosine phosphatase motif. The C-terminal unit constitutes a C2 tensin-type domain and PDZ domain at the C-terminus[26] (Figure 2).

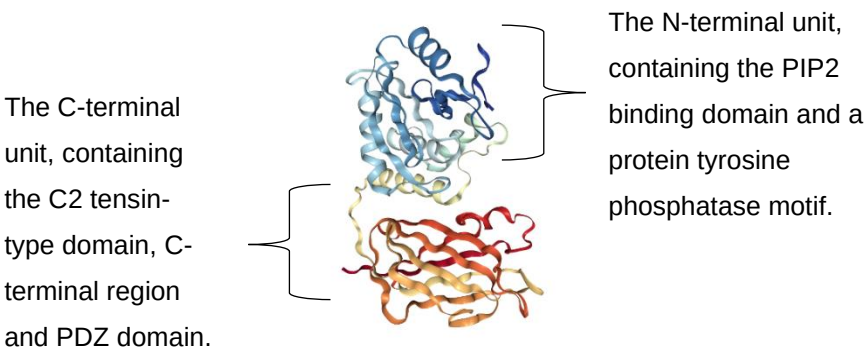

Figure 2. **The crystal structure of PTEN, PDB access number 1D5R.** The N-terminal domain is shown in blue, and the C-terminal domain in red. The structure shown above has deletions in the N-terminal region (amino acids 1-7) and in a loop region (residues 286–309) but has equivalent activity and affinity to PIP3 as wild-type PTEN. The deletions were created to stabilise the structure for crystallisation[27].

The protein tyrosine phosphatase motif (PTP), localised in the N-terminal unit, is similar to those in other dual-specificity phosphatases, but with a slightly wider active site to accommodate the larger substrate of PIP3[27]. The C2 domain of PTEN has been indicated to bind to the cell membrane and may also contribute to the correct positioning of the phosphatase active site at the membrane[26]. The C2/phosphatase domain interface is frequently mutated in cancer, with the residues mutated largely being involved in hydrogen bonding[26]. The instances of these localised mutations indicate that the interdomain hydrogen bonding is key for PTEN function. The PDZ domain plays a role in membrane localisation of PTEN, by interacting with the Pleckstrin homology (PH) domain in proteins such as MAGI2[28]. However, the significance of the PDZ domain in membrane localisation has been called into question in studies by Hanafusa and colleagues. This group postulated that the phosphatase domain and C2 domain have a more prevalent role in the membrane affinity of PTEN, as removing either of these domains reduced the membrane affinity of PTEN[29], whereas removing the PDZ domain did not significantly impact the activity of PTEN[30].

2.4. PTEN regulation

The functions of PTEN are multifaceted, and no less can be said of its regulation. Regulation of PTEN occurs at the transcriptional, translational and post-translational level, all of which contribute to a highly controlled, finely tuned system. Positive regulators of PTEN at the transcriptional level include early growth response protein

1 (EGR1), peroxisome proliferator activated receptor γ (PPARγ), and p53, all of which have the capacity to bind directly to the PTEN promoter region[31]. There are also negative regulators of PTEN transcription, and these include the Ras/Raf/MEK/ERK pathway through c-Jun and NF-κB through the sequestration of the transcriptional activator CBP/p300. In some cancer models, further transcription factors appear to be involved in down-regulating PTEN during tumour formation and progression, for example mitogen-activated protein kinase kinase 4 (MKK4)[32], transforming growth factor β (TGFβ)[33] and the polycomb group protein BMI1[34] have been identified.

Table 1. **Transcriptional regulation of PTEN.**

Regulator	Positive/Negative	Mechanism of action	Reference
P53[35]	Positive	Direct binding to PTEN promoter	Stambolic et al. (2001)
SPRY[36]	Positive	Direct binding to PTEN promoter	Edwin et al. (2006)
PPAR[37]	Positive	Direct binding to PTEN promoter	Patel et al. (2001)
EGR1[38]	Positive	Direct binding to PTEN promoter	Virolle et al. (2001)
NOTCH- RBPJ[39]	Positive	Direct binding to PTEN promoter	Whelan et al. (2007)
NOTCH- HES1[40]	Negative	Direct binding to PTEN promoter	Mumm et al. (2000)
MKK4[32]	Negative	Through up-regulation of NF-κB signalling	Xia et al. (2007)
TGFβ[33]	Negative	Through NF-κB signalling	Chow et al. (2010)

NF-κB[41]	Negative	Sequestration of CBP/p300 complex	Vasudevan et al. (2004)
RAS/Raf/MEK/Erk[42]	Negative	Via c-Jun binding to PTEN promoter	Hettinger et al. (2007)
BMI 1[43]	Negative	Direct binding to PTEN promoter	Song et al. (2009)
Promoter methylation	Negative	Epigenetic modification of the promoter identified in cases of breast[44], endometrial[45] and colorectal[46] cancers.	Bose et al. (2004), Salvesen et al. (2001), Goel et al. (2004)
Histone deacetylation[31]	Negative	Epigenetic modification by HDAC	Brito et al (2015)

(SPRY- protein sprout homolog; PPAR- peroxisome proliferator-activated receptor; EGR1- early growth factor 1; RBPJ- recombing suppressor of hairless; HES1- hairy and enhancer of split 1; MKK4- mitogen kinase kinase 4; TGFβ- transforming growth factor beta; NF-κB- Nuclear factor kappa light chain enhancer of activated B-cells; CBP/p300- cyclic adenosine monophosphate response element binding element binding protein; BMI1- HDAC- histone deacetylase)

NOTCH, a membrane-associated transcription factor[40], is able to both positively and negatively regulate PTEN transcription. If NOTCH recruits and activates hairy and enhancer of split 1 (HES1), PTEN expression is downregulated, whereas if NOTCH inhibits the recombining suppressor of hairless (RBPJ), PTEN expression is upregulated[40].

The promoter region for the PTEN gene may also be susceptible to epigenetic modifications leading to the silencing of PTEN gene expression. This is believed to be caused by the hypermethylation of the CpG islands present in the PTEN promoter region. This mechanism of PTEN gene silencing has been tentatively identified in instances of gastric, colon and breast cancer[31].

Numerous microRNAs (miRNAs) have been implicated in the post-transcriptional negative regulation of PTEN. miRNAs are negative regulators of mRNA translation which function by binding to the 3' untranslated region of the target mRNA, which either leads to prevention of translation or degradation of the target[47]. MiRNAs such as miR-130 and miR-21 are indicated to serve as tissue-specific regulators of PTEN synthesis[31]. MiR-21 negatively regulates PTEN by binding to the mRNA and preventing translation[48]. However, miR-130 is indicated to inhibit cell growth and increases apoptosis via direct interaction with PTEN in non-small cell lung cancer tissues, suggesting it plays a role as a positive regulator of PTEN activity[49]. MiR-130 is an example of a hairpin miRNA involved in PTEN regulation, and polycistronic miRNAs such as miR367-302b may also be involved.

Other post-translational modifications to the PTEN protein include phosphorylation,

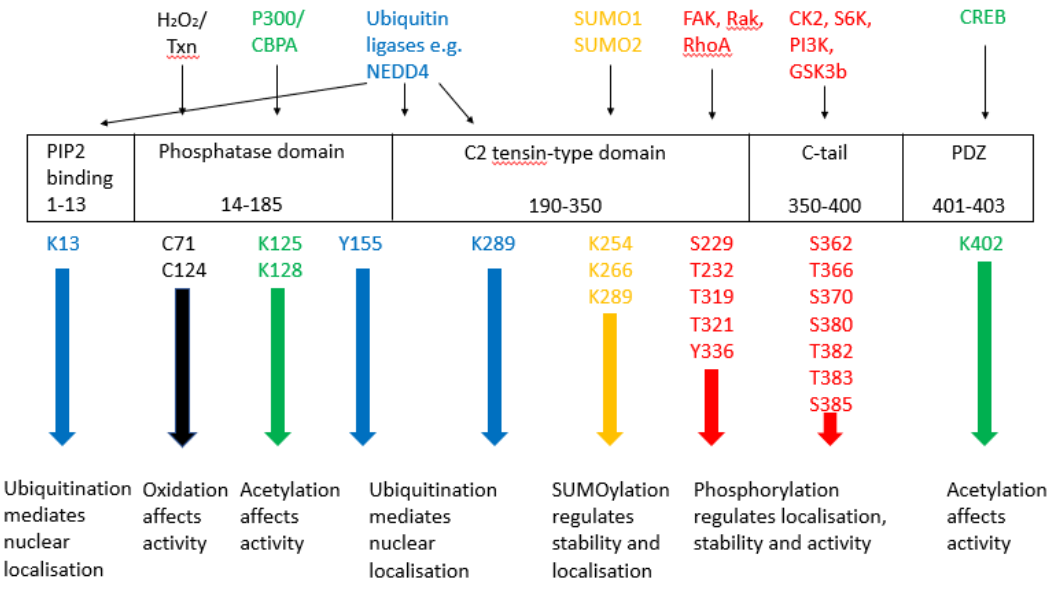

Figure 3. **An illustration of the domains of PTEN and how they are post-translationally modified.** The enzymes responsible for the PTMs are shown at the top of the diagram, with the residues they target shown beneath the domain. Shown in blue are the sites of ubiquitination, in black the sites of oxidation, in green the sites of acetylation, in yellow the sites of SUMOylation and in red, the sites of phosphorylation.

SUMOlyation, acetylation and oxidation (See figure 3). Phosphorylation of the C-terminal region of PTEN is mediated by casein kinase 2 (CK2) and retains PTEN in

a lipid-phosphatase inactive form in the cytoplasm[50]. Dephosphorylation of PTEN at the C-terminal region enables translocation to the plasma membrane and activation, but also destabilises PTEN and makes it more prone to ubiquitination by NEDD4[50]. It is possible that the dephosphorylation of the PTEN C-terminal region is regulated by PTEN itself, through its protein phosphatase activity[51], and that the ubiquitination of dephosphorylated PTEN by NEDD4 acts as a feedback regulation mechanism[50].

PTEN can also be oxidised by H_2O_2 produced as a result of epidermal growth factor or platelet-derived growth factor stimulation in cells with high levels of NADPH oxidase 1. Oxidation at cysteine 124 causes reversible, transient inactivation of PTEN[52].

2.4. Interactions between PTEN and viruses

2.4.1. Epstein-Barr Virus

PTEN is targeted by numerous different viruses during their replication. For example, during Epstein-Barr virus (EBV) infection, an EBV latent membrane protein has been found to cause hypermethylation of the PTEN gene promoter region via activation of DNA methyltransferase 1, leading to a decrease in PTEN protein production[53]. EBV is an enveloped, double stranded DNA virus which has been associated with several human cancers, including nasopharyngeal carcinoma, Hodgkins lymphoma and gastric carcinoma. By non-random, global hypermethylation of the promoter regions of cancer-associated genes including PTEN, EBV infection increases the likelihood of oncogenesis in human cells[53].

2.4.2. Hepatitis C Virus

PTEN has also been identified as a key host protein affected during Hepatitis C virus (HCV) infection. HCV is a small, enveloped, positive stranded RNA virus, strongly implicated in the development of hepatocellular carcinoma[54].

Immunofluorescence and Western blotting experiments have indicated that following HCV infection, the intracellular localisation of PTEN changes, in that there is a significant loss of PTEN from within the nucleus[55]. The loss of nuclear PTEN is suggested to favour virus production but may also contribute to genomic instability

and the formation of double-stranded DNA breaks, which in turn may be implicated in the oncogenic transformation of hepatocytes which can be associated with HCV infection. The loss of nuclear PTEN has been proposed to be caused by down-regulation of Transportin-2- a regulator of nucleocytoplasmic transport- by HCV viral non-coding RNA II.[55]

Furthermore, PTEN interacts with the HCV core protein to inhibit HCV replication. Overexpression of PTEN significantly reduced the levels of HCV RNA- by preventing post-binding step(s) in viral entry, possibly mediated by interaction between the lipid phosphatase domain of PTEN and the HCV core protein[56].

2.4.3. Avian Reovirus

Avian reovirus (ARV) is a non-enveloped virus with a segmented, double-stranded RNA genome. For the virus to replicate, it subverts the host cell autophagy process. Autophagy is a key process in cellular homeostasis and plays a key role in the stress-induced survival response, to maximise nutrient availability[57]. Autophagosomes may provide membranous support for viral transcription and replication, and thereby support ARV growth. P17 is an ARV non-structural protein which acts as a CRM1-independent nucleocytoplasmic shuttling protein and induces autophagy during infection, as well as contributing to regulation of the host cell cycle and translation, by interfering with host signalling pathways[58]. P17 stimulates the PTEN, AMPK and PKR/eIF2α pathways, leading to downregulation of Akt and mTORC1 activity, which triggers autophagy[58]. In addition, p17 mediates the suppression of Tpr, a component of the nuclear pore complex, leading to an accumulation of nuclear p53, which in turn upregulates transcription of PTEN[58]. Consequently, the PI3K/Akt/mTORC1 signalling pathway is downregulated, leading to a cellular translation shut-off alongside upregulation of autophagy, which benefits viral replication.

In conclusion, while interaction of viral proteins with PTEN have been demonstrated for several human viruses, there are many other viruses associated with human cancers (such as papillomaviruses and polyomaviruses) and other viruses that have the ability to transform human cells but for which no data on the interaction of these viruses with PTEN exists. One major group of such viruses is the Adenovirus family.

2.5. Adenovirus

Adenoviruses are double stranded, non-enveloped DNA viruses, with a genome of around 36kb. Four genera of adenoviruses exist, and they are so categorised based upon bioinformatic analysis. Human adenoviruses are from the Mastadenovirus genus and are divided into 7 species, named A through G, with at least 57 types existing between these species. Within human cells, adenoviruses exhibit some degree of cell tropism, where the differences between types may be attributed to differences in the fibre knob protein.[59]

2.5.1. Structure

The adenovirus capsid is constructed from 3 major proteins- penton, hexon and fibre proteins; and several other smaller proteins, known as cement proteins[60]. The capsid is an icosahedron of over 900Å in diameter, composed of 240 trimeric hexon proteins, with penton base and fibre proteins present at each of the 12 vertices of the icosahedron[61]. The penton base serves as the attachment site for cell surface integrins αvβ3 and αvβ5 during viral entry, which mediates viral internalisation. Furthermore, the penton base provides a site for the fibre shaft to penetrate and perhaps acts as an anchor[61] (Figure 4).

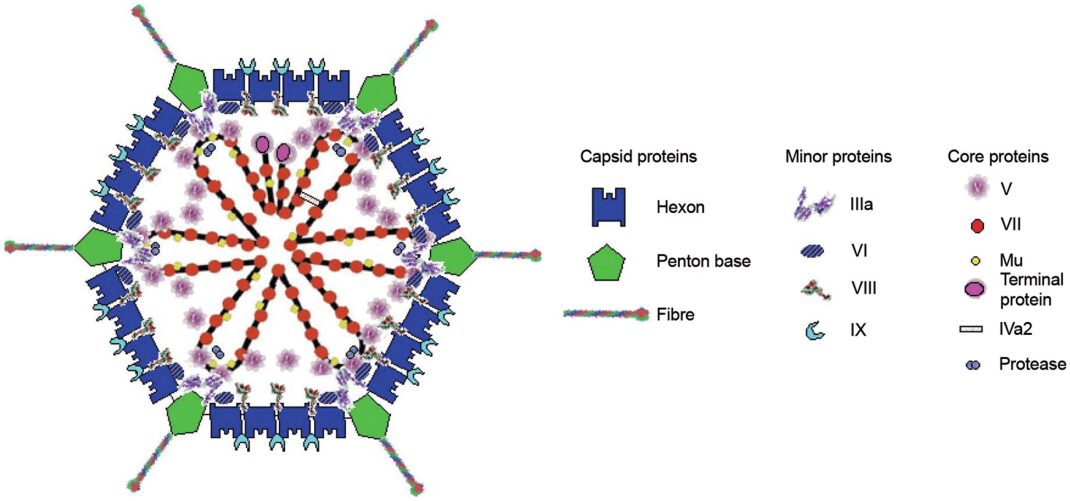

Figure 4. **A diagrammatic representation of the structure of human adenoviruses, from 'Adenoviruses: update on structure and function'.** A schematic to illustrate the major components of the adenovirus particle. Highlighted are the 3 major capsid proteins- fibre, hexon and penton base- the minor "cement" proteins IIIa, VI, VIII, IX, and the smaller core proteins- V, VII, Mu, terminal protein, IVa2 and protease. The proteins are not to scale, although approximate shapes are given based on X-ray crystallography and electron microscopy analyses[60].

The lifecycle of the adenoviruses can be divided into early phase and late phase events, with the early phase events occurring before viral DNA replication, and the late phase events occurring after.

Entry of adenoviruses into human cells is largely dependent on interaction of the fibre protein knob domain with the Coxsackie Adenovirus Receptor (CAR), although some types possess affinity for the CD46 receptor or desmoglein 2 instead, principally types from Species B[61]. Sialic acid and heparan sulphate-containing proteoglycans also facilitate virus entry, for some members of species D and G and B and C, respectively[62].

Adenoviruses also bind to soluble factors, including lactoferrin[63] and factor X[62].

CAR forms part of epithelial tight junctions and is present on most human cells. Three molecules of CAR bind to three molecules of the adenovirus fibre protein to induce endocytosis of the virion. To support virus internalisation, the penton base protein binds to integrins αvβ3 and αvβ5, via a conserved RGD motif, which causes integrin clustering and associated integrin transmembrane signalling via PI3K,

p130CAS and Rho GTPases[64]. These signalling events lead to the polymerisation of actin molecules localised to the site of penton binding, enabling endocytosis of the virion. In addition, the penton-integrin interactions initiate the uncoating of the virion at the cell surface through the loss of fibre proteins and exposure of cement protein VI, which prepares the virion for cell entry[65].

After the fibre-less virus particle has been endocytosed, it must then escape the endosome. For endosomal escape, cement protein VI penetrates the endosomal membrane, causing membrane disruption and allowing the virus particles to be released[64]. The acidification of the endosome during maturation may also have significance in the release of viral capsid proteins and also in the activation of the viral associated viral protease, which is required for the final disassembly of the virion at the nuclear pore[59].

After the virions have exited the endosome, they are transported to the nucleus along with microtubules, which is dictated by hexon binding. Hexon trimers are also responsible for the association of the viral components to the nuclear pore complex. Binding of the Ad virion to the nuclear pore complex triggers the complete uncoating of the virion and the transport of viral DNA into the nucleus[59]. Viral DNA enters the nucleus in complex with core protein VII at around 2 hours post infection.

The viral E1A gene is an immediate early gene that is transcribed without requirement for any other viral protein. It encodes two major phosphoproteins of 289 and 243 amino acids responsible for the regulation of viral and cellular protein expression at the transcriptional level[66], and the induction of the host cell cycle to enter S-phase[67], by interfering with proteins in the retinoblastoma (Rb) pathway[6].

Following entry into the nucleus, and transcription of early viral genes by host cell RNA polymerase II, the virus genome is replicated by the E2 gene products (E2-72K, E2B-DNA polymerase and terminal protein), assisted by host cell proteins[68].

Viral protein E1B-19K blocks apoptosis by inhibiting the downstream effectors of TRAIL and TNFα, which are pro-apoptotic signalling pathways to which the cell is sensitised to by the dysregulation of the cell cycle by E1A[69]. For example, it can bind to pro-apoptotic proteins Bak and Bax to prevent the opening of the mitochondrial permeability transition pore, and hence mitochondrial-dependent apoptosis[70]. E1B-55K is involved in the degradation of p53 alongside E4orf6[7], and hence suppresses apoptosis.

The E2 gene encodes the viral DNA polymerase, preterminal protein and the DNA-binding protein, all of which are essential for viral DNA replication[71].

E3 proteins are involved in the modulation of the host immune response in that they are involved in protecting the adenovirus infected cells from MHC-restricted cytotoxic T-cells and in preventing immune mediated inflammation. The E3 gene also encodes for the adenovirus death protein (ADP), which is involved in the efficient release of progeny virions[72].

The viral E4 gene is responsible for producing at least six viral polypeptides by alternative RNA splicing. The most important of these in the viral lifecycle are E4orf3 and E4orf6. Both proteins interact independently of the other indirectly to facilitate viral DNA replication, synthesis of late viral proteins and inhibition of host-cell protein synthesis[73]. E4orf3 is involved in SUMOlyating host proteins involved in DNA damage repair, to ensure high fidelity viral DNA synthesis[73]. It has also been proposed to regulate the structure and hence replication of the viral genome, by inhibiting the host cellular response to double-stranded DNA breaks[74]. E4orf6 is involved in the prevention of apoptosis by degrading p53- in association with E1B55K[7].

The L1-L5 gene products are involved in the structure and assembly of the capsid of the virus[69].

2.5.2. Adenoviruses as oncolytic therapeutics

Oncolytic viruses are able to selectively enter and replicate within cancer cells, while being unable to do so in normal cells. These viruses can be naturally occurring or genetically engineered for cancer cell specificity[75]. Oncolytic viruses aid the stimulation of the immunogenic response against the tumour cells by inducing active lysis of the cancer cells, or by delivering a transgene which initiates apoptosis or necrosis[76].

Adenoviruses present several advantages as a therapeutic- they are easy to genetically or chemically manipulate, they are able to be produced at high titres, and can transduce dividing and non-dividing cells. Furthermore, adenovirus DNA is not integrated into the host genome during infection, which reduces the risk of mutagenesis to host DNA[77]. However, the major issue surrounding adenoviral

therapy is the natural tropism of adenoviruses towards the liver, which may induce hepatocytotoxicity. This is mediated by the binding of hexon protein to Factor X, which enables the binding of Ad5 to the heparan sulphate proteoglycan receptors present on hepatocytes[78]. In addition, adenovirus infection induces a host immune response, either by the innate or adaptive immune systems if the patient has had previous exposure to the virus[79].

To prevent hepatotoxicity and the immunogenic response to wild-type adenoviruses, numerous methods of modification have been developed. Chemical modification by complexing the adenovirus with a synthetic polymer can be performed by chemical conjugation or by manipulating the anionic surface of the virus to encourage electrostatic interaction with an anionic polymer. By coating the virus surface in a polymer, it is possible to shield it from the host immune response. One of the benefits of using synthetic polymers to aid viral entry is the level of optimisation which can be performed, to maximise uptake efficiency and specificity, whilst maintaining the cancer cell-killing properties of the adenovirus.

In addition, affinity ligands can be attached to the polymer coat to encourage active targeting of cancer cells. Affinity ligands could be an antibody, a peptide, an aptamer or a polysaccharide with high affinity to a plasma membrane receptor which is over-expressed in cancer cells and under expressed in normal cells. For example, cRGD is a peptide with high affinity for αvβ3 and αvβ5 integrins, which are frequently expressed on growing tumour cells. Use of affinity ligands increases the selectivity and efficiency of viral accumulation at tumour cells[76].

A major drawback of chemically altering adenoviruses for oncolytic virotherapy is that the modifications cannot be replicated in the progeny virions. The progeny virions may then go on to cause unwanted, non-specific interactions with normal host tissues. Conditionally replicating adenoviruses have genetically modified genomes which ensure that cancer cell targeting modifications are passed onto the next viral generation[77].

One method of designing conditionally replicating viruses is to delete viral genes which are essential for viral replication during infection of normal cells but are complemented in cells displaying some of the hallmarks of cancer, such as aberrant cell cycling or cell death mechanisms.

For example, Onyx-015 is a genetically modified adenovirus with a deletion in the E1B55K gene, corresponding to the p53 binding domain[77]. In infection of normal cells, E1B55K interacts with p53, in conjunction with viral protein E4orf6, to prevent apoptosis triggered by viral E1A gene products. In approximately 50% of human cancers p53 is deleted or mutated[80], and Onyx-015 is able to successfully replicate in these p53-null cells but replicates poorly in normal cells with wild-type p53, as the lack of p53 binding causes the cell to undergo cell cycle arrest[81]. However, as E1B55K plays additional roles during the viral lifecycle, Onyx-015 replication in cancer cells is less efficient in replication than wild-type adenovirus as the mutant E1B55K prevents effective nuclear export of viral mRNA[79].

A modified virus that is similar to Onyx-015, named H101, has been approved for use in China for treatment of head, neck and oesophageal cancer[82]. It has deletions in both the E1B and E3 genes, leading it to replicate selectively in p53 null cells. The deletion to the E3 gene removes the coding region of the adenovirus death protein, which may improve the safety of the virus[83].

Other attempts to design a selectively replicating adenovirus involve making small, specific mutations to key genes, such as the E1A gene. Such small mutations are designed to interfere with one function of the viral protein, to retain viral potency whilst enabling selective replication[84]. E1A permits viral replication by interacting with cellular protein Rb to induce entry into the S-phase of the host cell cycle. Where the Rb-binding domain of the E1A gene is mutated, the virus is able to replicate in cancer cells with an already dysregulated cell cycle caused by, for example, mutation to Rb family genes[85].

Furthermore, tumour selectivity can also be conferred by placing the adenoviral early proteins under the control of a promoter which is upregulated in cancer cells. For example, placing the E1A gene under the transcriptional control of the human telomerase reverse transcriptase (hTERT) promoter enables specific replication in cancer cells, as hTERT is over expressed in cancer cells to prolong the lifespan of the cell[86].

2.5.3. Interactions between PTEN and Adenoviruses

Thus far, work by previous Blair group students has elucidated that there may be a paradoxical relationship between PTEN and adenoviruses during viral replication, in that Ad5 replicates poorly in PTEN-null cell lines and in cell lines in which PTEN was

depleted by RNA interference. However, the cellular level of PTEN is markedly decreased during the early phase of Ad5 infection in cells that contain normal, unmutated PTEN. Infection with Ad5 has been shown to decrease the cellular concentration of PTEN by 50% at 24 hours post infection (Beth Mason and Lisa DeCotret, unpublished results). The expression of PTEN mRNA was also reduced by approximately 50% in Ad5 infected A549 cells, as shown by RT-QPCR analysis and was decreased in both untreated A549 cells and in cells in which PTEN mRNA had been depleted by RNA interference (Amy Turner, unpublished results). However, PTEN expression was partly restored following inhibition of proteasomes by MG132, which implies that there may also be post-translational degradation of PTEN protein during Ad infection.

In investigating the contribution of p53 to PTEN regulation, it was found that the base level of PTEN was lower in p53 null cells, perhaps indicating that p53 partially contributes to the regulation of PTEN expression (Amy Turner, unpublished results). However, it was not determined whether p53 mediation of PTEN expression occurred in a cell specific manner.

In addition, it has been well documented that adenovirus proteins regulate p53 during infection, and therefore may also indirectly regulate PTEN.

2.6. Aims of this project

- Identify whether PTEN promoter activity changes during Ad5 infection
- Identify whether p53 status of cells affects the activity of the PTEN promoter during Ad5 infection
- Produce a PTEN-expressing U87MG cell line
- Compare progression of Ad5 infection in a PTEN-expressing cell line with wild-type U87MG and A549

3. Materials and Methods

3.1. Buffers

Table 2: Buffers used throughout this project and their composition

Buffer	Composition
TBST	20mM Tris HCl, 137mM NaCl, 0.05% Tween 20; pH 7.4
TBE	90mM Tris HCl, 90mM boric acid, 2mM Na_2EDTA
DNA loading buffer (New England Biolabs Cat No: B7025S)	2.5% Ficoll®-400, 10 mM EDTA, 3.3 mM Tris HCl, 0.02% Dye 1 (pink) 0.001% Dye 2 (blue); pH 8
RIPA	20mM Tris HCl, 150mM NaCl, 1mM Na_2EDTA, 1mM EGTA, 1% NP-40, 1% sodium deoxycholate, sodium pyrophosphate 2.5 mM, 1 mM β-glycerophosphate, 1 mM $Na_3 VO_4$, 1 µg/ml leupeptin
SDS running buffer	25mM Tris HCl, 192mM glycine, 3.5mM SDS; pH 8.3
SDS loading buffer	63 mM Tris HCl, 10% glycerol, 2% SDS, 0.0025% bromophenol blue, pH 6.8
Towbin transfer buffer	25mM Tris HCl, 192mM glycine, 20% methanol; pH 8.3
Passive lysis buffer	As supplied by Promega
PBS	137mM NaCl, 2.7mM KCl, sodium phosphate 10mM; pH 7.4

3.2. Cell Lines

Table 3: Cell lines. Cell lines used throughout this project, their PTEN and p53 status and origin.

Throughout this project, the following cell lines were used:

Name	PTEN status	P53 status	Origin	Notes
U87MG	PTEN-null	Wild-type p53	Glioblastoma	
A549	Wild-type PTEN	Wild-type p53	Non-small cell lung carcinoma	
293T	Wild-type PTEN	Wild-type p53	Embryonic kidney cells	Easily transfectable, immortalised with Adenovirus E1A and E1B
H1299	Wild-type PTEN	P53-null	Non-small cell lung carcinoma	
HCT116+/+	Wild-type PTEN	Wild-type p53	Large intestine carcinoma	
HCT116 -/-	Wild-type PTEN	P53 knockout	Large intestine carcinoma	
Phoenix Ampho[87]			Embryonic kidney	Based on 293T cell line, gives high transfection efficiency

3.3. Antibodies

Table 4: Antibodies. Antibodies used throughout this project, their species, application, working dilution, supplier and catalogue number (where relevant).

Antibody	Species	Supplier	Cat No	Application	Working Concentration
Anti-PTEN	Rabbit	Cell Signalling Technology	9559	Western blot	1:1000
Anti-PTEN	Mouse	Santa Cruz	Sc-7974	Immunofluorescence	1:100
Anti-GAPDH	Mouse	CalBiochem (Merk)	CB1001-500UG	Western blot	1:10000
Anti-fibre	Rabbit	Made in-house		Western blot, immunofluorescence	1:2000
Anti-penton	Rabbit	Made in-house		Western blot, immunofluorescence	1:1000
Anti-E1A	Mouse	Santa Cruz	Sc-430	Western blot, immunofluorescence	1:1000; 1:100
Anti-72K	Mouse	Kindly provided by K.Leppard (University of Warwick)		Western blot	1:5000
Anti-DBP	Rabbit	Kindly provided by K.Leppard (University of Warwick)		Immunofluorescence	1:10
Anti-mouse Horseradish Peroxidase		Sigma	1002231745	Western blot	1:1000
Anti-rabbit horseradish peroxidase		Sigma	1002144293	Western blot	1:1000

Anti-mouse Alexa Fluor-488	Goat	Invitrogen	A21203	Immunofluorescence	1:1000
Anti-rabbit AlexaFluor-488	Goat	Invitrogen	A27034	Immunofluorescence	1:1000

3.4. Mammalian cell culture

Cells were sub-cultured every two to three days, when approximately 80% confluent. Spent medium was removed, cells were washed with PBS, then trypsinised. DMEM with 10% FBS and 1% Pen/Strep was added and cells were dispersed by gentle aspiration. Approximately 2ml of cell suspension was retained in the flask, and the remainder discarded. Medium was added to the flask (around 10ml for a T75). Cells were incubated at 37°C in a humidified atmosphere containing 5% CO_2. For preparation of cells in six-well plates, the cells in solution following dispersion were counted using a haemocytometer and a seeding density of 0.3 x 10^6 cells per well was used. For a 12-well plate the seeding density was 0.1 x 10^6 cells per well, and for a 24 well plate the seeding density used was 0.05 x 10^6 cells per well.

3.5. Bacterial cell culture

Bacterial cultures were grown in LB medium supplemented with 100µg/ml ampicillin. Colonies were picked form LB agar plates and inoculated into 10ml LB medium plus ampicillin, followed by overnight growth with shaking at 37°C. From the liquid starter culture, 1ml starter was added to 100ml LB with ampicillin and left to grow overnight at 37°C with shaking for use in midi-prep plasmid DNA isolation.

3.6. Small and medium scale plasmid preparation

Small scale plasmid preparation (mini-prep) was performed using the QuiaGen system, following manufacturers instructions.

Medium scale plasmid purification (midi-prep) was performed using the QiaGen MidiPrep system, following manufacturers instructions. Cells from a 100ml overnight culture were harvested by centrifugation at 14000g and 4°C for 40 minutes. The cell pellet was resuspended in 4ml of buffer P1. Four millilitres of buffer P2 was added, followed by vigorous inversion. The mixture was incubated at room temperature for 5 minutes before 4ml of prechilled buffer P3 was added and vigorously inverted again. The tube was incubated on ice for 15 minutes. After buffer P3 was added, a white precipitate appeared which contained genomic DNA, proteins and cell debris. After centrifugation, the supernatant was transferred to a clean Falcon tube and centrifuged for a further 15 minutes, as described above. The QiaGen tip was equilibrated using 4 ml of buffer QBT, which was emptied from the column by gravity flow before the supernatant from the previous step was applied to the resin. The column was washed with two washes of 10ml buffer QC. DNA was eluted from the column into a clean 15ml Falcon tube using 5ml buffer QF. An aliquot (3.5ml) of

room-temperature isopropanol was added to the eluate to precipitate the DNA. The tube was centrifuged at 14000g for 60 minutes at 4°C. The supernatant was carefully decanted and discarded. The DNA pellet was washed with 2ml 70% ethanol and centrifuged in the same conditions as before for 60 minutes. The supernatant was discarded, and the pellet resuspended in 100µL nuclease-free water. A nanodrop at 260nm was used to calculate the concentration of DNA.

3.7. Agarose gel electrophoresis

A 0.75% agarose gel was made by heating 0.75g of agarose and 100ml of TBE buffer in a microwave oven, until the agarose had completely dissolved. The gel mixture was left to cool slightly, until it reached 50°C, and 1µL SybrSafe Gel Stain (ThermoFisher) was added. The mixture was then gently cast into a stand with a comb already inserted. The gel was left to set completely before use. Before being loaded onto the gel, 0.5µg of each plasmid was combined with 2µL of Loading Buffer (New England Biolabs). The gel was placed into an electrophoresis tank, and TBE buffer was added to the tank until a layer of buffer covered the gel. The plasmids were then loaded alongside a 1kb DNA ladder (New England Biolabs), and a voltage of 100V was applied for 1 hour. A fluorescent image of the agarose gel was captured using a Fuji FLA5000 imager.

3.8. E.coli transformation

An aliquot of competent *E.coli* DH5α (kindly provided by Vikki Easton, University of Leeds) was thawed on ice, and 1µL of miniprep or 2µL of plasmid was added. The tube was gently agitated and incubated for 30 minutes on ice. The mixture was heat-shocked at 42°C for 45 seconds and incubated on ice for two minutes. Eighty microlitres of SOC medium (2% tryptone, 0.5% yeast extract, 10 mM NaCl, 2.5 mM KCl, 10 mM $MgCl_2$, 10 mM $MgSO_4$, and 20 mM glucose, ThermoFisher)was added and incubated at 37°C for 30 minutes with shaking. Bacteria were spread on LB agar plus ampicillin plates, warmed to room temperature, left to adsorb for several minutes, inverted and incubated at 37°C overnight.

3.9. Mammalian cell transfection

Twenty-four hours prior to transfection, cells were seeded into antibiotic-free DMEM + 10% FBS in the wells of a 6, 12 or 24-well plate to achieve 50-80% confluency at the time of transfection. On the day of transfection, two tubes were made up; Tube A contained 1µg of plasmid DNA in 224µL of OPTIMEM, tube B contained 4µL Lipofectamine 2000 and 21µL OPTIMEM. Tube B was prepared first and incubated at room temperature for 5 minutes. The contents of tube B were added to tube A

and incubated at room temperature for a further 20 minutes. The cells to be transfected were washed twice with PBS. OPTIMEM (900µL) was added to the combined tube A plus B, and the contents added to cells. The plate was incubated at 37°C for 4 hours before an additional two millilitres of serum-free medium was added. Cells were harvested 24 or 48 hours post-transfection.

3.10. Production of retroviruses and cell transduction

Phoenix Ampho cells were seeded at $4.5x10^5$ cells per well in a 6-well plate. At 24 hours after seeding, cells were transfected with 2.5µg pBABE PTEN plasmid, and Lipofectamine 2000, at a ratio of DNA to lipofectamine of 1:2.5 as described above. Cells were incubated overnight with the transfection complex and medium was replaced with DMEM + 10% FBS + 1% P/S, supplemented with 20mM HEPES-KOH (pH 7.5). At 48 hours post transfection, the supernatant containing retroviruses was harvested, filtered through a 0.45µm filter and polybrene was added to a final concentration of 4µg/ml and gently pipetted to mix. The removed medium was replaced with the HEPES supplemented DMEM+FBS+P/S. At seventy-two hours post transfection (24 hours later), a second batch of retroviral supernatant was harvested, filtered and treated with polybrene as described above. Supernatants were used immediately to transduce U87MG as described below.

Twenty-four hours prior to infection, U87MG cells were seeded at $4.5x10^5$ cells per well of a 6-well plate. For transduction, the medium was removed and replaced with the retrovirus-containing supernatant that had been harvested at 48 hours post transfection. Cells were incubated for 4 hours at 37°C, with agitation every 15 minutes. The retrovirus-containing supernatant was removed, cells were washed twice with PBS and fresh growth medium was added. At twenty-four hours after the initial transduction, a second round of transfection was performed using the second batch of harvested retrovirus-containing supernatant.

Twenty-four hours after the second round of transduction, the growth medium was changed to medium containing 2µg/ml puromycin, to select for stably transduced cells. Selection was performed for 14 days, with medium changes every two days. Cells were expanded to T25 flasks and the concentration of puromycin was reduced to 1µg/ml.

3.11. Limiting dilution

Cells from a stable polyclonal population were counted using a haemocytometer and diluted into conditioned medium (derived from confluent U87MG cells, sterile filtered using a 0.22 µ syringe filter) plus 2mg/ml puromycin to a final concentration of 5

cells per ml. Medium used throughout isolation was supplemented with puromycin at 2mg/ml. The corner well of a 96-well plate was seeded with 1000 cells to act as a focal plane, and all other wells were seeded with 100µL of the 5 cells/ml solution. The plates were incubated for 7 days before being checked for cell growth using an inverted microscope.

Wells that contained single colonies were considered to be candidate monoclonal cell lines and expanded into wells of a 24-well plate once 80% confluency was reached. From the 24-well plate, growing cells were expanded into wells of a six well plate once 80% confluent. Before reaching confluency, cells from each well were expanded into a T25, then a T75 flask.

3.12. Preparation of mammalian cell lysates

Cells were washed with PBS, treated with trypsin for five minutes at 37°C, and complete medium was added. The cell suspension was centrifuged at 15,000 rpm for 5 minutes at room temperature to pellet cells. Cells were resuspended in PBS, centrifuged, and resuspended in RIPA buffer + protease inhibitors and left on ice for 30 minutes. The samples were centrifuged at 15000 g for 5 minutes at 4°C. The supernatant was carefully removed and stored at -80°C until further use.

3.13. Protein assay

To determine the protein concentration of samples, a BCA assay was performed. Standard protein concentration samples of 0, 0.05, 0.1, 0.2, 0.4, 0.6, 0.8 and 1 mg/ml were prepared using BSA and added in duplicate into wells of a 96 well plate. Cell lysates, prepared in RIPA as described above, were diluted 1:10 before addition in duplicate, to the wells of the 96 well plate. BCA reagent (ThermoScientific) was added to each well and the plate incubated for 30 minutes at 37°C in the dark. Absorbances were recorded at 562nm using a plate reader and used to calculate the protein concentration of each sample.

3.14. SDS PAGE

SDS-polyacrylamide gels for SDS-PAGE were cast in an Atto gel apparatus. For 12% gels the resolving and stacking gels were prepared as follows:

Table 5: SDS-PAGE gel composition.

Component	Resolving Gel	Stacking Gel
DH_2O	3.95ml	4.83ml
30% acrylamide	4.8ml	1ml
1.5M Tris HCl pH 8.8	3ml	
0.5M Tris HCl pH 6.8		2ml
10% SDS	120µL	80µL
10% APS	120µL	80µL
TEMED	12µL	8µL

The resolving gel was made first, mixed gently then poured into the gel plates. A layer of butanol was gently pipetted over the top of the gel and was left to polymerise 15-30 minutes. Once polymerised, the butanol was removed, and the stacking gel was made up and gently added on top of the resolving gel. The comb was inserted, and the gel left to polymerise for 30-45 minutes.

Once the gel had set completely, the casting stand, spacer and comb were removed, and the gel was assembled in the running tank. The chamber was filled with 1x SDS Running buffer so that both the bottom of the gel and the wells were completely submerged, taking care to remove any air bubbles.

The cell lysates were prepared by adding 4µL of SDS loading buffer to the volume of sample which contained 25-50µg protein (as measured by BCA assay) before heating at 95°C for 5 minutes. Samples were loaded alongside 6µL protein molecular mass ladder (MagiMark XP). Electrophoresis was performed at 100V for 20 minutes, until the samples had migrated through the stacking gel, then the voltage was increased to 150V for around 50 minutes to one hour, ensuring the bromophenol marker dye was close to the bottom of the gel.

3.15. Western blotting

Proteins were transferred from the gel to a PVDF membrane (Immobilion). The membrane was soaked in methanol for 5 minutes, then in Towbin transfer buffer for a further 5 minutes. Two filter pads (BioRad) were soaked in Towbin buffer for 5

minutes. The gel was removed from the tank and the glass plates and was sandwiched between the two filter pads, with the PVDF membrane on the underside. The sandwich was rolled to remove air bubbles, assembled into a semi-dry blotting apparatus and transferred at 15V for one hour using PowerPac 300 (BioRad).

The membrane was removed from the transfer apparatus and treated with blocking buffer (0.5g milk powder in 0.1% TBS-Tween 20 (TBST)) for one hour at room temperature with gentle rocking. The blocking buffer was removed, and the primary antibody at an appropriate dilution (see Table 4) in blocking buffer was added and rocked overnight at 4°C. The membrane was washed six times with 0.2% TBST for 5 minutes each time, before the secondary antibody (diluted 1:1000 in blocking buffer) was added and rocked for one hour at room temperature. The membrane was washed as before and imaged using Amersham ECL Select Western Blotting Detection Reagents (400µl of both A and B) that were pipetted onto the membrane which was sandwiched between two acetate sheets. Images were captured using a Fuji LAS-3000 after 30 seconds, one-minute or two-minute exposure times, applying fresh ECL reagents for each exposure. When analysing two different proteins, the membrane was blocked as before after imaging, followed by repeating the antibody treatment and washing steps as above.

3.16. Infection with Adenovirus

Cells were cultured on the appropriate plate until 80-90% confluent. Medium was removed and replaced with 0.5ml serum-free medium. Cells were infected with Ad5 (kindly provided by Ms Binta Bettaye, University of Leeds) at 300 virus particles per cell (vp/cell) for wtAd5 and 600vp/cell for Ad5EGFP. Cells were incubated at 37°C for one hour with regular agitation, a further 2ml of serum-free medium was added and incubated at 37°C in a humidified atmosphere containing 5% CO_2 for either one or two days.

3.17. Luciferase assay

For transfection of luciferase-gene-containing plasmids, all plasmids were diluted to around 20ng/µL. Transfection was performed as described as above with Tube B containing 4µL of Lipofectamine 2000 and 21µL of OPTIMEM per well to be transfected, and after addition of the two components, tubes were incubated at room temperature for 5 minutes. Tube A was prepared using 1µL of plasmid DNA (at 20ng/µL), 19µL of Renilla luciferase plasmid DNA (also at 20ng/µL), and 224µl OPTIMEM. After Tube B was added to tube A, the tubes were incubated at room

temperature for 20 minutes. Meanwhile, cells were washed twice with PBS. After Tubes A and B combined had been incubated, 900µl of OPTIMEM was added to each tube and the contents were added to the washed cells. Cells were incubated at 37°C for 4 hours, an additional two millilitres of serum-free medium was added and incubated for a further two days.

To measure luciferase activity, the Promega Dual Luciferase Assay system was used. In brief, the medium was removed from the cells, the monolayer washed with PBS and cells were lysed with Passive Lysis Buffer (PLB) for 15 minutes at room temperature, with rocking. Each cell sample was assayed at various dilutions- between no dilution and 1:500 dilution in PLB. Twenty microlitres of each dilution was dispensed in triplicate into wells of a white 96 well plate. A FLUOstar OPTIMA luminometer (BMG Labtech) was used to dispense 50µL each of LAR II and Stop & Glo reagents per well and to measure the resulting luciferase activity.

3.18. Statistical Analysis

For each measured sample, the mean firefly:renilla activity was calculated using 12 values recorded for each luciferase activity. For each biological repeat (composed of a set of triplicate measurements), the average mean firefly:renilla of the three triplicates was calculated, then normalised to the corresponding pGL3-basic sample or to the mock-infected value.

A two-tailed, unpaired student's t-test was used to assess the significance of any difference within the data sets, with a p-value of less than 0.05 determining differences between experimental data as statistically significant.

3.19. Immunofluorescent antibody staining

Cells were grown in the appropriate plates until approximately 70% confluent, medium was removed and cells were washed twice with cold PBS. Cells were fixed using ice-cold 100% methanol for 10 minutes, washed three times with PBS and blocked with 10% normal goat serum (NGS) for 20 minutes at room temperature. Cells were washed with PBS three times and incubated with 200µL of the appropriate antibody diluted in PBS plus 1% NGS and 0.1% Triton X-100 for one hour at room temperature, with rocking. The cells were washed three times with rocking, for 10 minutes each time, with PBS, before being incubated with 200µL Alexa Fluor-488-conjugated anti-mouse or rabbit immunoglobulin (diluted in PBS plus 1% NGS +0.1% Triton X-100) for 30 minutes at room temperature, in the dark, with rocking. Cells were washed three times with PBS, for 10 minutes each with

rocking. DAPI (200µL of a 1µg/ml stock solution) was added to the cells and incubated at room temperature, in the dark, with rocking, for 15 minutes. Cells were washed three times with PBS before being stored in PBS at 4°C in the dark. Images were obtained using an EVOS FL Auto Fluorescence Imaging System microscope (Life Technologies).

3.20. Flow Cytometry of infected cells

Cells were seeded at $0.3x10^6$ cells per well of a six well plate. Twenty-four hours post-seeding, cells were infected with Ad5EGFP at approximately 600 vp/cell, as described above. Cells were transduced at 37°C for 24 hours. After infection, medium was removed from cells, cells were washed gently with PBS and trypsinised at 37°C for 5 minutes. Cells were resuspended in serum-free medium and transferred to an Eppendorf tube. The cell suspension was centrifuged for 5 minutes at 180 x g. The supernatant was removed, and the cell pellet was resuspended in PBS. The cell suspension was recentrifuged as before, and the supernatant removed. To fix the cells, the cell pellet was resuspended in 4% PFA and incubated at room temperature for 10 minutes. The cells were centrifuged again, and the supernatant was removed. The cell pellet was then resuspended in 500µL of PBS. Samples were then analysed using flow cytometry.

Flow cytometry was performed on a Cytoflex S cytometer, using the 488-525 laser. A total of 10,000 cells were measured for fluorescence in each sample. Gates were set using mock-infected A549 cells as the negative control, whereby fluorescence detected above the background fluorescence exhibited by mock-infected A549 cells was deemed due to Ad5EGFP transduction.

4. Effect of Ad5 infection on the activity of the PTEN promoter region

Previous research by the Blair group identified a 50% decrease in steady-state levels of PTEN protein and mRNA following Ad5 infection. This decrease could be attributed to viral effects at the level of transcription of the PTEN gene, for example by reduced activity of the PTEN promoter, reduced pre-mRNA splicing or other post-transcriptional modification, or by reduced transport of PTEN mRNA from the nucleus to the cytoplasm. The PTEN promoter region has previously been identified and characterised, and contains a p53 binding region[35], which may be relevant as p53 is targeted for proteasomal degradation during Ad5 infection by the Ad5 proteins E1B55K and E4orf6[7].

To identify whether Ad5 infection results in any change to the activity of the PTEN promoter, PTEN promoter-luciferase plasmids were transfected into several human cell lines known to support Ad5 replication and luciferase assays were performed as a measure of promoter activity.

Luciferase reporter assays can be used to monitor the activity of a genetic response element of interest (such as a promoter/enhancer region) by placing a luciferase gene under its control. During the assay, the luciferase enzyme in cell-free extracts of transfected cells reacts with its substrate, luciferin, to produce bioluminescence. The luciferase genes from firefly (*Photinus pyralis*) and sea pansy (*Renilla reniformis*) are commonly used for this purpose as their properties and the luciferase enzymes produced have been well-characterised.

In dual luciferase assays, a plasmid containing the gene for Renilla luciferase under the control of a constitutively-active promoter (such as the cytomegalovirus, CMV, immediate early promoter) is co-transfected with a plasmid containing the promoter/enhancer element of interest driving firefly luciferase. Renilla luciferase acts as an internal control that monitors transfection activity, as its expression is independent of cell-type specific transcription factors. Renilla luciferase activity can therefore be used to “normalise” firefly luciferase activity by correcting for any variation due to transfection efficiency between samples. The Promega Dual Luciferase system first generates a luminescent signal from the firefly luciferase, using LAR II reagent; and subsequent addition of the “Stop and Glo” reagent both quenches this luminescence and activates the bioluminescence of the Renilla luciferase.

In these experiments, PTEN promoter regions were used extending from either -1359 to -427 base pairs upstream of the PTEN transcription start site (defined as

+1) or –2526 to -427 base pairs upstream of the transcription start site linked to firefly luciferase. These plasmids were kindly provided by Dr V. Stambolic (Amgen Research Institute and Ontario Cancer Institute, Toronto). If the PTEN promoter region is active, the firefly luciferase gene will be transcribed and translated, resulting in bioluminescence when the Stop and Glo reagent is added. The use of Renilla luciferase as a control permits comparison of transfections in different cell lines by providing a normalisation control.

Luciferase assays were performed in triplicate and the mean luciferase activity was calculated for each sample.

4.1. Initial characterisation of PTEN promoter-luciferase plasmids

The two plasmids received from V.Stambolic (Amgen Research Institute and Ontario Cancer Institute) were named PTEN full (region -2526 to -427) and PTEN short (region -1359 to -427).

Initially, the plasmids were sent for sequencing to ensure the promoter regions were accurate. A BLAST search on the sequencing results revealed a 97.06% identity of PTEN full to the PTEN RefSeqGene on chromosome 10. PTEN short showed a 99.36% identity to the same reference sequence.

The plasmids were analysed by agarose gel electrophoresis.

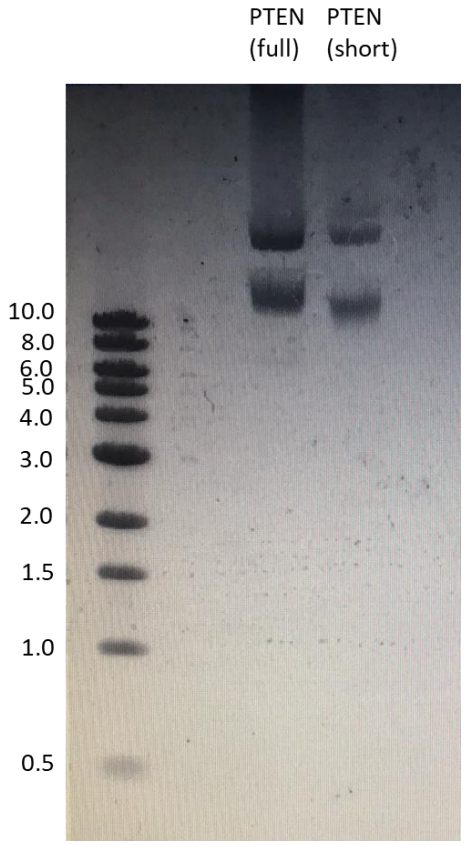

Figure 5: **Analysis of PTEN promoter plasmids by agarose gel electrophoresis**. Aliquots (containing 0.5µg DNA) were separated by electrophoresis on a 0.75% agarose gel at 100V for an hour, and the image obtained using an FLA5000 imager. SybrGreen was used to visualise DNA within the gel. Each plasmid separates into two bands on the agarose gel- the top band is likely to be linear plasmid, as it migrates more slowly through the gel, and the bottom band likely to be supercoiled plasmid, which migrates quickly through the gel[88].

Dual luciferase assays were performed following transfection of each plasmid (along with the control Renilla plasmid) in two different cell lines to identify which promoter region showed greater activity for use in subsequent experiments.

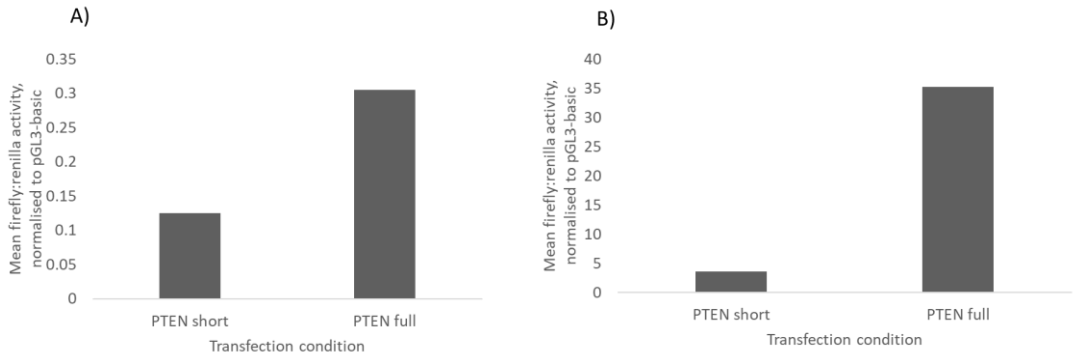

Figure 6: **Initial characterisation of the activity of PTEN promoter regions.** Dual luciferase assays were performed using lysates of cells transfected by each PTEN promoter plasmid. Mean firefly:renilla values were normalised to the luciferase activity of pGL3-basic, the negative control, in (A) 293T cells and (B) A549 cells.

As the mean firefly:renilla activity of the full PTEN promoter was significantly greater than that of the shorter variant in both cell lines, it was used in subsequent transfections. As A549 cells support Ad5 infection and also represent an epithelial cell type targeted during Ad5 infection in humans, most experiments were performed using this cell line.

4.2. The activity of the PTEN promoter in Ad5-infected A549 cells

A549 cells were transfected with the PTEN full-luciferase plasmid and Renilla luciferase, using Lipofectamine 2000 for transfection. At 24 hours post-transfection, samples were either mock infected or infected with Ad5 at 300vp/cell. 24 hours post-infection, cells were harvested using Passive Lysis Buffer (Promega) and diluted appropriately. The luciferase activity of each sample was measured in triplicate, the firefly:renilla activity for each repeat calculated, and an average taken. The mean firefly:renilla activity for each condition was then normalised to the mean firefly:renilla luciferase activity calculated for pGL3-basic, the negative control. Raw luciferase and normalised data are shown in Appendix. Results were expressed as fold change in luciferase activity with respect to mock-infected A549 cells which was set as 1. In Fig.7, 10 biological repeats of this transfection were performed. A student's t-test (n=10) was performed to identify whether any change to the PTEN promoter activity post-infection was significant. The p-value calculated was 0.922. Using $p \geq 0.05$ to identify a null hypothesis, the t-test indicates that any trend in these data is not statistically significant.

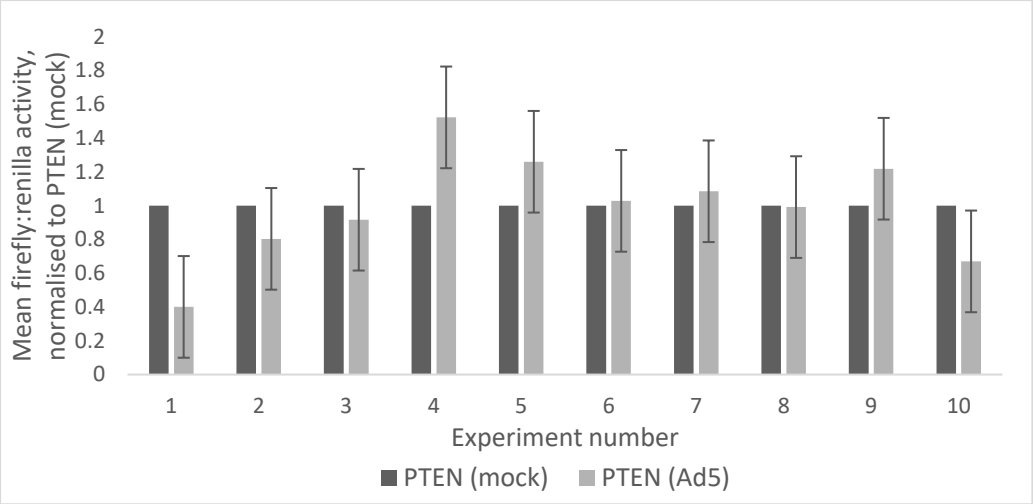

Figure 7: **Activity of the PTEN promoter in A549 cells during Ad5 infection.** Dual luciferase assays were performed in A549 cells transfected with the PTEN promoter-luciferase plasmid and Renilla luciferase followed by mock- or Ad5-infection. This basic experiment was repeated 10 times. At 24 hours post-transfection samples were either mock infected (black bars) or infected with Ad5 at 300 vp/cell (grey bars). The lysates from each biological repeat were assayed in triplicate, and the mean firefly:renilla activity calculated. The mean firefly:renilla activity was normalised to the mock infected sample in each experiment. The error bars show +/- one standard deviation calculated from the 10 repeats. The raw data and standard deviations for each experimental repetition can be found in the Appendix (Table 1).

The data shown in Fig. 7 were also analysed for percentage change in PTEN promoter activity in mock- and Ad5-infected A549 cells (Fig. 8). The majority of samples do not show a significant change in promoter activity, which is in agreement with the high p-values calculated by the student's t-test.

When comparing the percentage change in promoter activity between mock and Ad5 infected samples, it is likely that experiment 1 presents an anomalous result, as it does not fit the trend of the other 9 experiments, which all show a less pronounced % change in promoter activity.

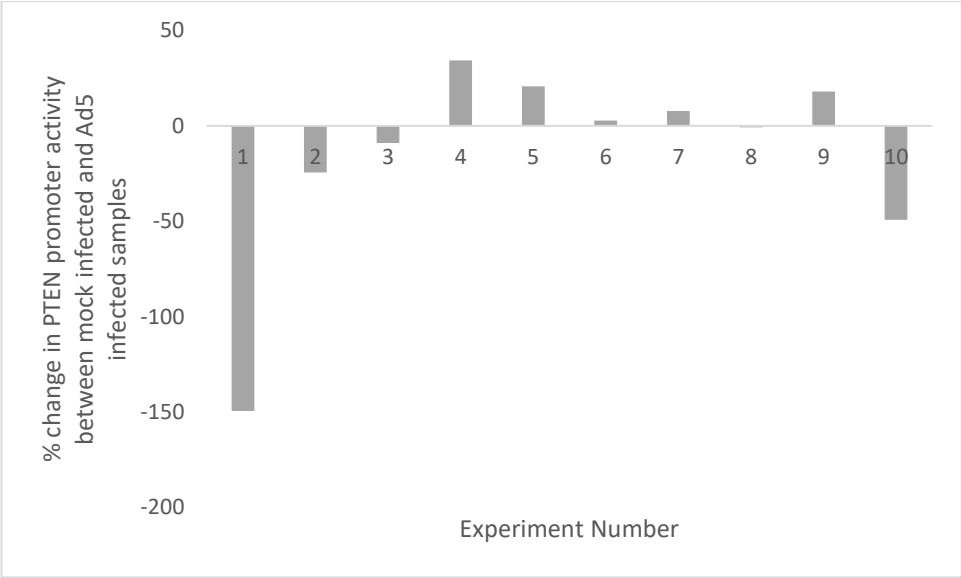

Figure 8: **PTEN promoter activity in A549 cells 24hpi is variable**. The percentage change in PTEN promoter activity 24 hours post infection was calculated for each experiment, after the mean firefly:renilla activity had been normalised to mock infected samples.

In certain experiments, lysates were also made using RIPA and protease inhibitors for use in Western blotting. Western blotting for the Ad5 protein, fibre, was analysed to demonstrate that virus replication had taken place 24 hours post-infection when samples were harvested for luciferase assays. Western blotting of the lysates was also used to monitor expression of PTEN protein in the mock and Ad5 infected transfected cell samples (Fig. 9).

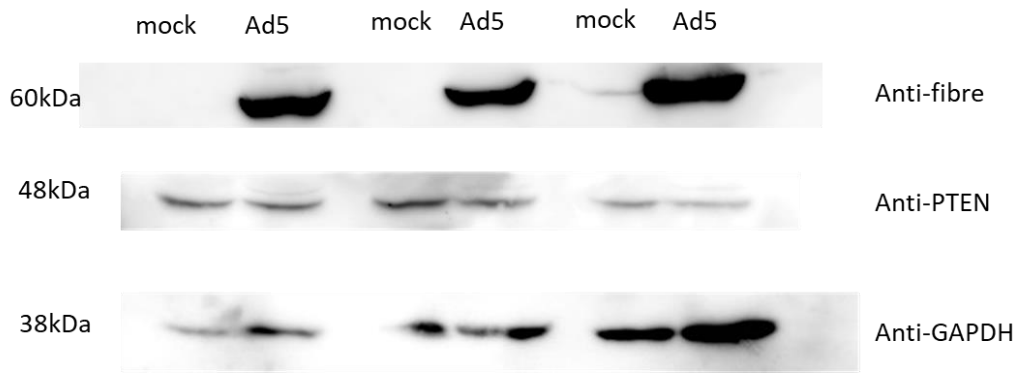

Figure 9: **Ad5 infection in three experiments of the transfection/infection experiments in A549 cells.** The presence of the late adenovirus fibre protein was detected by Western blotting of cell extracts (corresponding to 25µg of protein) prepared from mock- and Ad5-infected A549 cells, following transfection of

luciferase plasmids. A rabbit polyclonal antibody was used against fibre, at concentration indicated in Table 4. Images were captured using a LAS3000 imager.

The protein of approximately 62kDa detected with anti-fibre is a good indicator that Ad5 has entered and replicated within the cells in question. GAPDH was used as a loading control, and its presence at 38kDa in all lanes is an indicator that approximately equivalent masses of protein were analysed. As expected, PTEN was detected in all samples from transfected cells.

Since no significant differences in PTEN promoter activity were detected between A549 cells that were either mock or infected with Ad5, this raised the question of the role of p53 in PTEN transcriptional regulation in Ad infection. P53 activates transcription of PTEN by directly binding to a p53 binding site in the PTEN promoter region (at -1190 to -1157 base pairs upstream of the PTEN transcription start site)[35]. As p53 is targeted for proteasomal degradation by the Ad5 gene products E4orf6 and E1B55K during infection[7], it is perhaps surprising that no decrease in PTEN promoter activity was observed during Ad5 infection. This question was addressed further using a p53-null cell line, H1299, for transfection and Ad5 infection.

4.3. The activity of the PTEN promoter in Ad5-infected H1299 cells

Dual luciferase assays were performed in H1299 cells in the same way as performed in A549 cells. H1299 cells were co-transfected with the PTEN promoter-luciferase plasmid and CMV-immediate early promoter-Renilla luciferase plasmid. Twenty-four hours post-transfection, samples were either mock infected or infected with Ad5 at 300 vp/cell. After a further 24 hours, samples were harvested, lysed with PLB and diluted appropriately for luciferase assay. All assays were performed in triplicate, and the mean firefly:renilla luciferase activity was calculated for each experiment, then was normalised to the mean firefly:renilla luciferase activity of the mock infected sample (Fig. 10). This basic experiment was repeated 9 times.

A students' t-test was performed on all the experimental repeats (n=9), to identify whether any overall difference between the PTEN promoter activity in mock or Ad5 infected cells is statistically significant. The p-value calculated was 0.371, indicating any overall change observed in PTEN promoter activity following infection with Ad5 is not significant, using a p value of less than 0.05 to reject a null hypothesis.

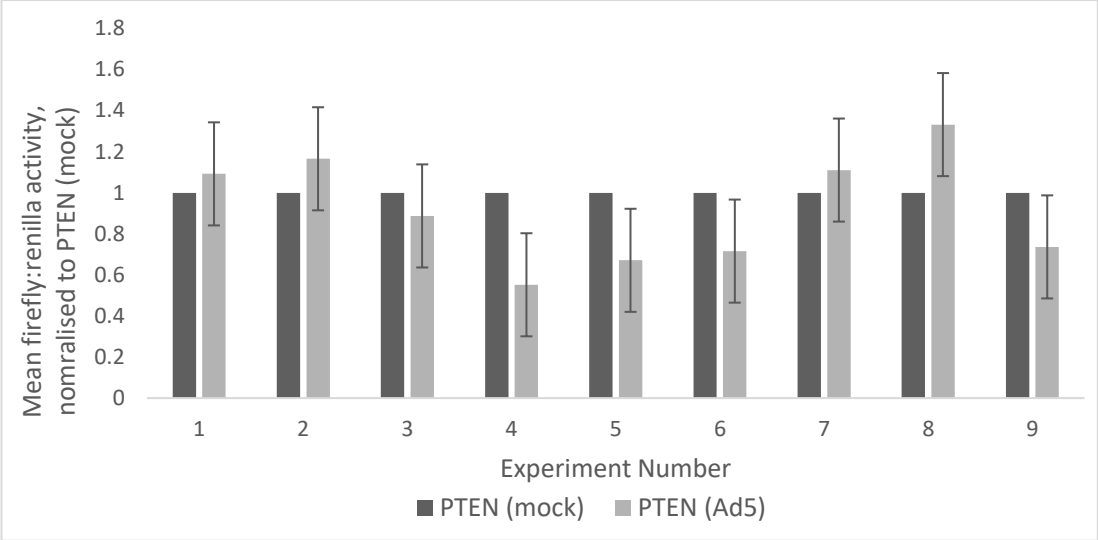

Figure 10: **PTEN promoter activity in mock and Ad5-infected H1299 cells**. H1299 cells were transfected with a firefly luciferase gene under the control of the PTEN promoter region and co-transfected with Renilla luciferase as an internal control. At 24 hours post-transfection, samples were either mock (black bars) or Ad5 infected (grey bars). Samples for luciferase assay were harvested 24hpi. The lysates from each biological repeat were assayed in triplicate, and the mean firefly:renilla activity calculated for both conditions in each experiment. The experiment was repeated on nine separate cell samples. To allow direct comparison, the values for Ad5 infected samples were normalised to the mock value. The error bars represent +/- one standard deviation calculated from the nine repeats. The standard deviation within the raw data for each repeat can be found in the Appendix (Table 2).

The data shown in Fig. 10 were also analysed for percentage change in PTEN promoter activity in mock- and Ad5-infected cells (Fig. 11).

When comparing the percentage change in promoter activity, it appears that there are two clusters of experiments. Biological repeats 1,2, 7 and 8 all show a less than 25% increase in promoter activity in Ad5-infected H1299 cells, whereas biological repeats 4, 5, 6 and 9 show marked decrease in PTEN promoter activity in Ad5-infected calls.

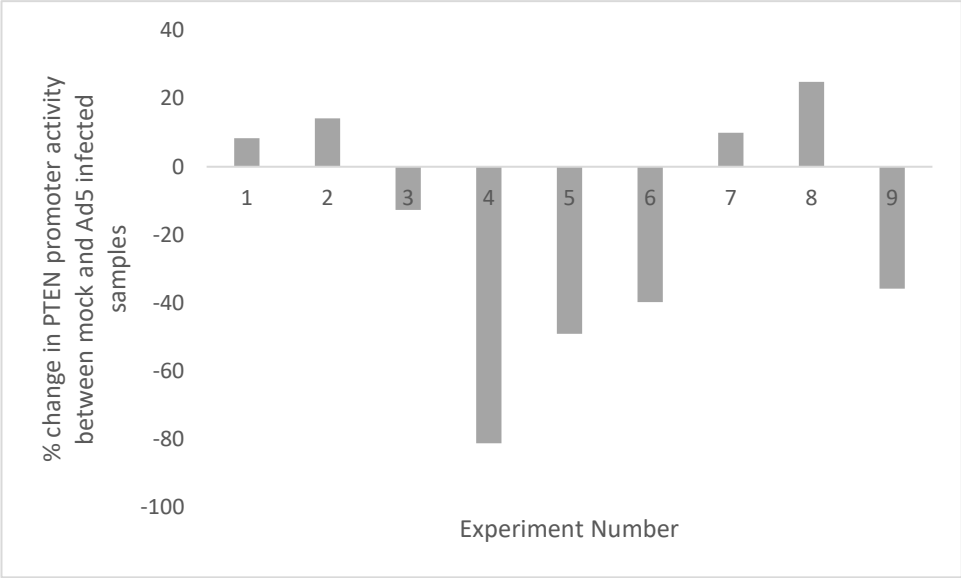

Figure 11: **The percentage change of PTEN promoter activity between Ad5 and mock infected H1299 cells was highly variable**. The percentage change was calculated from the mean renilla:firefly activity of each sample once normalised to the mock infected sample.

To confirm Ad5 replication had taken place 24 hours after infection, in certain experiments lysates were also made using RIPA + PI for Western blotting. Samples from these experiments were analysed for the presence of the late Ad5 protein, fibre. If fibre is present in the Ad5 infected samples, this is an indicator that viral replication had occurred in these samples, and therefore any changes in luciferase activity and hence PTEN promoter activity were due to Ad5 infection of H1299 cells.

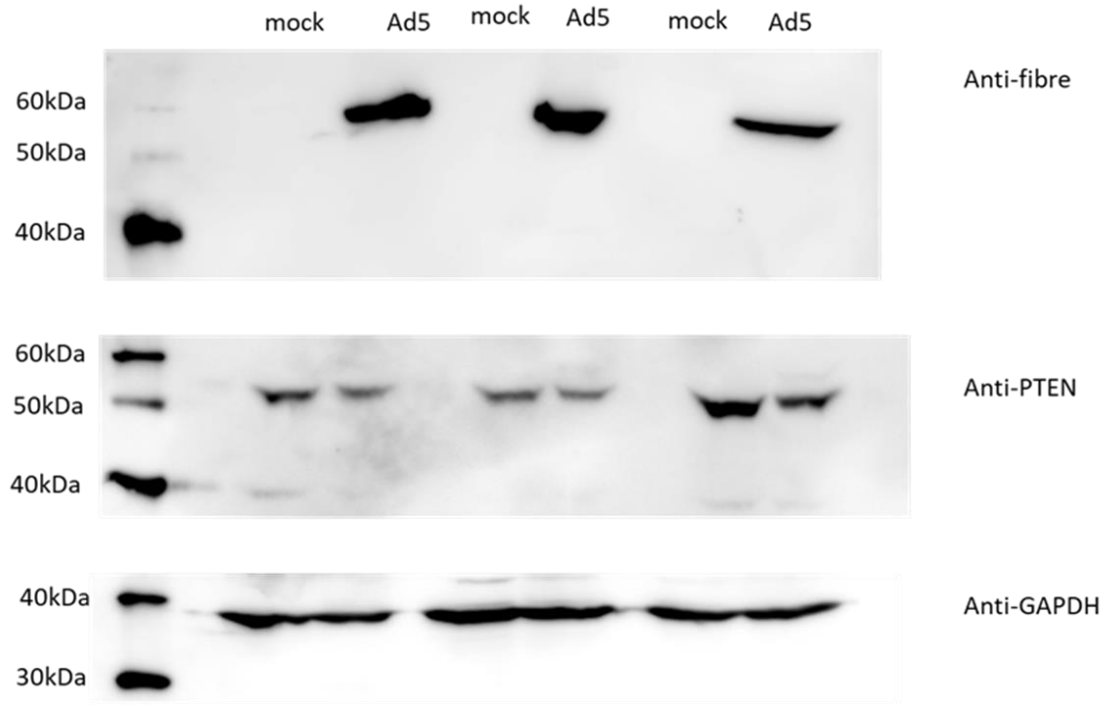

Figure 12: **Ad5 infection in three of the transfection/infection experiments in H1299 cells.** The presence of the late adenovirus fibre protein was detected by Western blotting of cell extracts prepared from mock- and Ad5-infected H1299 cells, following transfection of luciferase plasmids. The volume of lysate corresponding to 25µg of protein was loaded onto the gel, and protein was detected using a rabbit polyclonal antibody against fibre protein. Images were captured using a LAS3000, with HRP secondaries used for antibody detection.

The presence of protein at 62kDa detected with anti-fibre in all three of the wells containing post-infection lysates indicates that Ad5 replication has occurred in the cells. GAPDH (which migrated at 38kDa) was using as a loading control to ensure equivalent masses of protein were loaded in each well.

Overall, in H1299 cells, there was no significant difference in PTEN promoter activity between mock- and Ad5-infected samples. This tends to exclude p53 as a factor in regulating the PTEN promoter in Ad5 infection.

4.4. Comparison of A549 and H1299 luciferase results

To identify whether p53 status affects PTEN promoter activity during Ad5 infection, the luciferase assays results above, from a cell line with normal levels of p53 (A549) and a cell line with no expression of p53 (H1299) can be compared.

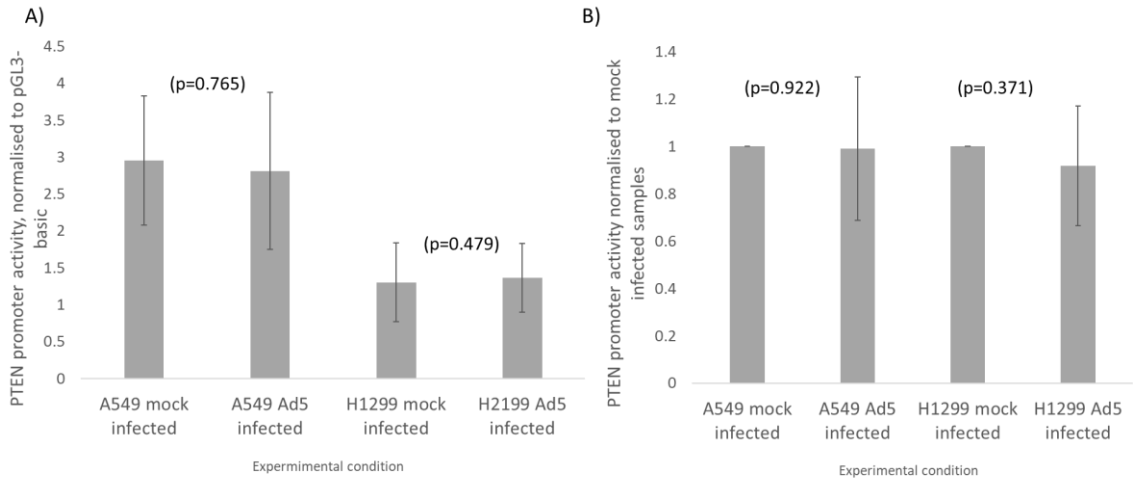

Figure 13: **PTEN promoter activity in mock- and Ad5-infected A549 and H1299 cells**. The activity of the PTEN promoter was normalised to A) pGL3-basic, the negative control, and B) mock infected samples. The PTEN promoter activity was around twice as high in A549 cells compared to H1299 (when normalised to pGL3-basic) but neither sample showed change to the PTEN promoter activity post infection. This indicates that p53 positively regulates PTEN transcription, but is not important in regulating PTEN promoter activity during Ad5 infection. As p53 upregulates the activity of the PTEN promoter, the difference in PTEN promoter activity between the two cell lines is expected, due to the p53 null status of H1299 cells. The error bars represent +/- one standard deviation for the data in each experimental condition. The p-values calculated from student's t-tests performed on each cell line are shown above the respective bars.

A students' t-test was performed to identify if any difference in activity of the PTEN promoter in Ad5 infected A549 and H1299 cells is significant (n=10 for A549, and n=9 for H1299). The p-value equalled 0.602 when comparing A549 and H1299 cells, both of which had been transfected with the PTEN promoter-luciferase construct and infected with Ad5.

Since no significant difference in PTEN promoter activity was detected post-infection in either H1299 or A549 cells, it might be informative to co-transfect H1299 with the PTEN promoter plasmid and a wild-type p53 expression plasmid to give a clearer indication as to whether p53 affects the activity of the PTEN promoter region during Ad5 infection. Such co-transfection experiment would mitigate for any differences in gene expression between cell lines that might affect PTEN promoter activity.

4.5. The effect of exogenous p53 expression on PTEN promoter activity during Ad5 infection

To identify whether p53 changes the activity of the PTEN promoter during Ad5 infection, a co-transfection/dual luciferase assay was performed in H1299 cells, which are p53 null. H1299 cells were co-transfected with same PTEN promoter/firefly luciferase plasmid as above, with either a p53-containing plasmid or a pUC19 plasmid that acted as a negative control. pUC19 was used to ensure the same mass of DNA was being transfected in each condition, without impacting the luciferase activity of the samples.

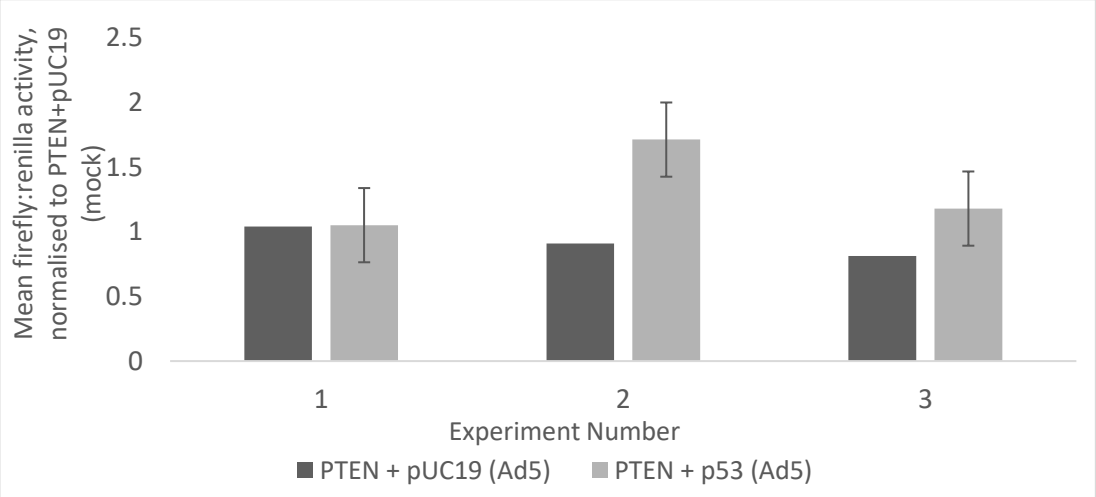

Figure 14: **PTEN promoter activity in H1299 cells co-transfected with a p53 expression plasmid or pUC19 and infected with Ad5.** The PTEN + pUC19 samples (black bars) reflect the luciferase activity in control H1299 cells infected with Ad5. PTEN promoter activity in H1299 cells co-transfected with a p53 expression plasmid followed by Ad5 infection are shown by the grey bars. H1299 cells were transfected with the same PTEN promoter-luciferase plasmid as before, as well as the Renilla luciferase plasmid. At 24 hours post-transfection, samples were either infected with Ad5 or mock infected, and after a further 24 hours, samples were harvested for luciferase assay. Assays were performed in triplicate, and the mean firefly:renilla luciferase activity calculated. Results are shown relative to the normalised luciferase activity of pUC19 co-transfected cells which is set to a value of 1. Three independent repeats of the experiment were performed. The error bars represent +/- one standard deviation calculated from the 3 independent experiments.

In one of the three experiments, restoration of p53 expression appeared to increase PTEN promoter activity in Ad5-infected cells. The remaining experiments showed very little difference in PTEN promoter expression between the H1299 sample and the p53-transfected H1299 sample. This could be due to inefficient transfection of p53, or Ad5 replication not being successful.

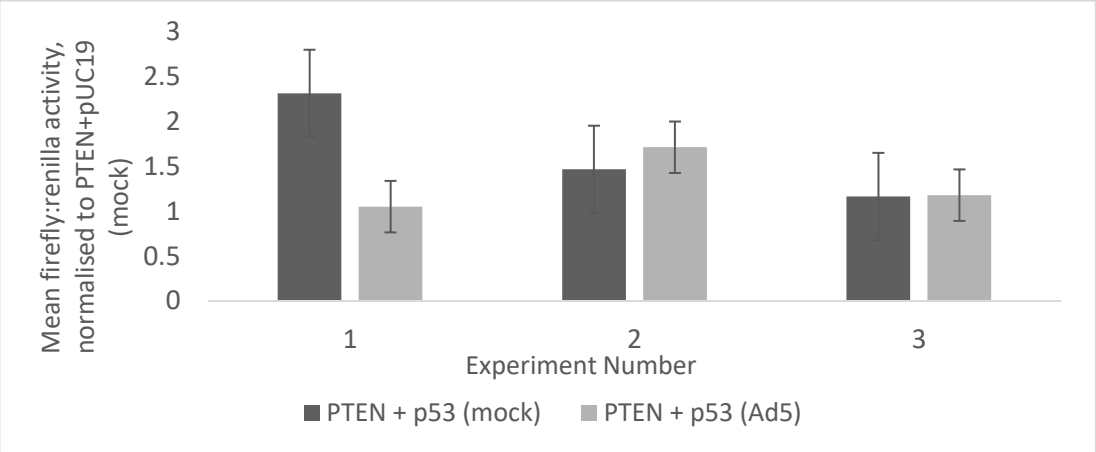

Figure 15: **Comparing change to the activity of the PTEN promoter post infection, dependent on the presence of p53.** H1299 cells were transfected with the firefly luciferase gene under the control of the PTEN promoter region, which contains a p53 binding site. Samples were either co-transfected with p53 or pUC-19 as a control, and infected or mock infected with Ad5. 24 hours post infection, cells were harvested, and the activity of the luciferase genes was measured. Transfection with RSV or pGL3-basic were used as the positive and negative controls, respectively. The error bars represent +/- one standard deviation of the data shown on the graph.

In these experiments, Western blotting could not be used to detect a marker of Ad5 infection or p53 expression.

It was therefore decided to use cell lines in which there was targeted disruption of p53, and compare the luciferase activity in these cell lines following PTEN promoter-luciferase transfection and mock or Ad5 infection.

4.6. Further analysis of the effect of p53 on the activity of the PTEN promoter region during Ad5 replication

HCT116+/+ is a cell line with normal expression of p53, for which a p53 knockout is available, termed HCT116-/- [88]. Using cell lines where the only difference is the p53 status enables the luciferase activity experiment to define the role of p53 in PTEN promoter activity during Ad5 infection.

Transfection and infection were performed as above, with three independent experiments in each cell line used. Twenty-four hours after transfection, cells were either infected with Ad5 at 300 vp/cell, or mock infected. After a further 24 hours, cells were harvested with Passive Lysis Buffer, and the luciferase assay performed on the lysates. Each experiment was analysed in triplicate, and a mean value for firefly:renilla activity calculated from the triplicate repeats.

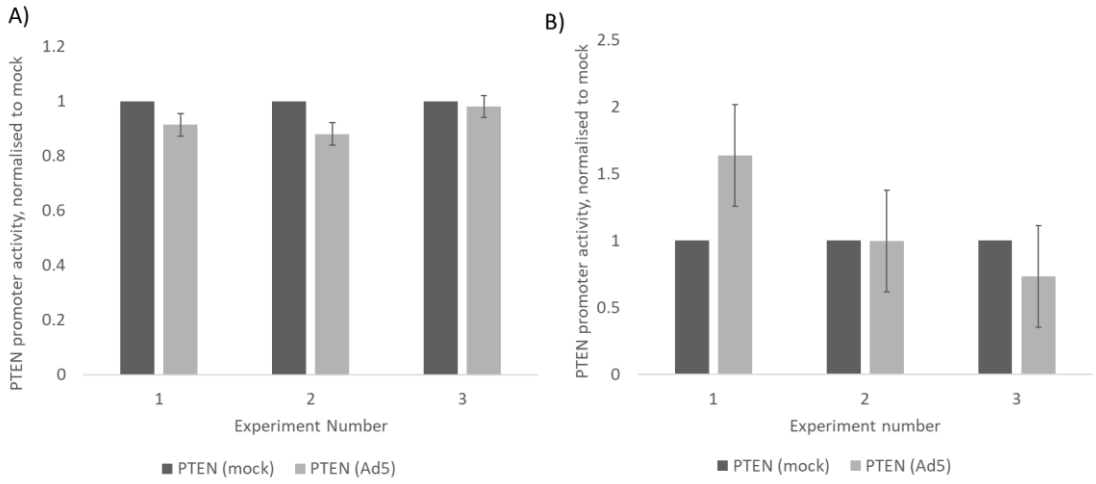

Figure 16: **Activity of the PTEN promoter region in mock- or Ad5-infected HCT116+/+ and HCT116-/- cells**. Dual luciferase assays were performed on A) HCT116+/+ and B) HCT116 -/- cells transfected with a plasmid containing the firefly luciferase gene under the control of the PTEN promoter region. Renilla luciferase was co-transfected as an internal control. At 24 hours post-transfection, cells were either mock infected or infected with Ad5 at 300vp/cell. A further 24 hours later, cell lysates were harvested. The error bars represent +/- one standard deviation of the data shown on the graph.

A students' t-test was performed on the three experimental repeats (n=3), after normalisation to mock infected samples, and p= 0.06 for HCT116 +/+ cells. Although this p-value is closer to the 0.05 value indicating statistical significance, it is still too high to give confidence that differences in PTEN promoter activity shown in these data (Fig. 16) are significant. The p-value for the t-test (n=3) carried out on the

HCT116-/- samples was 0.68, further confirming that any difference in PTEN promoter activity was not statistically significant within this cell line.

4.7. Comparing PTEN promoter activity in HCT116+/+ and HCT116-/- cells

The activity of the PTEN promoter in both HCT116+/+ and HCT116-/- was compared to identify whether the p53 status of the cells affected PTEN promoter activity in Ad5 infected samples.

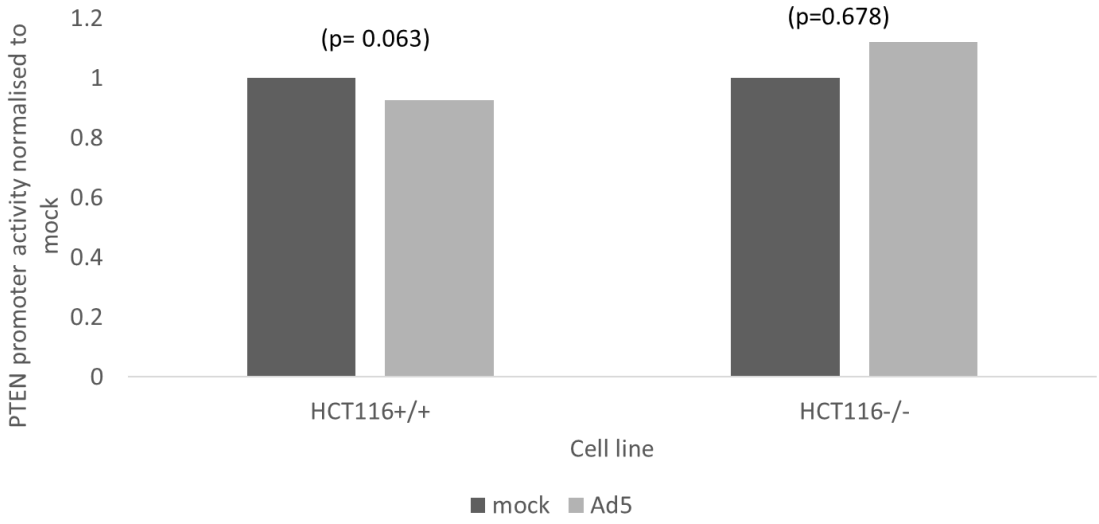

Figure 17: **PTEN promoter activity in either mock- or Ad5-infected HCT116+/+ and HCT116-/- cells.** Cells were transfected with the PTEN promoter-luciferase constructs and a Renilla plasmid. After 24 hours, cells were either mock infected or infected with Ad5 at 300vp/cell. A further 24 hours later, cells were detached and lysed with PLB. Dual luciferase assays were performed in triplicate on the cell lysates, and the mean firefly:renilla activity for each sample calculated. This basic experiment was repeated three times for each cell, and the average of the mean firefly:renilla activity calculated and normalised to the mock value.

A students t-test was performed to compare the significance of any difference in PTEN promoter activity in Ad5-infected HCT116+/+ and HCT116-/- cells (Fig. 17). The calculated p-value was 0.510, indicating that any difference in PTEN promoter activity between the two infected cell lines is not significant.

4.8. Collating all luciferase results

The results of the luciferase experiments in each cell line were collated into a table for easy comparison. The p53 status of each cell line or experimental condition has been noted, along with the p-value calculated by a student's t-test on the biological repeats performed in each cell line. None of the cell lines show significant difference between the luciferase activity in mock and Ad5 infected cells, indicating that the p53 status of the cell line does not impact the activity of the PTEN promoter during Ad5 infection.

Table 6: The luciferase activity of all cell lines used for assays. The values given are the mean of the biological repeats of each cell line for each condition, all normalised to the mock value in each cell line. The p-value was calculated using a student's t-test. For A549, n=10, for H1299 n=9, and for H1299+p53, HCT116+/+ and HCT116-/-, n=3.

		Luciferase activity		
Cell line	p53 status	mock	Ad5	p-value
A549	+	1	0.990061	0.922
H1299	-	1	0.91808	0.371
H1299+p53	+	1	0.797343	0.45
HCT116+/+	+	1	0.924987	0.063
HCT116 -/-	-	1	1.119975	0.678

5. Construction and molecular characterisation of PTEN-expressing U87MG cell lines

5.1. Production of a PTEN-retrovirus and transduction of U87MG cells

The retroviral transduction method of establishing stable transgene expression exploits the ability of a retrovirus to integrate its genetic material into the host cell DNA. Phoenix Ampho cells produce the retrovirus proteins derived from the gag, pol and env genes. However, Phoenix Ampho cells are unable to package RNA into viable retroviruses due to mutation of the packaging signals in the retroviral genome. By transfecting the Phoenix Ampho cells with a pBABE plasmid containing a gene of interest flanked by wild-type packaging signals and a selectable marker, this gene is incorporated into the retrovirus which, on subsequent transduction of human cells, is reverse transcribed and integrated into the cellular genome. The selectable marker permits selection of stably integrated retroviral genomes.

The plasmid was analysed by electrophoresis on an agarose gel to confirm the presence of plasmid DNA. This confirmed the presence of plasmid DNA in the midi-prep. The PTEN insert in the pBABE plasmid was sent for sequencing by GeneWiz and analysis of the sequencing results showed a greater than 99% percentage identity with various retroviral vectors, and a 100% identity to PTEN mRNA sequences, as shown using NCBI BLAST.

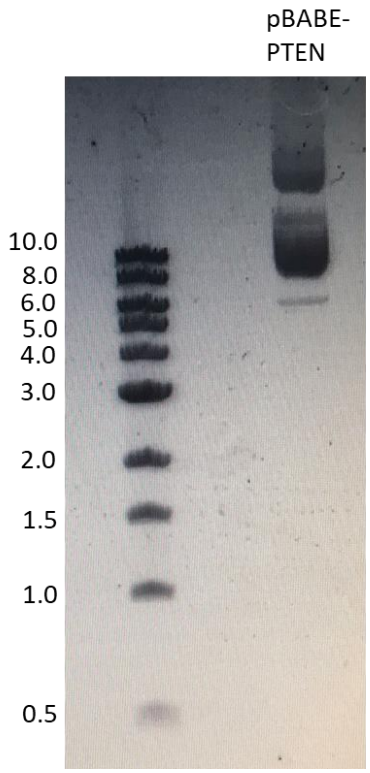

Figure 18: **Analysis of the pBABE-PTEN plasmid by agarose gel electrophoresis**. Plasmid (0.5µg) was separated by electrophoresis on a 0.75% agarose gel at 100V for an hour, then visualised using an FLA5000 imager. SybrGreen was added to the gel to enable visualisation of the DNA. The expected size of the plasmid was around 6300 bp. There are 3 bands present on the gel, due to the different migration rates of different plasmid conformations. The highest band on the gel is likely to be nicked, open circular plasmid, which migrates slowly. The middle band at approximately 8kDa is most likely linear plasmid, and the lowest band may be supercoiled plasmid, which migrates the fastest through the gel[88].

The pBABE-PTEN plasmid was transfected into Phoenix Ampho cells using Lipofectamine 2000, and the resulting virus harvested. This virus was used to transduce U87MG cells. Puromycin resistance was used as the selectable marker, and after transduction, cells were maintained in puromycin-containing medium.

5.2. Detection of PTEN in transduced cells

After U87MG cells were transduced with the PTEN gene by retroviral transduction, the pool of infected cells was analysed for presence of the PTEN protein by Western blotting.

It had previously been established that U87MG is PTEN-null and, as expected, no band was present at 57kDa in the Western blot with anti-PTEN antibody that could correspond to PTEN. A549 cells express normal PTEN and a 57kDa protein was detected by Western blotting with anti-PTEN. The band in the lane corresponding to a sample of the U87MG cells transduced with the PTEN retrovirus (U87MG/PTEN) is a good indication that the retroviral transduction performed as described in Methods was successful, and the pool of U87MG cells expressed PTEN at a level similar to that of A549 cells.

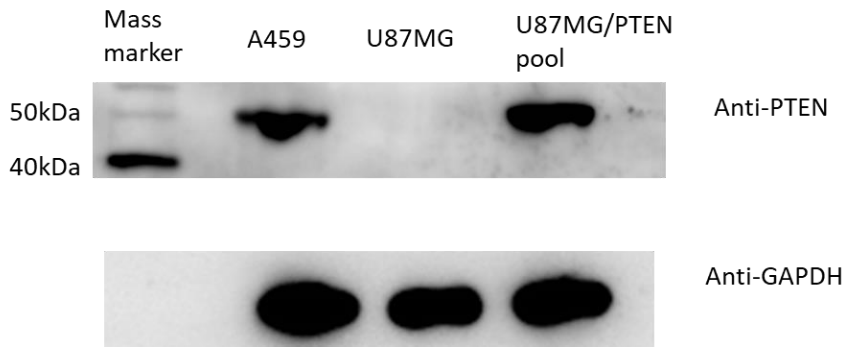

Figure 19: **PTEN expression in U87MG, A549 and the transfected U87MG pool.**

To compare levels of PTEN protein in the PTEN-transduced U87MG pool, a Western blot was performed on the volume of lysate corresponding to 25µg of protein in U87MG, A549 and the pooled U87MG/PTEN cells, using an anti-PTEN antibody (Cell Signalling Technology) (Fig. 19). Detection of GAPDH served as a loading control, to ensure equivalent masses of protein were loaded in each sample.

To isolate clonal populations of PTEN-expressing U87MG cells, limiting dilution was performed, and the resulting populations expanded into wells of 6-well plates. Clones were named after the well of the 6-well plate from which they were taken (A1 through 6 and B1 through 6). Levels of PTEN between the clones was variable and was quantified by normalising to the level of GAPDH present in the sample. The clones with the most similar level of PTEN to A549 were considered for further analysis to confirm monoclonality.

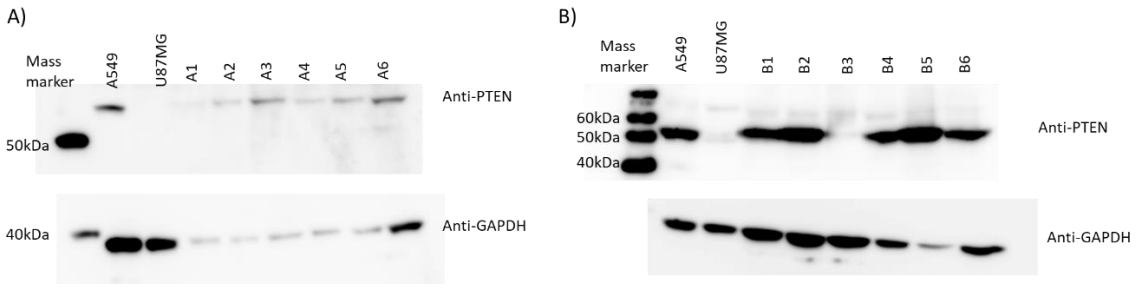

Figure 20: **Levels of PTEN protein in U87MG/PTEN clones**. Cell lysates were harvested, and protein content resolved by SDS-PAGE. Once transferred to a PVDF membrane, lysates were tested using anti-PTEN (1:1000, Cell Signalling Technology) and anti-GAPDH (1:1000) with the corresponding HRP secondary to allow imaging.

25µg of protein per sample as calculated by BCA assay was loaded onto the gel. Blotting with anti-GAPDH as a loading control illustrated that more protein was loaded for A549, U87MG and U87MG/PTEN A6 than the other “A” clones. Loading of the U87MG/PTEN “B” clones was fairly even, save for clone B5. Densitometry analysis was performed on each sample, with the PTEN band isolated using Fujifilm Multi-Gauge software and normalised to the isolated GAPDH band for each sample (Tables 7 and 8).

Table 7: **Comparing PTEN protein levels in U87MG/PTEN "A" clones with A549**.

Cell Line	PTEN/GAPDH signal compared to A549	Ranking PTEN similarity to A549
U87MG/PTEN A1	0.20	2
U87MG/PTEN A2	0.36	4
U87MG/PTEN A3	0.51	6
U87MG/PTEN A4	0.34	3
U87MG/PTEN A5	0.38	5
U87MG/PTEN A6	0.14	1

Table 8: **Comparing PTEN protein levels in U87MG/PTEN "B" clones with A549**.

Cell Line	PTEN/GAPDH signal compared to A549	Ranking PTEN similarity to A549
U87MG/PTEN B1	0.15	4
U87MG/PTEN B2	0.22	5
U87MG/PTEN B3	0.66	6
U87MG/PTEN B4	0.14	3
U87MG/PTEN B5	-0.009	1
U87MG/PTEN B6	0.02	2

PTEN-expressing U87MG clones were carried forward for further analysis based on the similarity of PTEN protein levels when compared to A549. U87MG/PTEN B5 was discounted as the level of PTEN was lower than that of A549. Clones B6, B4 and B1 were carried forward for immunofluorescence.

Immunofluorescence analysis enables the proportion of PTEN-expressing cells within each cell line to be estimated and gives an indication of the localisation of PTEN within the cells.

5.3. Immunofluorescence analysis of PTEN in A549 and U87MG

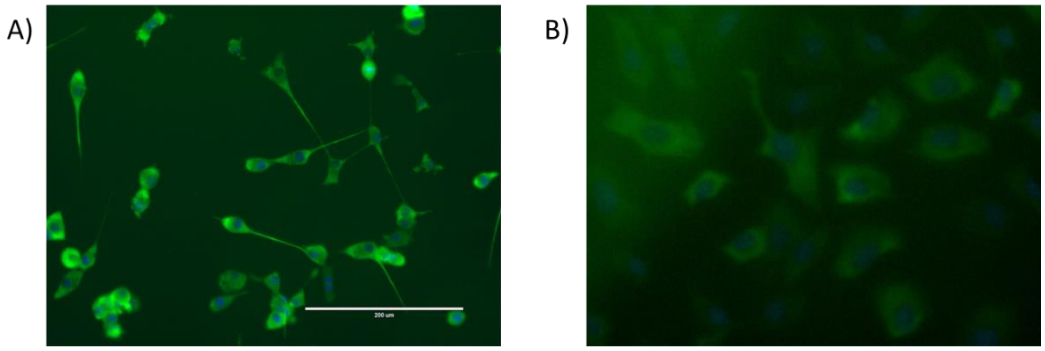

Figure 21: **Initial immunofluorescence of U87MG and A549 cells for anti-PTEN**. A) U87MG cells and B) A549 cells were fixed with methanol and stained for PTEN, then imaged using an EVOS microscope at a 20x magnification. Nuclei were stained with DAPI, shown in blue. Immunofluorescent antibody staining was performed using a mouse monoclonal anti-PTEN (SantaCruz) at 1:100 dilution, with secondary AlexaFluor-488-labelled goat anti-mouse at 1:1000 dilution.

This experiment identified an issue with the antibodies used. As U87MG is a PTEN-null cell line, there should have been no green fluorescence present corresponding to PTEN. However, as seen in the images above, the U87MG cells were fluorescing green to a degree not explained by background fluorescence. The levels of fluorescence present meant estimating the proportion of the U87MG/PTEN populations expressing PTEN was not possible.

5.4. Characterising the Santa Cruz and Cell Signalling Technology anti-PTEN Antibodies

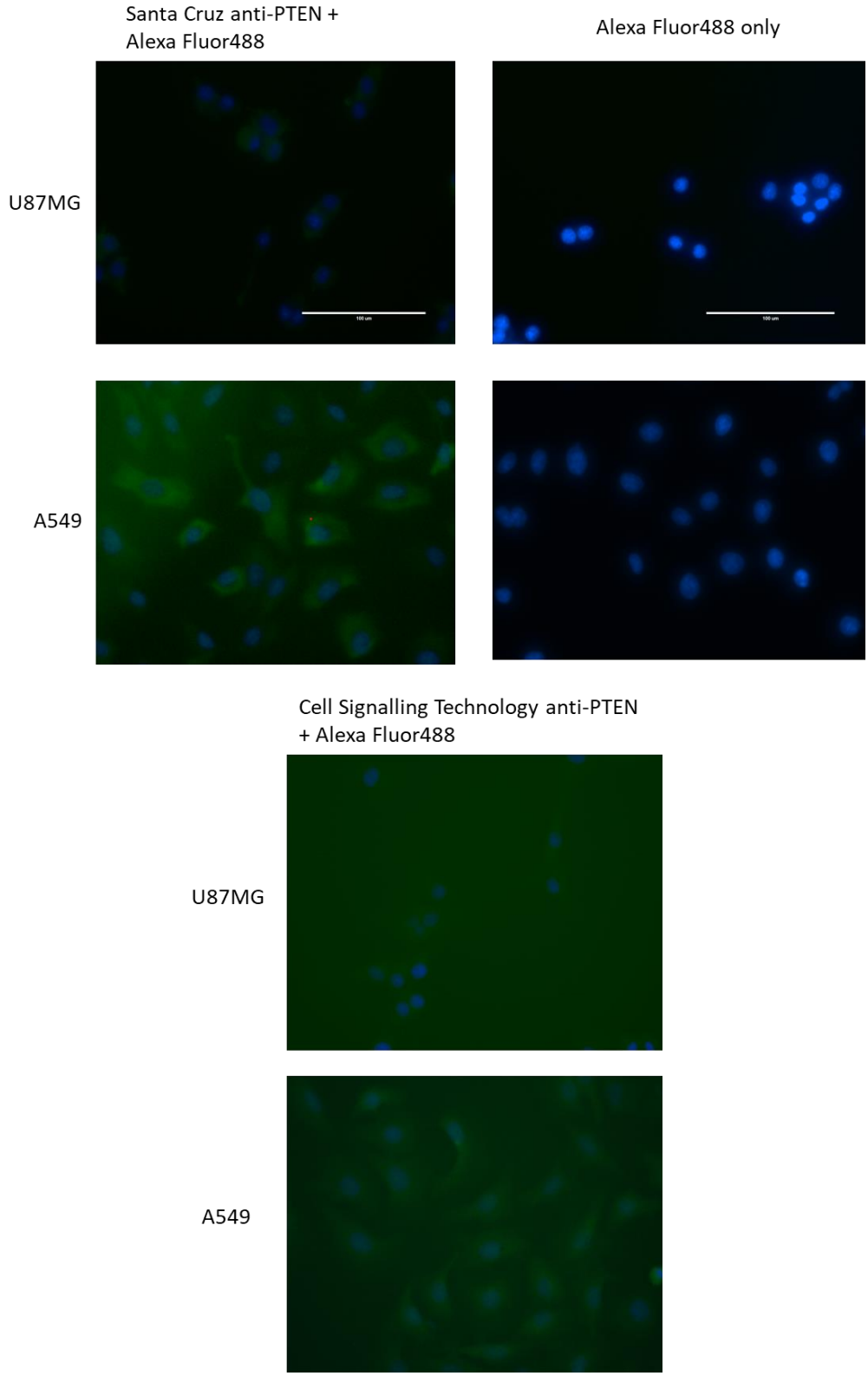

Figure 22: **Immunofluorescence of PTEN in A549 and U87MG cells to compare the Santa Cruz PTEN antibody with the Cell Signalling anti-PTEN.**

As established previously, the Cell Signalling (CST) anti-PTEN antibody shows one clear band at approximately 47kDa in A549 cells on a Western blot. To identify if the Santa Cruz (SC) PTEN antibody forms non-specific interactions in any of the cell lines used for IF, a Western blot was performed on the cell lysates using Santa Cruz anti-PTEN.

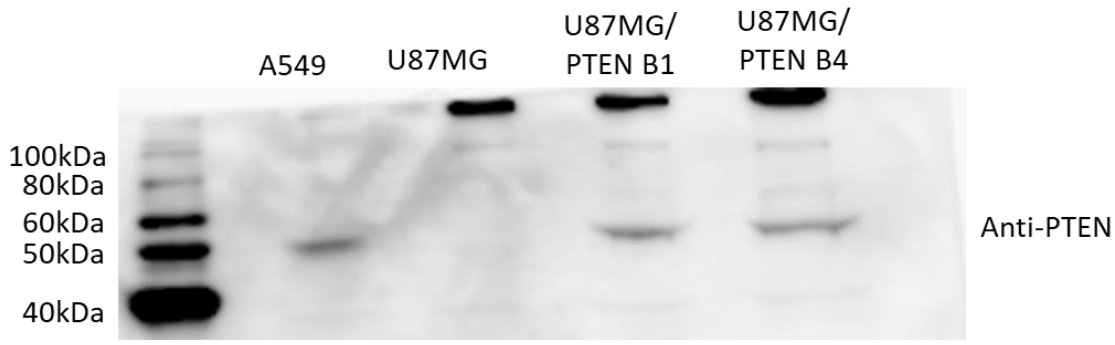

Figure 23: **Western blot analysis of the Santa Cruz anti-PTEN antibody**.

The Western blot shown in Figure 23 revealed additional bands in U87MG and PTEN-expressing U87MG cell lysates, but not in A549. As the additional bands were located at the very top of the gel, it is difficult to identify whether said bands were an artefact or non-specific binding that might cause the fluorescence in U87MG cells noted in Figure 23.

As these higher molecular mass bands were more intense than the band at the expected molecular mass of PTEN, it is important to ascertain what they represent. A 10% acrylamide gel followed by Western blotting was therefore performed on the samples to give greater clarity to what these bands may have been.

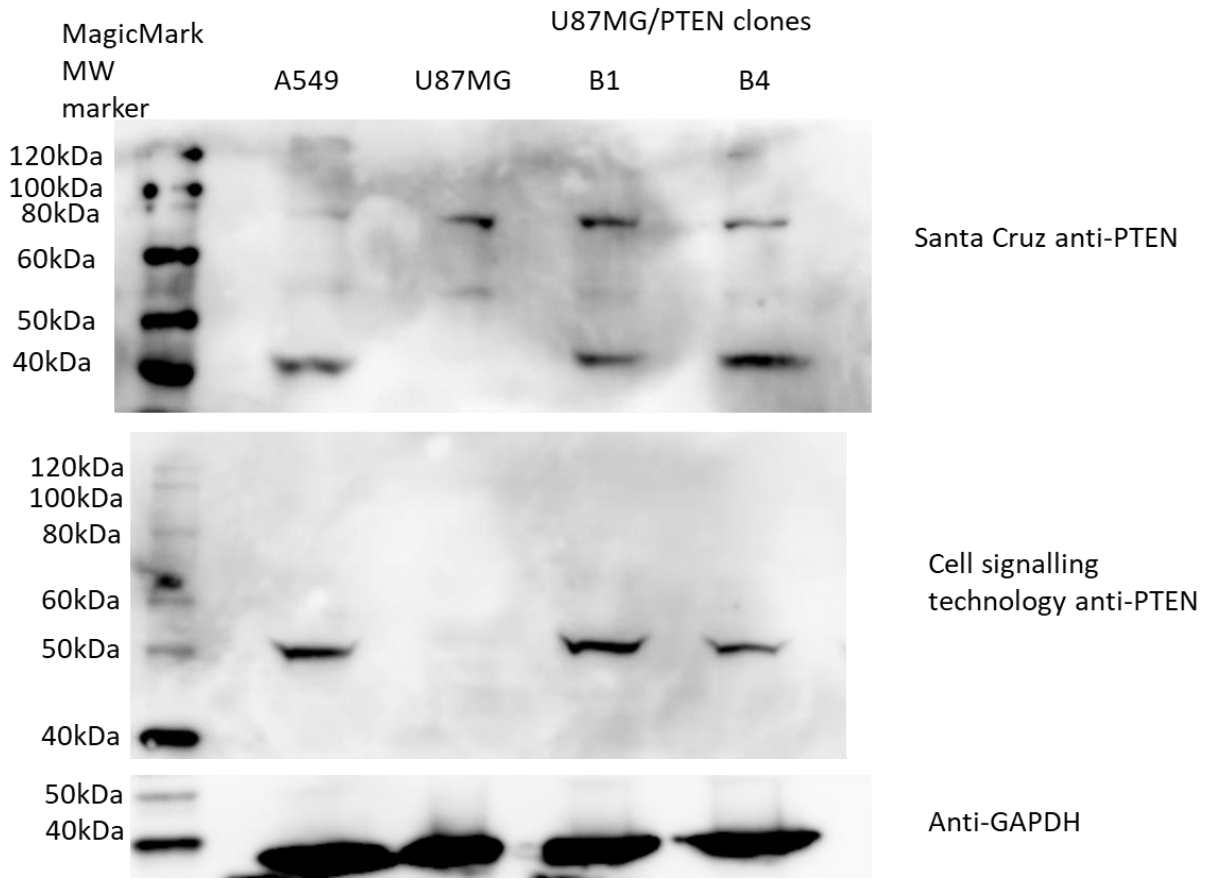

Figure 24: **Further comparison of the Santa Cruz and Cell Signalling Technology antibodies by Western blotting following electrophoresis in a 10% acrylamide gel.**

The higher molecular mass bands detected in U87MG and PTEN-expressing U87MG cell lines with the Santa Cruz PTEN antibody migrated into the 10% gel. This indicates that the bands in the blot shown in Figure 23 are not artefacts but may, instead, be a result of interactions of the antibody with an unidentified protein within the U87MG and U87MG-derived cell lines. These bands were not detected when the CST anti-PTEN was used, and therefore may represent non-specific binding of the Santa Cruz antibody to other proteins in U87MG cells.

Alternatively, these additional proteins may be caused by the Santa Cruz antibody binding to PTEN-long, another epitope of PTEN present in certain human cell lines. This protein species was notably absent from A459 cell lysates.

5.5. Immunofluorescence of U87MG/PTEN clones for PTEN protein

To visualise the proportion of each cell population that was expressing PTEN, immunofluorescent staining of PTEN was performed, with DAPI used to locate the nucleus of each cell. Immunofluorescence also gave an indication of the localisation of PTEN within the cell.

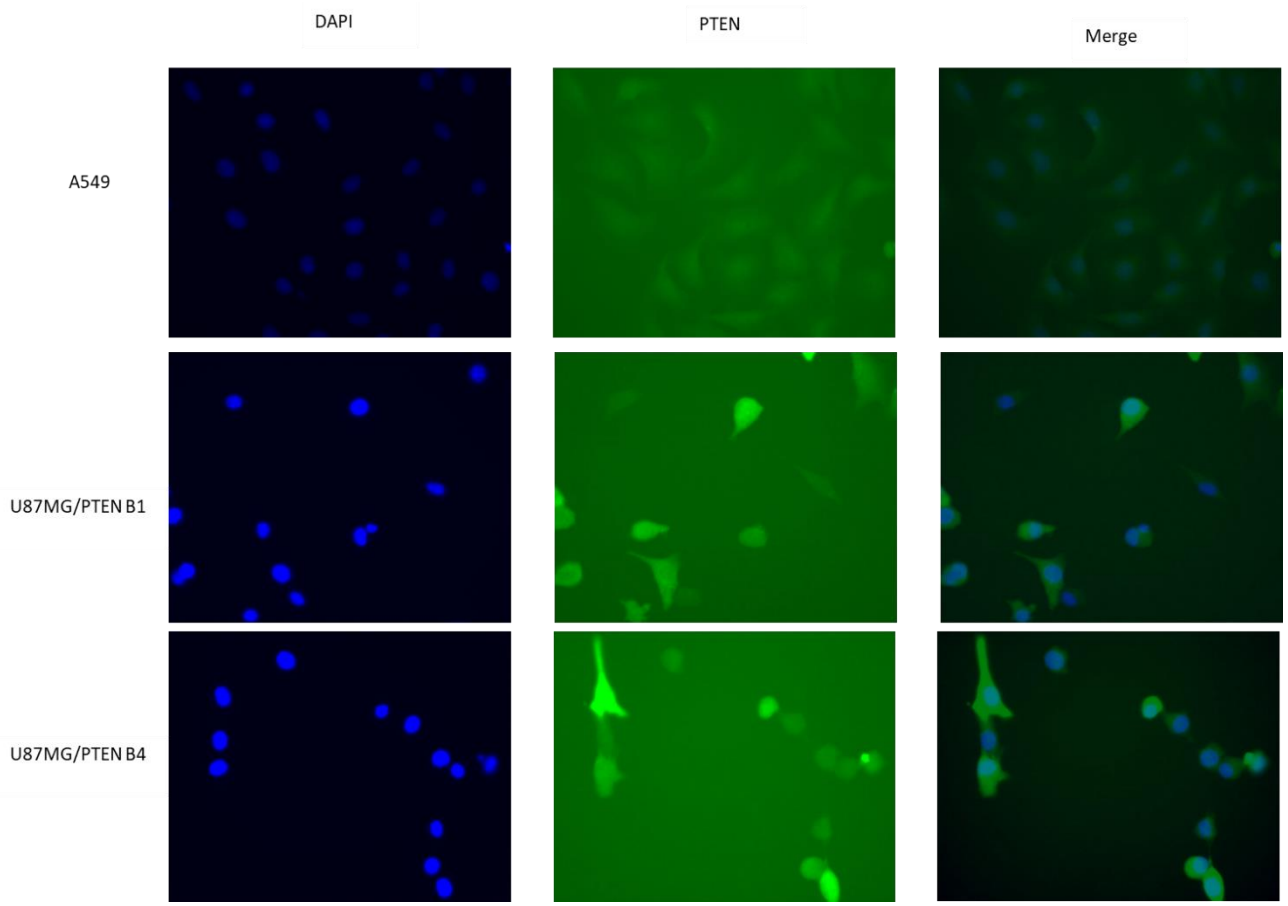

Figure 25: **Characterisation of PTEN protein expression in U87MG/PTEN clones**. Cells were fixed with methanol, and immunofluorescence analysis performed using CST anti-PTEN at 1:100 dilution with secondary AlexaFluor-488-labelled goat anti-rabbit at 1:1000 dilution as the secondary. Images were captured using an EVOS microscope at a 20x magnification.

The number of PTEN-expressing cells within each population was counted from around 100 cells per clone. U87MG/PTEN B1 was expressing PTEN to the same degree as A549 (or higher) in 77% of cells, and U87MG/PTEN B4 expressed PTEN to the same degree as A549 (or higher) in 70% of cells.

5.6. Infection of PTEN-expressing U87MG cells.

Given that Ad5 is unable to replicate efficiently in U87MG yet replicates in A549 -a cell line with normal PTEN- it is of interest to elucidate whether restoring PTEN protein to U87MG cells will restore the ability of Ad5 to replicate.

Once the presence of PTEN in the transduced clones was confirmed, the clones B1, B4 and B6 were infected with Ad5, alongside U87MG and A549 as negative and positive controls for PTEN, respectively. Western blotting was performed on infected cell lysates to identify the level of viral protein produced, with immunofluorescence also being employed to visualise the cellular localisation of the viral proteins.

5.6.1. Detecting viral protein in infected cells

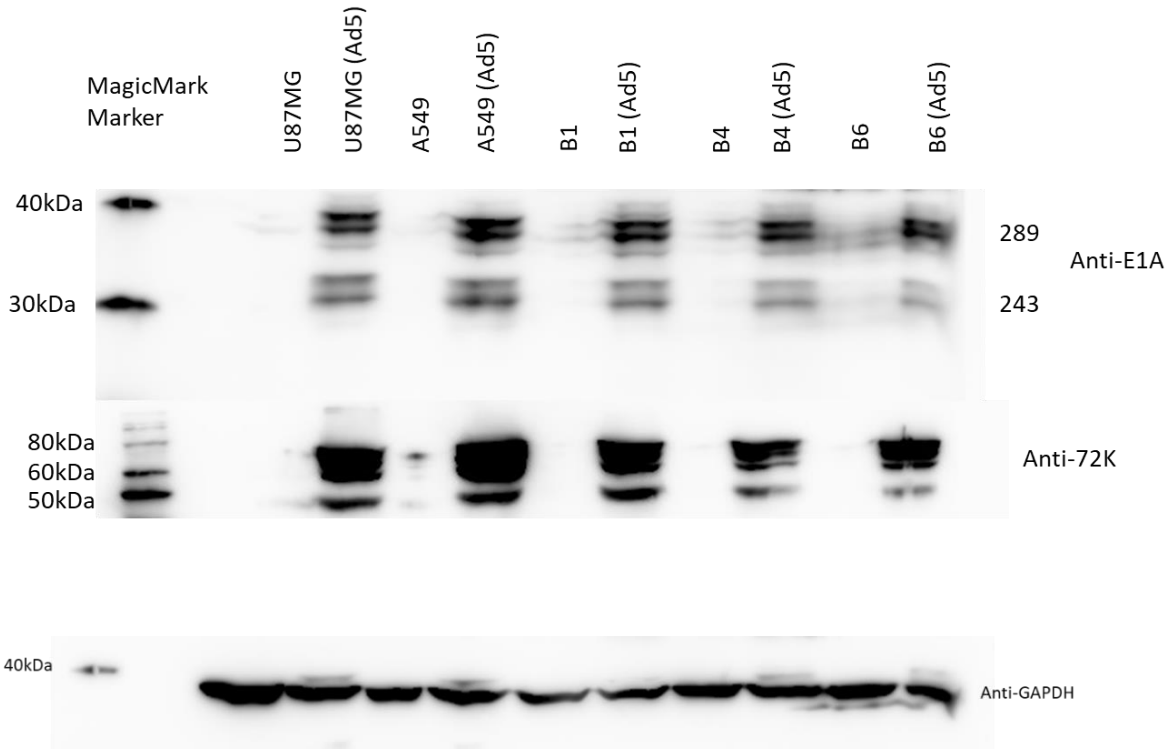

Figure 26: **Expression of early viral proteins in mock and Ad5 infected cells**. Samples were probed using anti-E1A (1:1000) and anti-72K (1:5000) and their respective HRP antibodies. The two groups of bands in the E1A blot are representative of the multiple phosphorylated protein species encoded by E1A, of 243 and 289 amino acids. The two bands in each division are representative of phosphorylated derivatives of the E1A proteins. The second early virus protein detected is the 72K DNA binding protein, which is detected at the expected 72kDa in all infected samples. Anti-GAPDH (1:10000) was used as a loading control, with 25µg of protein being loaded per sample.

In conjunction with the early viral proteins, the samples were also tested for the presence of late viral proteins.

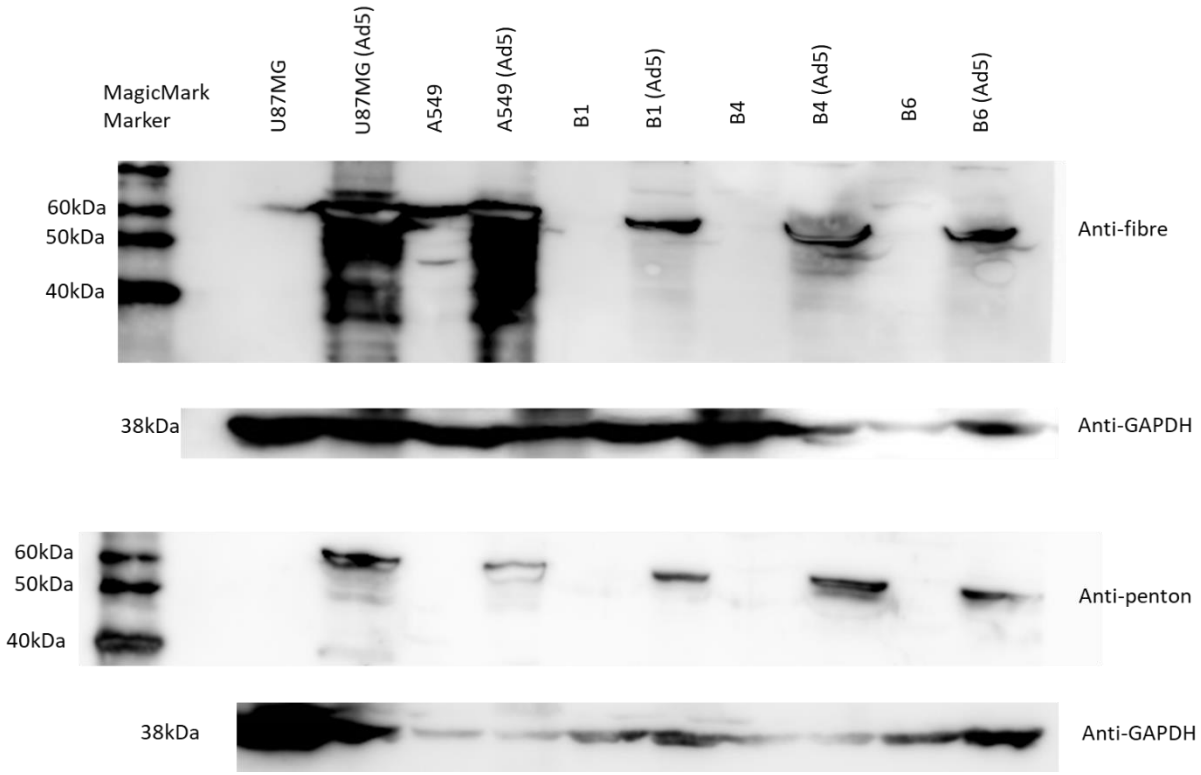

Figure 27: **Expression of the late viral proteins-fibre and penton-in Ad5 infected cells.** Owing to the large quantities of viral protein present, the amount of protein loaded onto the gel was decreased to 10µg per sample. Cell lysates were tested using rabbit anti-fibre (1:2000) and rabbit anti-penton base (1:1000), with rabbit anti-HRP used as the secondary antibody. Protein was imaged using a LAS3000 imager.

Protein bands at around 62kDa are present in infected samples when blotting with anti-fibre, with a lesser amount present in the infected U87MG/PTEN clones. The density of the protein bands in infected lysates at around 63kDa when blotting for anti-penton base are consistent in all samples.

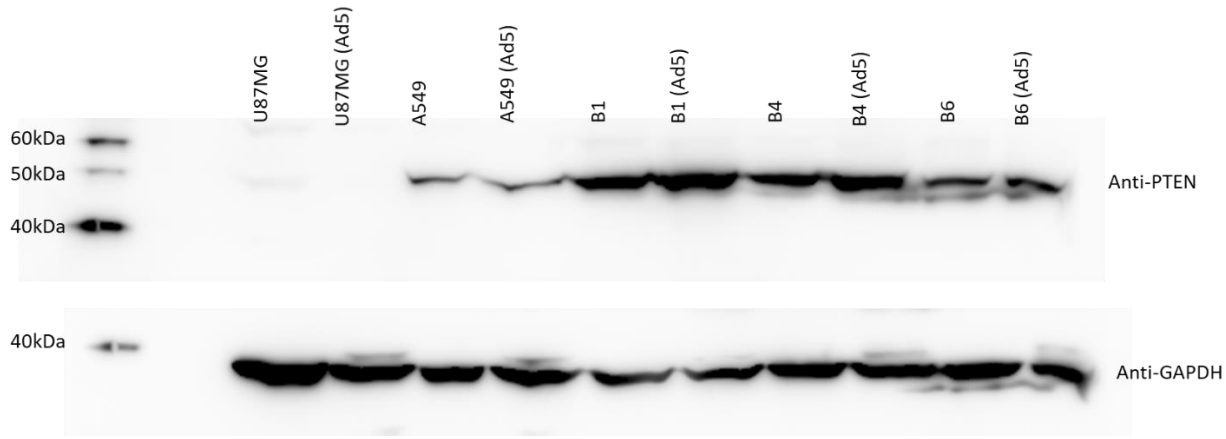

Figure 28: **Expression of PTEN in mock and infected cells**. The presence of PTEN was also tested for in mock and infected cells, to identify whether the 50% decrease in PTEN protein following infection observed by previous members of the Blair group also occurs in the PTEN-expressing U87MG cell lines.

Densitometry analysis of these blots was performed using FujiFilm Multi-Gauge software. The bands for each viral protein were isolated and normalised to the respective GAPDH band for each sample.

Table 9: **Densitometry analysis of protein levels in infected cell lines**. Cells were infected with virus at 300vp/cell, then harvested 24 hours post infection. Bands were isolated using FujiFilm MultiGuage software and normalised to the density of the corresponding GAPDH band.

	Viral protein normalised to GAPDH					
Cell line	E1A 243	E1A 289	72K higher	72K lower	penton	fibre
A549	0.69	1.09	1.46	1.30	4.37	1.17
U87MG	0.69	1.12	1.41	1.11	1.53	1.07
U87MG/PTEN B1	0.68	1.04	1.51	1.29	3.25	0.72
U87MG/PTEN B4	0.45	0.88	0.98	0.66	9.86	3.50
U87MG/PTEN B6	0.43	1.04	1.57	0.65	2.57	6.47

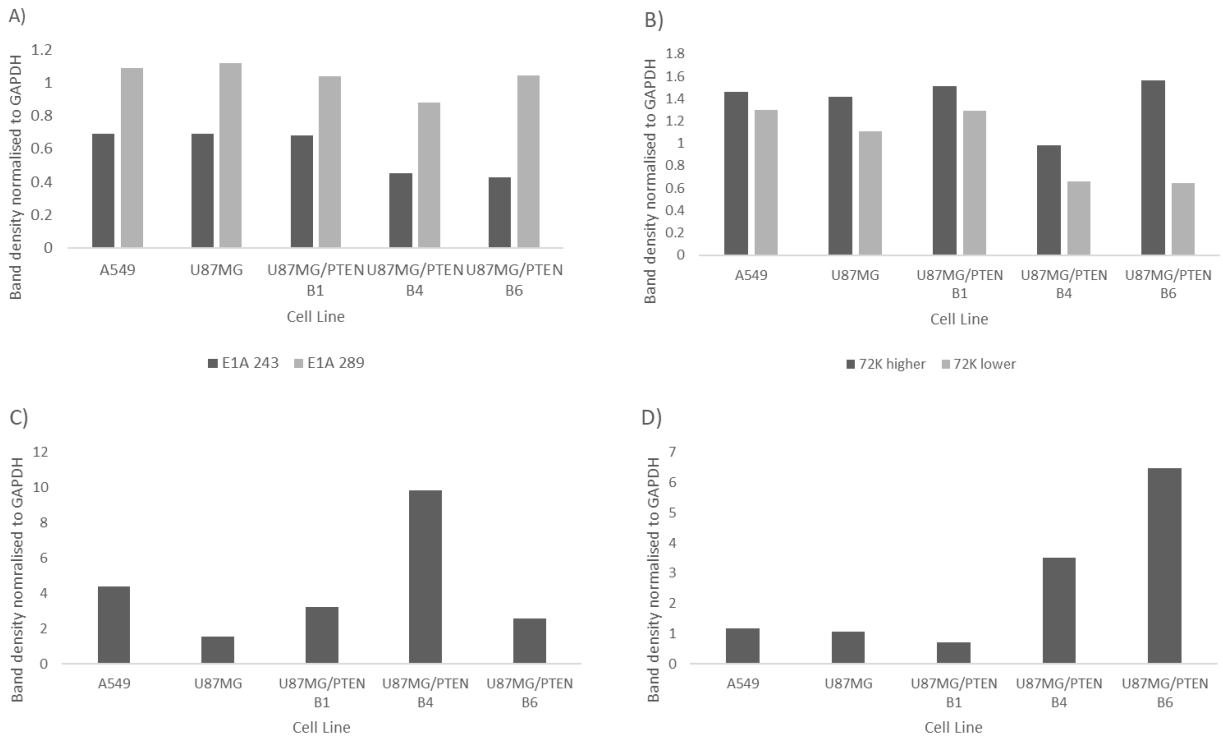

Figure 29: **Comparing viral protein levels in A549, U87MG and U87MG/PTEN cell lines**. The level of A) E1A proteins, B) 72K proteins, C) fibre protein and D) penton base protein present in each cell line 24 hours post infection was isolated by Western blot and normalised to the level of GAPDH within each sample.

These results were unexpected as there appeared to be little difference between the level of viral protein expressed in U87MG cells and A459 cells, which did not conform with previous results by the Blair group. Additionally, there was no consistency within each infected U87MG/PTEN cell line as to whether viral protein has increased or decreased when compared to infected U87MG cells.

5.6.2. Immunofluorescent antibody staining of Ad5 proteins in infected cells

A) Infection of A549 cells

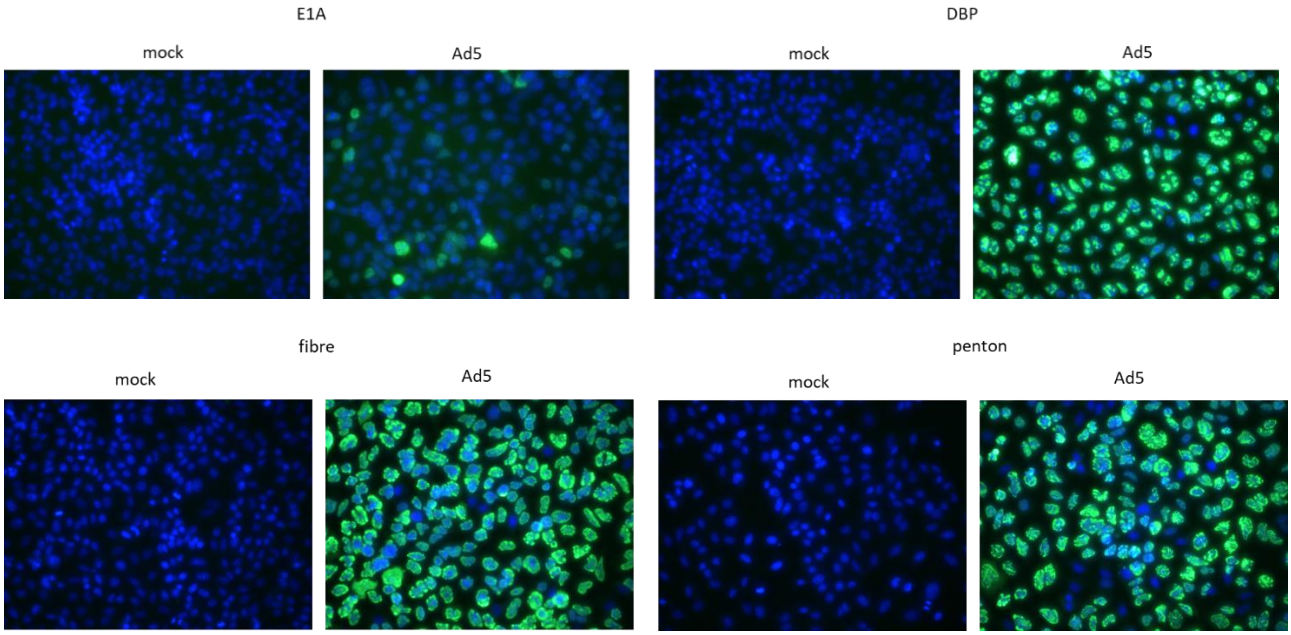

Figure 30: **Immunofluorescence imaging of Ad5 infected and mock infected A549 cells**. Cells were infected with virus at 300vp/cell, and incubated for 24hours at 37°C. During fluorescence staining, the viral proteins were labelled with an Alexa-Fluor 488 secondary antibody, which fluoresced green. The nucleus of the cells was labelled with DAPI , which fluoresced blue. Primary antibodies were used at the following concentrations: E1A at 1:100, DBP at 1:10, fibre at 1:2000 and penton at 1:1000. Cells were scanned using a 20x objective by an EVOS microscope.

E1A was present in lower levels than the other viral proteins, and did not form notable structures. DBP formed granular structures, localised to the nucleus. Fibre formed a combination of linear and granular structures, localised to the periphery of the nucleus. Finally, penton also formed a combination of linear and granular structures, and was located within the nucleus, with higher intensity areas existing towards the periphery of the nucleus.

B) Infection of U87MG cells

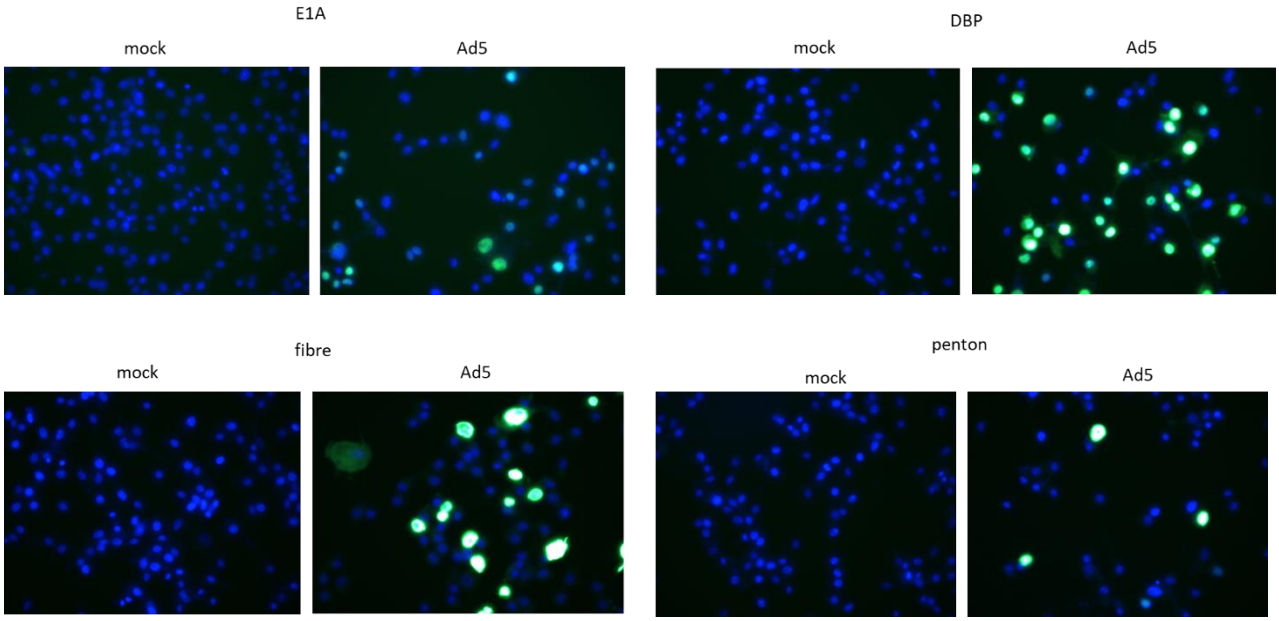

Figure 31: **Immunofluorescence imaging of U87MG cells that had either been mock infected or infected with Ad5**. Cells were infected with Ad5 at 300vp/cell, then incubated at 37°C for 24 hours. Imaging was performed at a 20x magnification, with DAPI (blue) used to locate the nucleus. The viral proteins were imaged using an Alexa-Fluor488 secondary antibody, and therefore fluoresced green. Unlike A549 cells, where the majority of cells exhibited fluorescence for each viral antibody, U87MG cells presented with bright “hotspots” of fluorescence in few cells. Little in the way of structures formed by viral proteins could be ascertained.

C) Infection of U87MG/PTEN cell lines

PTEN-expressing U87MG cell lines were infected with Ad5 at 300 vp/cell. Twenty-four hours post-infection, cells were fixed with methanol and stained using the four viral antibodies (as in figure 31) and DAPI. Images were taken at a range of magnifications, to identify a proportion of cells positive for viral protein, and to identify the localisation of the viral protein within the infected cells. Imaging was carried out using an EVOS microscope.

i) Infection of U87MG/PTEN B1

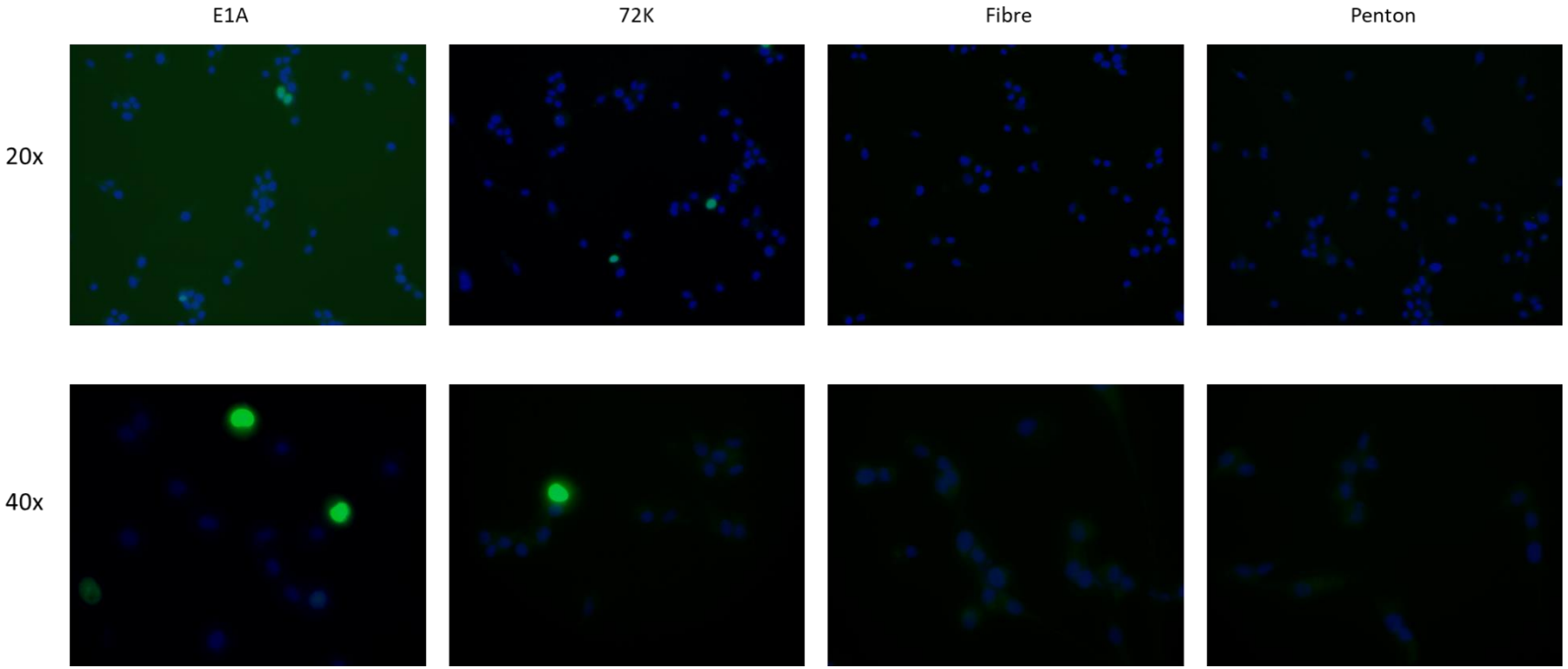

Figure 32: **Immunofluorescence analysis of virus proteins in Ad5-infected U87MG/PTEN B1 cells**. Immunofluorescence was performed 24 hours after cells were infected with Ad5 at 300vp/cell. DAPI (blue) was used to locate the nucleus, and the appropriate virus protein antibody with an AlexaFluor-488 anti-goat secondary was used to show the virus protein (green). Primary antibodies were used at the following concentrations: E1A at 1:100, DBP at 1:10, fibre at 1:2000 and penton at 1:1000. Cells were scanned with a 20x or 40x objective by an EVOS microscope.

ii) Infection of U87MG/PTEN B4

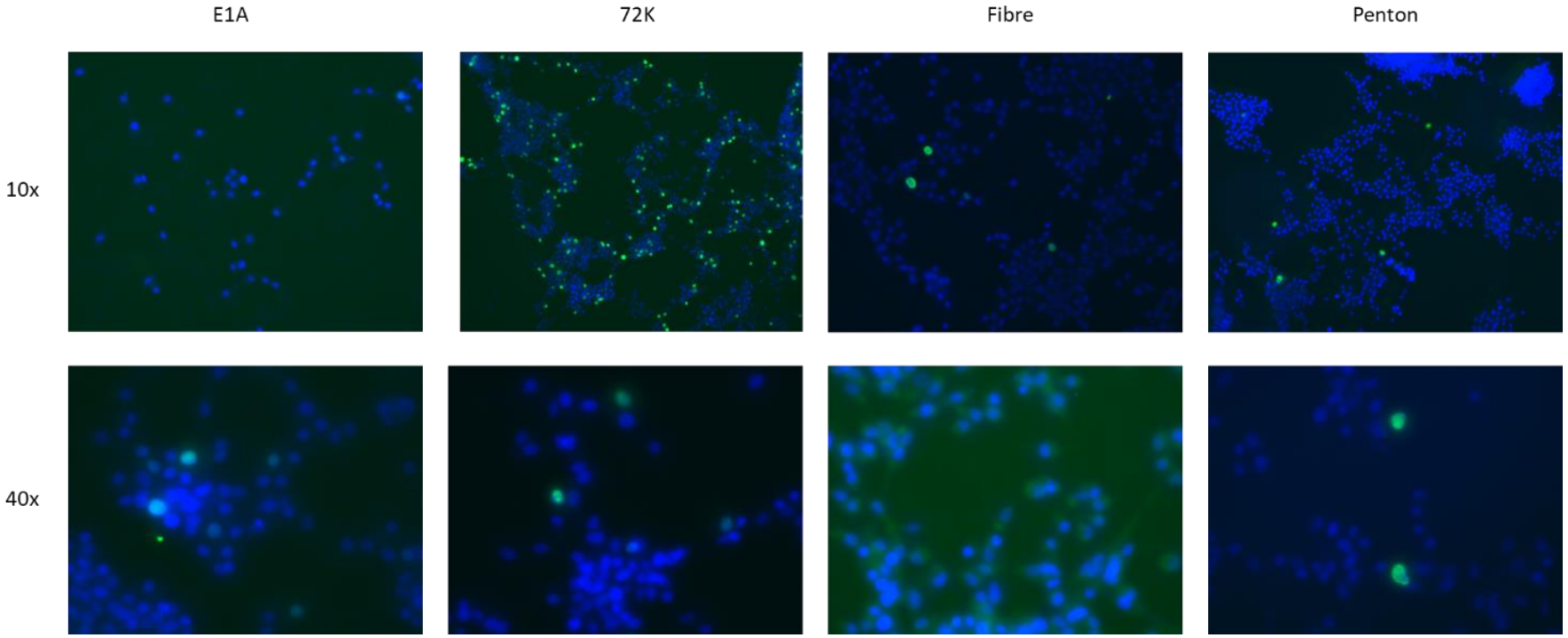

Figure 33: **Viral protein in infected U87MG/PTEN B4 cells, shown by fluorescence microscopy**. Cell were incubated with the viral antibodies at appropriate dilutions, and Alexa-Fluor488 was used as the secondary antibody. Viral proteins were shown in green, and DAPI, which localises to the nucleus, was shown in blue. Cells were scanned using either a 10x or 40x objective.

Unlike infected A549 cells, infected U87MG/PTEN B4 cells showed sparse fluorescence for early viral proteins E1A and 72K. A small proportion of the cells present exhibited green fluorescence, as shown by the 10x objective. When the same samples were viewed with a 40x objective, it was difficult to discern a notable structure to the viral protein fluorescence, which again, is unlike that noted in A549 cells.

Additionally, similar to infected U87MG cells, very few of the U87MG/PTEN B4 cells showed green fluorescence for the late viral proteins, fibre and penton. Where fibre and penton were present, it is in “hotspots”, where the green fluorescence was highly concentrated to a single cell, and the brightness of the microscope used was adjusted to accommodate this.

iii) Infection of U87MG/PTEN B6

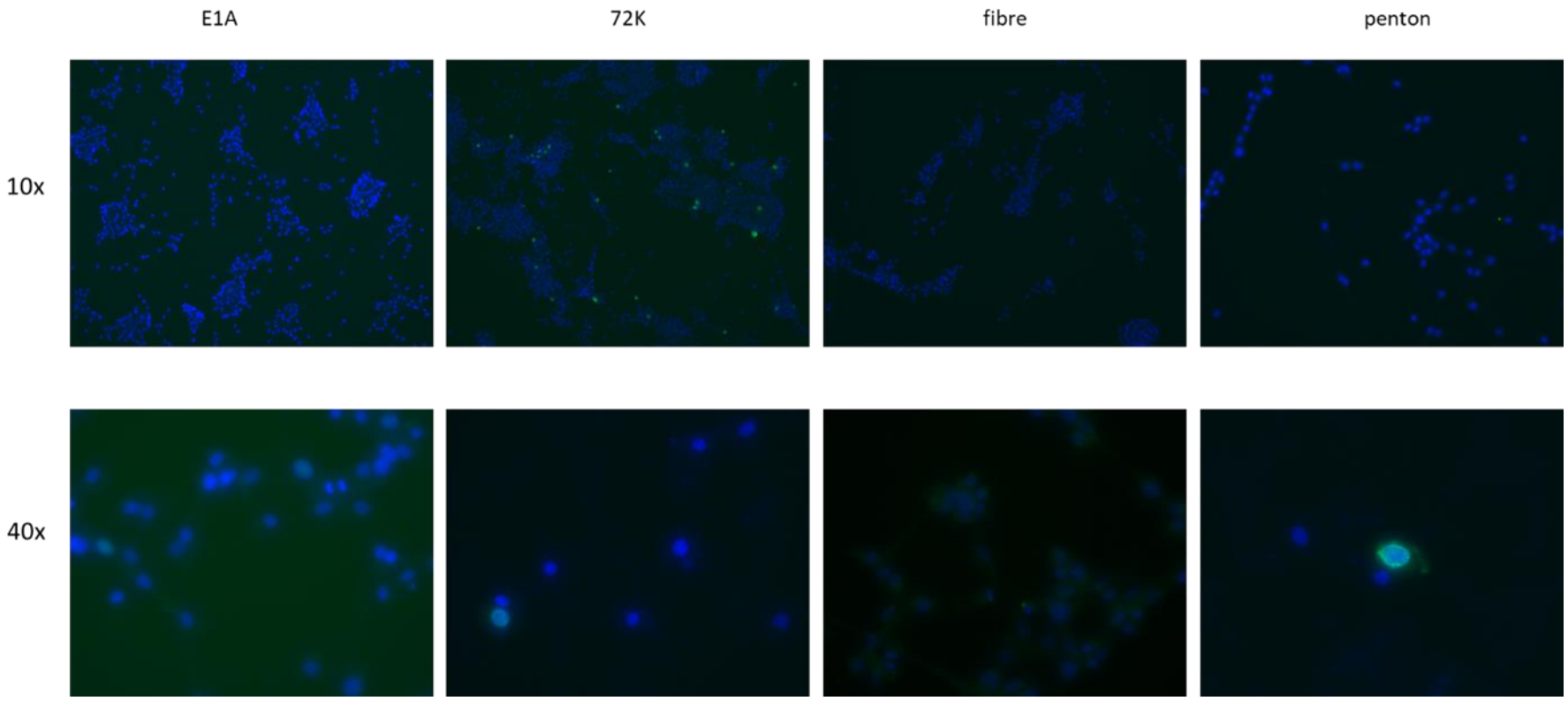

Figure 34: **Viral protein in Ad5 infected U87MG/PTEN B6 cells, shown by fluorescence microscopy**. The antibodies for the viral proteins were used as primary antibodies, with Alexa Fluor-488 used as the secondary. Viral proteins will therefore fluoresce green, and DAPI fluoresces blue to locate the nucleus of each cell.

U87MG/PTEN B6 cells infected with Ad5 show very little evidence of viral replication by fluorescence microscopy. In the cells treated with anti-72K, some green fluorescence was captured at a 10x objective, but the vast proportion of cells showed no fluorescence. Of interest for future work may be the co-staining and immunofluorescence of PTEN and the viral proteins.

5.7. Transduction of cells with Ad5EGFP

To ascertain whether Ad5 entered the PTEN-expressing U87MG cell lines, the cell lines were transduced with a replication-deficient Ad5-EGFP virus, where an EGFP gene replaced the E1A and E1B genes. Therefore, EGFP is used as a marker for cell entry and migration of virus to the nucleus where the EGFP transgene is transcribed. The newly-synthesised EGFP was viewed by fluorescence microscopy.

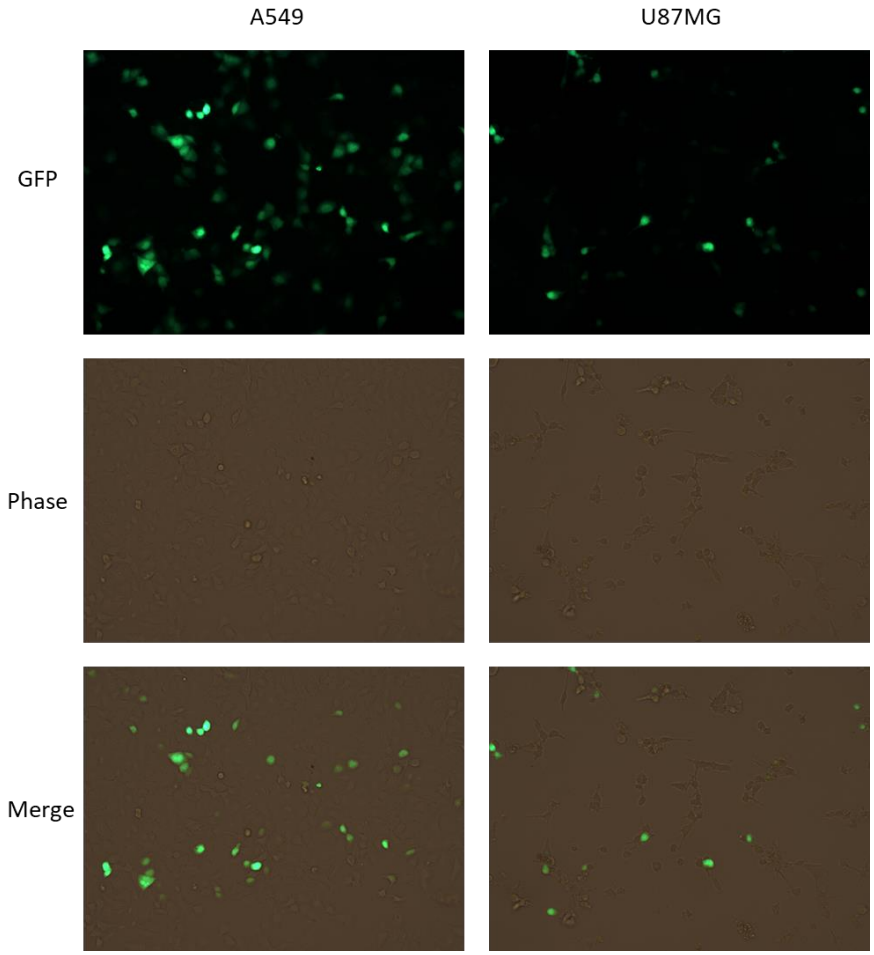

Figure 35: **Entry of Ad5EGFP into A549 and U87MG cells**. Cells were infected with virus at 600vp/cell, incubated for 24 hours, then imaged using an EVOS microscope.

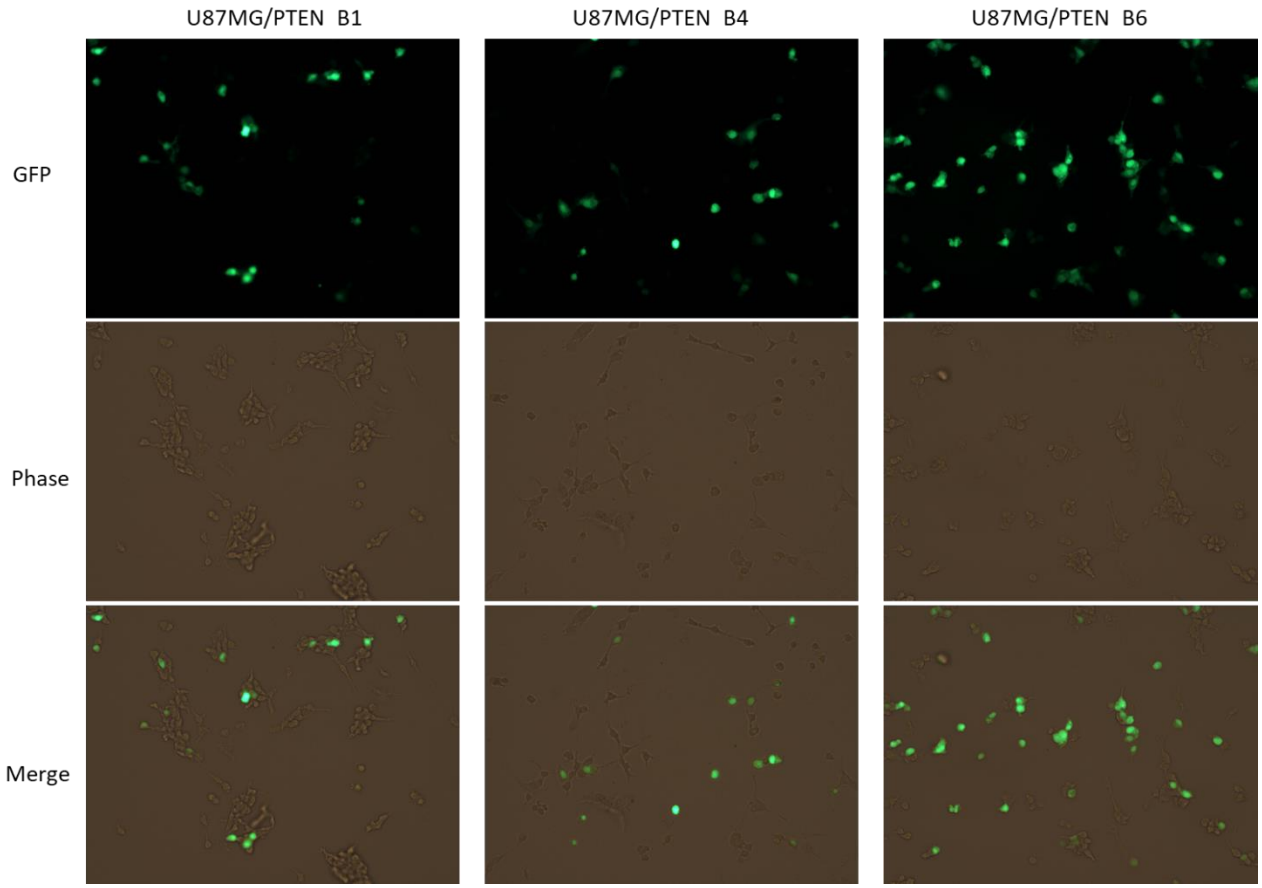

Figure 36: **Ad5EGFP entry into PTEN-expressing U87MG cell lines**. Cells were transduced with virus at 600vp/cell, incubated for 24 hours, then imaged using an EVOS microscope.

Flow cytometry was performed on PFA-fixed mock and Ad5EGFP infected cell lines, to quantify the successfully transduced cells. Gates were set around an unlabelled control sample, then an additional gate was set using each mock sample to isolate cells positive for EGFP.

A)i.

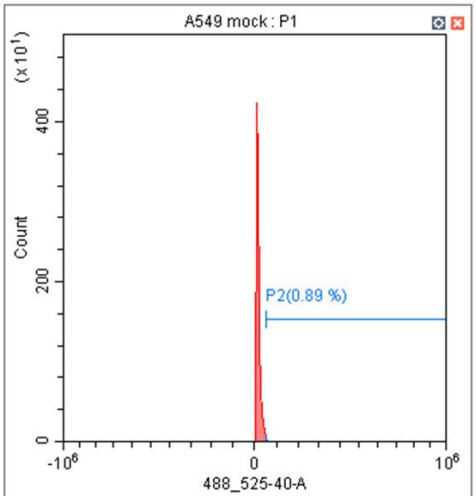

ii.

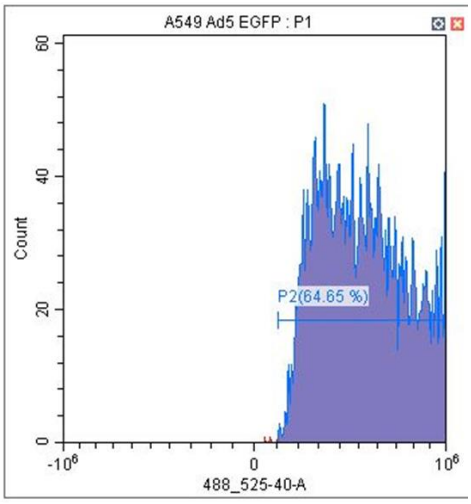

B) i.

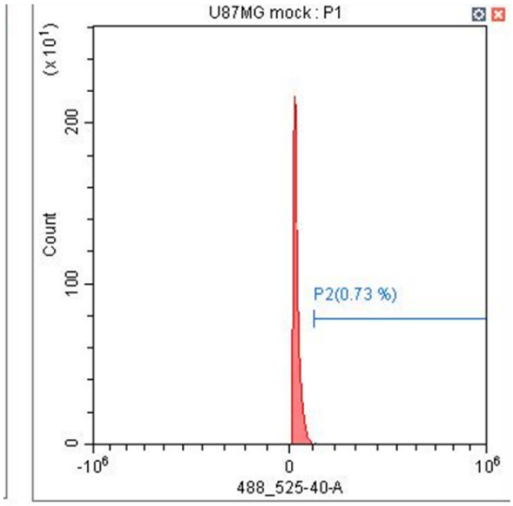

ii.

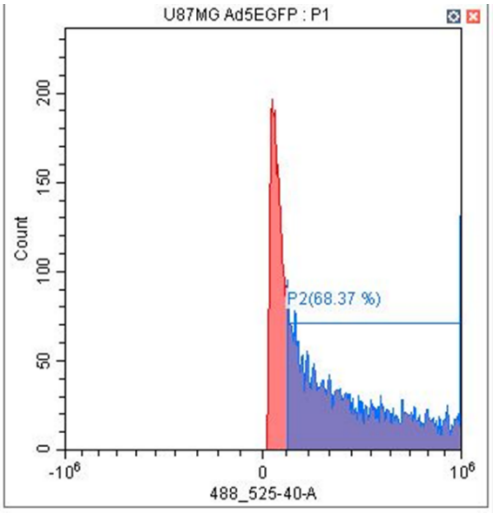

C) i.

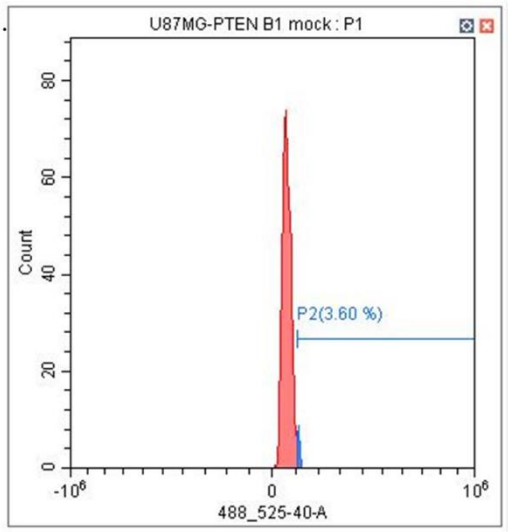

ii.

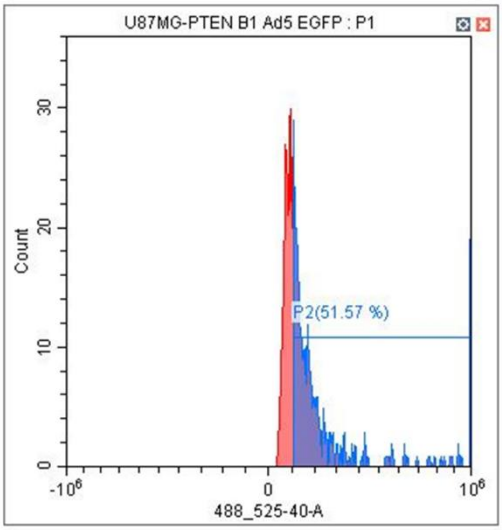

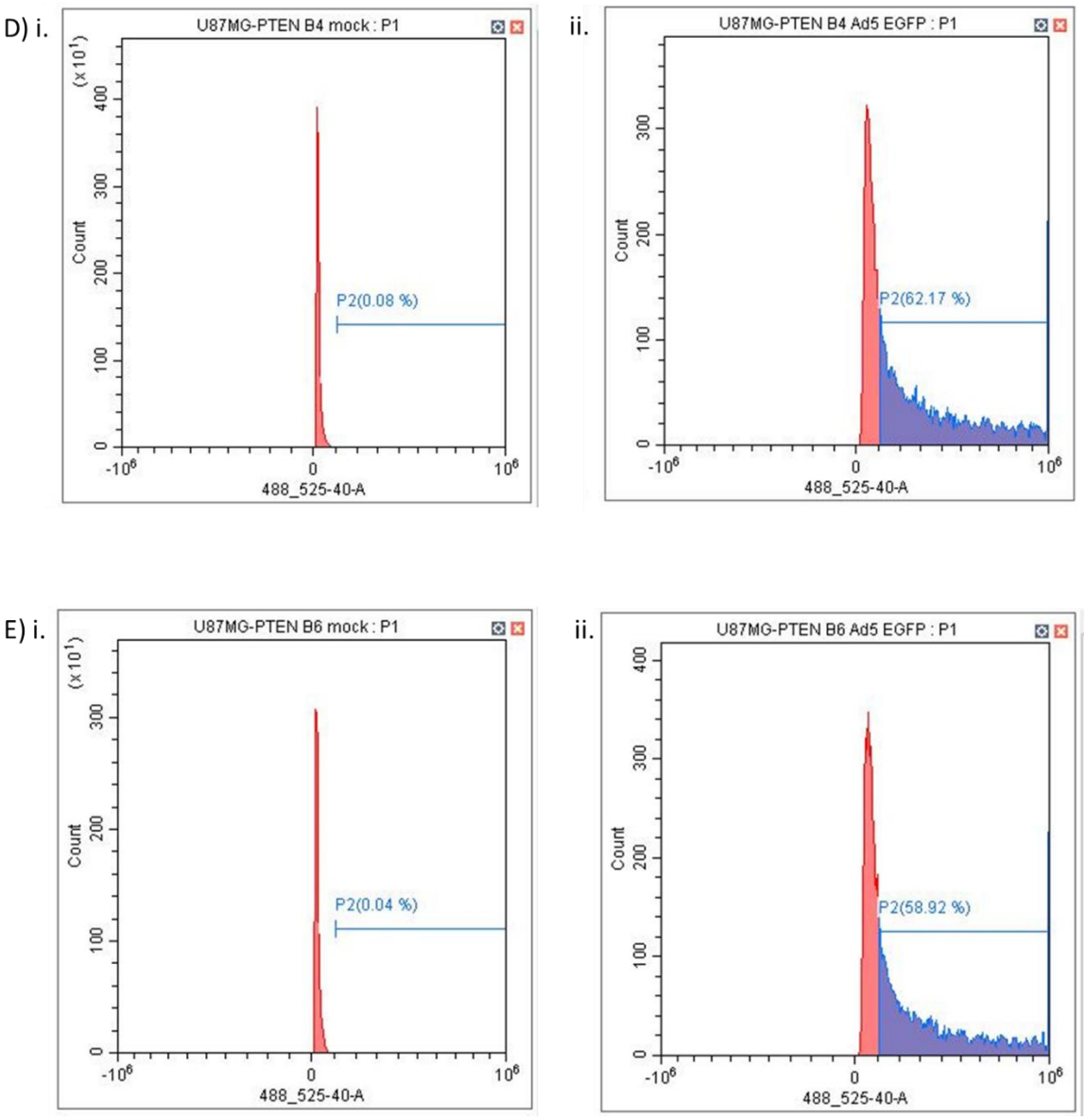

Figure 37: **Quantification of cell entry by Ad5EGFP**. A) A549, B) U87MG, C) U87MG/PTEN B1, D) U87MG/PTEN B4, Cells and E) U87MG/PTEN B6 cells were transduced with Ad5EGFP at 600vp/cell and incubated for 24 hours. Cells were detached from the plate, fixed with 4% PFA and analysed by flow cytometry.

The percentage of EGFP-expressing cells were taken for both mock- and Ad5EGFP-infected cells.

Table 10: **Quantification of cell entry by Ad5EGFP.**

	Percentage EGFP positive cells		Percentage transduced cells
Cell Line	Mock	Ad5	
A549	0.89	64.65	63.76
U87MG	0.73	68.37	67.64
U87MG/PTEN B1	3.60	51.57	47.97
U87MG/PTEN B4	0.08	62.17	62.09
U87MG/PTEN B6	0.04	58.92	58.88

All cell lines except U87MG/PTEN B1 were successfully transduced with Ad5EGFP where over half of cells were expressing EGFP at 24 hours post-transduction. The similar values for A549 and U87MG was expected, as indicated by previous work by the Blair group. However, it was expected that A549 cells would be more highly transduced than U87MG. It could be that a proportion of successfully transduced cells were removed during the washing step, resulting in smaller percentages of transduced cells by flow cytometry.

6. Discussion

6.1. Regulation of the PTEN promoter during Ad5 infection

PTEN regulation is highly complex, with regulation of protein expression occurring at the transcriptional, translational and post-translational level.

Previous work in the Blair group has found a 50% reduction in PTEN protein during Ad5 infection, and this project aimed to identify whether the cause for this reduction is transcriptional regulation of PTEN.

Numerous cellular factors are able to regulate PTEN transcription, both positively and negatively. P53, for example, is known to upregulate PTEN transcription by directly binding to the PTEN promoter region.

6.1.1. The PTEN promoter region

The PTEN promoter region is a GC-rich, TATA-less region with multiple transcription start sites89. A minimum promoter region has been identified at -958 to -821 base pairs from the ATG start codon of the PTEN protein, which contains consensus binding sites for numerous transcription factors, including GATA1, GATA2, and Dof3 (a single zinc finger transcription factor)89. Direct binding of transcription factors such as p53[35] and c-Jun[42] to the PTEN promoter region have been implicated in regulation of PTEN transcription.

Of particular interest to this project is the regulation of PTEN transcription by p53. Wild-type p53 is known to upregulate PTEN transcription[35] and is targeted for proteasomal degradation by adenovirus proteins E1B-55K and E4orf6[7]. Thus, a decrease in p53 in Ad5 infected cells may cause a decrease in activity at the PTEN promoter, leading to the decrease in PTEN mRNA and protein identified by previous members of the Blair group.

However, the transient expression of PTEN promoter-luciferase plasmids and subsequent luciferase assays performed demonstrate that there was no significant change to the activity of the PTEN promoter during Ad5 infection in various cell lines, both p53-positive and p53-null, which indicates that the 50% decrease in PTEN protein and mRNA previously detected during Ad5 infection was not caused by a decrease in promoter activity. Instead, it may be caused by virus-mediated post-transcriptional mRNA processing or degradation, as PTEN mRNA is also decreased by 50%. Viruses are able to directly target host proteins or can manipulate host systems such as miRNA regulation of mRNAs and hence steady-state levels of protein. Adenoviruses are able to deregulate host miRNAs during infection90, and as PTEN is regulated by many

different miRNAs, it is possible that virus-mediated dysregulation of host miRNAs leads to the lowered level of PTEN mRNA.

6.1.2. miRNA regulation of PTEN

Alongside transcriptional and post-translational regulation of PTEN, PTEN can also be regulated by microRNAs (miRNAs). miRNAs target mRNAs through complementary base pairing of the 'seed' region of the miRNA to the mRNA. The miRNA can then either destabilise the mRNA or inhibit its translation[47]. miRNAs can bind to multiple targets, and work in conjunction with one another91.

PTEN is known to be regulated by miRNAs in a largely cell-type specific manner. miR-21, for example, has been identified as a negative regulator of PTEN in gastric cancer, head and neck squamous cell carcinoma92 and clear cell renal cell carcinoma. Further examples of negative PTEN regulators include miR-130 in lung adenocarcinoma and bladder cancer93, miR-221/222 in non-small cell lung cancer94, miR-301a in breast cancer95 and melanoma96, and miR-155-5p in hepatocellular carcinoma97. PTEN can also be upregulated by miRNA, either by direct targeting of the PTEN mRNA or by miRNA mediated upregulation of hypomethylation of the PTEN promoter region[49].

6.1.3. miRNA dysregulation by Adenovirus infection

During Adenovirus infection, host miRNAs are targeted to dysregulate the cell cycle and thus create an environment conducive to viral replication91.Adenovirus infection has been noted to deregulate host miRNAs in stages, similar to the dysregulation of host genes. In stage 1 of viral infection (0-12 hours post-infection), miRNAs with roles in the host immune response such as miR-22, miR-181b, miR320 and let-7e are upregulated98.

In the second stage of infection (hours 12-24 post-infection), the cell environment begins to change as host gene expression is altered by the presence of the viral E1A protein. At this timepoint, additional miRNAs involved in the host immune response are upregulated, and the first virus-mediated down-regulation of host miRNA is observed. The downregulated miRNAs are largely tumour suppressive miRNAs, such as miR-34a and miR-185. There is also an upregulation in a small number of oncogenic miRNAs (miR-21 and the miR-17/92 cluster) at this timepoint, believed to be a cell response to combat viral replication98.

In the late stages of viral replication (24 hours post-infection onwards), previously overexpressed host miRNAs involved in the immune response are downregulated, alongside oncogenic miRNAs miR-193 and miR-221. Whether the downregulation of oncogenic miRNA is a host "last defence" or a viral downregulation has yet to be elucidated98.

At 36 hours post-infection onwards, there is a marked deregulation of both host genes and miRNAs, with around 146 host miRNAs being differentially expressed by over 1.5 fold compared to mock samples98. These data for miRNAs dysregulated in Ad infection comes from experiments with Ad2, these data may be somewhat similar to Ad5 infection, as both Ad5 and Ad2 belong to species C of the human Adenoviruses.

The cell-type specificity of PTEN regulation by miRNAs does make analysis of the literature difficult, but we can identify potential miRNAs of interest by looking at any overlap in miRNAs involved in the regulation of PTEN and those that are dysregulated during Adenovirus infection.

By comparing miRNAs that regulate PTEN with miRNAs dysregulated in Ad infection, numerous miRNAs of interest can be identified.

Table 11: **Comparing miRNAs that regulate PTEN and are dysregulated during Ad infection.**

Regulates PTEN	Dysregulated during Ad infection
Upregulates PTEN miR-29 miR-185	Upregulated during infection miR-155 (early) miR-29 (early) miR-10a-5p
Downregulates PTEN miR-21 miR-221 miR-155-5p miR-10a	Downregulated during infection miR-155 (late) miR-29 (late) miR-21 miR-185 miR-29a miR-221

For example, miR-155-5p is known to downregulate PTEN mRNA49,97, and is also subjected to change in expression during Ad infection98. Initially, miR-155-5p expression is increased during Ad infection, but after 24hpi, expression decreases98. The increase in miR-155-5p during the early stages of infection may therefore contribute to the decrease in PTEN mRNA and protein. MiR-130a is also a known downregulator of PTEN expression, and is upregulated at 24 hours post-infection with adenovirus98. As with miR-155-5p, the downregulatory effect of miR-130a on PTEN may contribute to the decrease in PTEN protein observed.

miR-29a is a positive regulator of PTEN expression that functions by inhibiting DNA methyltransferases DNMT1 and DNMT3b. MiR-29 is also initially upregulated as part of

the host immune response to Ad infection, then downregulated[99], which may affect the level of PTEN in the cells.

An additional consideration is the role of viral miRNAs on the expression of host miRNAs.

6.1.4. Adenovirus miRNAs

Adenovirus genomes encode for one or two non-coding RNAs (ncRNAs). The first is $VARNA_I$ which is present in all Adenovirus types, and the second is $VARNA_{II}$, which is present in around 80% of Ad types91. Although the length of the VA RNAs is similar (157-160 nucleotides for VA RNA_I and 158-161 nucleotides for VA RNA_{II}) and the presence conserved 5' and 3' terminal sequences, the nucleotide sequences of the VA RNAs are diverse, both within a specific virus type and between species90. VA RNAs deregulate host miRNA processing through binding and sequestration of DICER, the complex that produces mature miRNAs from pre-miRNAs90,91. VA RNAs can also saturate Exportin-5, which exports host pre-miRNAs from the nucleus91. This disruption of the miRNA biogenesis pathway by VA RNAs may contribute to the reduction in PTEN during Ad5 infection.

VA RNAs contribute to viral deregulation of host proteins, and 462 genes have been shown to be downregulated following transfection of cells with VA RNA_I and VA RNA_{II}, a large proportion of which have complementary sequences to the seed region of mivaRNAs99. The downregulated genes performed roles in cell signalling, cell growth and apoptosis control as well as DNA repair.

VA RNAs are processed in a similar way to host miRNAs, through cleavage by DICER to produce viral-associated microRNAs (mivaRNAs). The mivaRNAs can occupy RISC complexes, contributing to the post-transcription downregulation of host gene expression100. The high abundance of mivaRNA isoforms means identifying and verifying direct targets of mivaRNAs is difficult.

6.2. Role of PTEN in Adenovirus Replication

A PTEN-expressing variant of U87MG cells was created to enable cell-type specific analysis of the role of PTEN expression in Adenovirus infection. As mentioned above, PTEN is regulated by a very complex system, and the prevalence of different regulatory mechanisms may differ between cell types.

The Western blots for viral proteins expressed following infection of U87MG/PTEN clones showed a reduction in viral protein expression for the majority of viral proteins in the clones compared to both A549 and U87MG (Figs. 26 and 27), This was an

unexpected result, firstly because previous findings by the Blair group illustrated a significant decrease in Adenovirus proteins between A549 and U87MG. The level of penton base in Ad5-infected U87MG cells was 5% that of the penton base level in infected A549 cells, and fibre had decreased to 30% of the level of A549 cells in U87MG cells. Similar differences were seen in the early Adenovirus proteins E1A and DBP.

Secondly, previous findings that Adenovirus proteins are expressed at a lower level in infected A549 cells with reduced PTEN levels led to the construction of a hypothesis that restoration of PTEN expression in a normally PTEN-null cell line may restore the ability of Ad5 to replicate. It was therefore expected that an increase in virus protein would be observed between U87MG and the PTEN-expressing clones. This was observed in some instances, for example, the U87MG/PTEN clone B4 exhibited a 6.4 and 3.3 fold increase in penton base and fibre protein, respectively, when compared to U87MG. However, a corresponding increase in early viral proteins was not observed, calling into question the validity of these results.

Overall, the Western blot analysis of infection gives no consensus as to whether restoring PTEN expression to U87MG cells affects the replication of Ad5.

Of interest is the similarity between localisation of viral proteins illustrated by IF in U87MG and the PTEN-expressing clones, although high-resolution imaging would be needed to confirm this. Both normal U87MG and U87MG/PTEN clones show an uneven distribution of viral proteins (both early and late), with very little fluorescence except in intense “hotspots”. The PTEN-expressing clones appear to have less viral protein present than U87MG by immunofluorescence. This may indicate that the role of PTEN in Adenovirus infection is not as significant as expected, and that another difference between the cell lines is responsible for the differences in adenovirus replication previously identified by the Blair group.

Alternatively, if the transduced PTEN protein is not functional, this might account for the similarity between U87MG and U87MG/PTEN cell lines. To clarify this, a Western blot against phospho-AKT in U87MG and U87MG/PTEN cell lines would be useful, as if the transduced PTEN is functional, a decrease in phospho-AKT would be observed.

Previous work (Painter, unpublished results) had identified that reducing PTEN protein levels by around 70% by RNA interference caused a decrease in both early and late Adenovirus proteins following infection. Penton base protein levels were reduced by 70% and fibre was reduced by around 50% in the reduced-PTEN A549. Similarly, DBP and E1A were reduced by around 40% and 50% respectively. It would therefore be beneficial to knock-out PTEN expression in A549 using CRISPR-Cas technology, and

test for viral protein expression following Ad5 infection. If virus proteins were similarly expressed in PTEN-null A549 and U87MG cells, then this would be a good indicator that PTEN plays a significant role in Ad5 replication.

7. Conclusions and Future Directions

Adenoviruses are pathogens which have the capacity to cause life-threatening illness in the immunocompromised101. Confirming that PTEN is necessary for Adenovirus infection would provide a potential avenue for anti-virals as by inhibiting PTEN, viral replication would also be inhibited. This project has not been able to ascertain whether Ad5 infection is dependent on PTEN status, but additional work to confirm that PTEN is functional in the U87MG/PTEN cell lines would be beneficial to this regard. In addition, designing a PTEN-knockout A549 cell line using Crispr-Cas technologies would enable further analysis of the role of PTEN during Ad5 infection. Having the PTEN-knockout A549 cell line would enable the isolation of the role of PTEN, as currently it is not known whether the cause for poor Adenovirus replication in U87MG is the PTEN-null status or the role of another cellular factor. Furthermore, relatively specific, reversible PTEN inhibitors are available, such as bisperoxovandium compound bisperoxovanadium 1, 10-phenatroline102. It would be of interest to use these inhibitors to identify whether the catalytic activity of PTEN is required for Adenovirus replication in A549, as a decrease in PTEN by RNA interference led to a decrease in virus replication.

Gaining an understanding of how PTEN is regulated and the role it plays in Adenovirus replication has potential implications for both oncolytic adenovirotherapy as well as the development of anti-virals. Ad5-based vectors are being studied more frequently as cancer therapeutics103,104, and therefore it is important to understand whether the PTEN-null status of U87MG cells is the limiting factor to Ad5 replication, so that oncolytic virotherapies targeting PTEN-null cancers can be modified to combat the poor replication observed.

The possibility that PTEN regulation by p53 is significant during Adenovirus infection has also been investigated. We found no significant change in PTEN promoter activity following Ad5 infection, in both wild-type p53 and p53-null cell lines, indicating that although p53 does positively regulate PTEN transcription[35] (Figure 13), this regulation of PTEN is not affected by Ad5 infection (Figures 13, 14 and 16) . This therefore opens the field of investigation to the role of miRNAs in regulating PTEN during Ad5 infection. Identification of miRNas that both regulate PTEN and are dysregulated by Adenovirus infection provides a starting point for screening which miRNAs may be responsible for the 50% decrease in PTEN mRNA and protein previously observed by the Blair group. Inhibition of specific miRNAs by Anti-miRs105 could provide insight into which of the miRNAs identified is involved in the decrease of PTEN.

8. Bibliography

1. Lodish, H. *et al.* (2000) Molecular Cell Biology. 4th Edition. New York: W H Freeman.
2. Munoz-Fontela, C. *et al.* Control of virus infection by tumour suppressors. *Carcinogenesis* **28**, 1140–1144 (2007).
3. Münger, K. *et al.* Mechanisms of Human Papillomavirus-Induced Oncogenesis. *Journal of Virology* **78**, 11451–11460 (2004).
4. Tornesello, M. L., Annunziata, C., Tornesello, A. L., Buonaguro, L. & Buonaguro, F. M. Human oncoviruses and p53 tumor suppressor pathway deregulation at the origin of human cancers. *Cancers* vol. 10 213 (2018).
5. Fridman, J. S. & Lowe, S. W. Control of apoptosis by p53. *Oncogene* vol. 22 9030–9040 (2003).
6. Helt, A.-M. Mechanisms by which DNA tumor virus oncoproteins target the Rb family of pocket proteins. *Carcinogenesis* **24**, 159–169 (2003).
7. Querido, E. *et al.* Degradation of p53 by adenovirus E4orf6 and E1B55K proteins occurs via a novel mechanism involving a Cullin-containing complex. *Genes and Development* **15**, 3104–3117 (2001).
8. Wang, Z. G. *et al.* Role of PML in cell growth and the retinoic acid pathway. *Science* **279**, 1547–1551 (1998).
9. Pharos : Target Details - P29590. https://pharos.nih.gov/targets/P29590.
10. Song, M. S. *et al.* The deubiquitinylation and localization of PTEN are regulated by a HAUSP-PML network. *Nature* **455**, 813–817 (2008).
11. Carvalho, T. *et al.* Targeting of adenovirus E1A and E4-ORF3 proteins to nuclear matrix-associated PML bodies. *Journal of Cell Biology* **131**, 45–56 (1995).
12. Flinterman, M., Gäken, J., Farzaneh, F. & Tavassoli, M. E1A-mediated suppression of EGFR expression and induction of apoptosis in head and neck squamous carcinoma cell lines. *Oncogene* **22**, 1965–1977 (2003).
13. Papa, A. & Pandolfi, P. P. The pten–pi3k axis in cancer. *Biomolecules* vol. 9 (2019).
14. Xu, F., Na, L., Li, Y. & Chen, L. Roles of the PI3K/AKT/mTOR signalling pathways in neurodegenerative diseases and tumours. *Cell & Bioscience 2020 10:1* **10**, 1–12 (2020).

15. Stambolic, V. *et al.* Negative regulation of PKB/Akt-dependent cell survival by the tumor suppressor PTEN. *Cell* **95**, 29–39 (1998).

16. Zhou, X. P. *et al.* Germline PTEN promoter mutations and deletions in Cowden/Bannayan-Riley-Ruvalcaba syndrome result in aberrant PTEN protein and dysregulation of the phosphoinositol-3-kinase/Akt pathway. *American Journal of Human Genetics* **73**, 404–411 (2003).

17. Mingo, J. *et al.* A pathogenic role for germline PTEN variants which accumulate into the nucleus. *European Journal of Human Genetics* **26**, 1180–1187 (2018).

18. Lee, Y. R., Chen, M. & Pandolfi, P. P. The functions and regulation of the PTEN tumour suppressor: new modes and prospects. *Nature Reviews Molecular Cell Biology* vol. 19 547–562 (2018).

19. Mansour, W. Y. *et al.* Loss of PTEN-assisted G2/M checkpoint impedes homologous recombination repair and enhances radio-curability and PARP inhibitor treatment response in prostate cancer. *Scientific Reports* **8**, (2018).

20. Blanco-Aparicio, C., Renner, O., Leal, J. F. M. & Carnero, A. PTEN, more than the AKT pathway. *Carcinogenesis* vol. 28 1379–1386 (2007).

21. Kurose, K. *et al.* Frequent somatic mutations in PTEN and TP53 are mutually exclusive in the stroma of breast carcinomas. *Nature Genetics* **32**, 355–357 (2002).

22. Freeman, D. J. *et al.* PTEN tumor suppressor regulates p53 protein levels and activity through phosphatase-dependent and -independent mechanisms. *Cancer Cell* (2003) doi:10.1016/S1535-6108(03)00021-7.

23. Mayo, L. D., Dixon, J. E., Durden, D. L., Tonks, N. K. & Donner, D. B. PTEN protects p53 from Mdm2 and sensitizes cancer cells to chemotherapy. *Journal of Biological Chemistry* **277**, 5484–5489 (2002).

24. Trotman, L. C. & Pandolfi, P. P. PTEN and p53: Who will get the upper hand? *Cancer Cell* vol. 3 97–99 (2003).

25. Nakanishi, A., Kitagishi, Y., Ogura, Y. & Matsuda, S. The tumor suppressor PTEN interacts with p53 in hereditary cancer (Review). *International Journal of Oncology* vol. 45 1813–1819 (2014).

26. Molinari, F. & Frattini, M. Functions and Regulation of the PTEN Gene in Colorectal Cancer. *Frontiers in Oncology* **3**, (2014).

27. Lee, J. O. *et al.* Crystal structure of the PTEN tumor suppressor: Implications for its phosphoinositide phosphatase activity and membrane association. *Cell* **99**, 323–334 (1999).

28. Vazquez, F. *et al.* Phosphorylation of the PTEN Tail Acts as an Inhibitory Switch by Preventing Its Recruitment into a Protein Complex. *Journal of Biological Chemistry* **276**, 48627–48630 (2001).

29. Georgescu, M. M., Kirsch, K. H., Akagi, T., Shishido, T. & Hanafusa, H. The tumor-suppressor activity of PTEN is regulated by its carboxyl-terminal region. *Proceedings of the National Academy of Sciences of the United States of America* **96**, 10182–10187 (1999).

30. Sanchez, T. *et al.* PTEN as an effector in the signaling of antimigratory G protein-coupled receptor. *Proceedings of the National Academy of Sciences of the United States of America* **102**, 4312–4317 (2005).

31. Brito, M. B., Goulielmaki, E. & Papakonstanti, E. A. Focus on PTEN regulation. *Frontiers in Oncology* vol. 5 (2015).

32. Xia, D. *et al.* Mitogen-activated protein kinase kinase-4 promotes cell survival by decreasing PTEN expression through an NFκB-dependent pathway. *Journal of Biological Chemistry* **282**, 3507–3519 (2007).

33. Chow, J. Y. C. *et al.* TGF-β downregulates PTEN via activation of NF-κB in pancreatic cancer cells. *American Journal of Physiology - Gastrointestinal and Liver Physiology* **298**, (2010).

34. Song, L. B. *et al.* The polycomb group protein Bmi-1 represses the tumor suppressor PTEN and induces epithelial-mesenchymal transition in human nasopharyngeal epithelial cells. *Journal of Clinical Investigation* **119**, 3626–3636 (2009).

35. Stambolic, V. *et al.* Regulation of PTEN transcription by p53. *Molecular Cell* **8**, 317–325 (2001).

36. Edwin, F., Singh, R., Endersby, R., Baker, S. J. & Patel, T. B. The tumor suppressor PTEN is necessary for human sprouty 2-mediated inhibition of cell proliferation. *Journal of Biological Chemistry* **281**, 4816–4822 (2006).

37. Patel, L. *et al.* Tumor suppressor and anti-inflammatory actions of PPARγ agonists are mediated via upregulation of PTEN. *Current Biology* **11**, 764–768 (2001).

38. Virolle, T. *et al.* The Egr-1 transcription factor directly activates PTEN during irradiation-induced signalling. *Nature Cell Biology* **3**, 1124–1128 (2001).

39. Whelan, J. T., Forbes, S. L. & Bertrand, F. E. CBF-1 (RBP-Jκ) binds to the PTEN promoter and regulates PTEN gene expression. *Cell Cycle* **6**, 80–84 (2007).

40. Mumm, J. S. & Kopan, R. Notch signaling: From the outside in. *Developmental Biology* vol. 228 151–165 (2000).

41. Vasudevan, K. M., Gurumurthy, S. & Rangnekar, V. M. Suppression of PTEN Expression by NF-κB Prevents Apoptosis. *Molecular and Cellular Biology* **24**, 1007–1021 (2004).

42. Hettinger, K. *et al.* c-Jun promotes cellular survival by suppression of PTEN. *Cell Death and Differentiation* **14**, 218–229 (2007).

43. Song, L. B. *et al.* The polycomb group protein Bmi-1 represses the tumor suppressor PTEN and induces epithelial-mesenchymal transition in human nasopharyngeal epithelial cells. *Journal of Clinical Investigation* **119**, 3626–3636 (2009).

44. Khan, S. *et al.* PTEN promoter is methylated in a proportion of invasive breast cancers. *International Journal of Cancer* **112**, 407–410 (2004).

45. Salvesen, H. B. *et al. PTEN methylation is associated with advanced stage and microsatellite instability in endometrial carcinoma*. http://bozeman.mbt. (2001) doi:10.1002/1097-0215.

46. Goel, A. *et al.* Frequent Inactivation of PTEN by Promoter Hypermethylation in Microsatellite Instability-High Sporadic Colorectal Cancers. *Cancer Research* **64**, 3014–3021 (2004).

47. Cai, Y., Yu, X., Hu, S. & Yu, J. A Brief Review on the Mechanisms of miRNA Regulation. *Genomics, Proteomics and Bioinformatics* vol. 7 147–154 (2009).

48. Meng, F. *et al.* MicroRNA-21 Regulates Expression of the PTEN Tumor Suppressor Gene in Human Hepatocellular Cancer. *Gastroenterology* **133**, 647–658 (2007).

49. Li, W., Zhang, T., Guo, L. & Huang, L. Regulation of PTEN expression by noncoding RNAs 06 Biological Sciences 0601 Biochemistry and Cell Biology. *Journal of Experimental and Clinical Cancer Research* vol. 37 (2018).

50. Wang, X. & Jiang, X. Post-translational regulation of PTEN. *Oncogene* vol. 27 5454–5463 (2008).

51. Leslie, N. R. & Downes, C. P. PTEN function: How normal cells control it and tumour cells lose it. *Biochemical Journal* vol. 382 1–11 (2004).

52. Kwon, J. *et al.* Reversible oxidation and inactivation of the tumor suppressor PTEN in cells stimulated with peptide growth factors. *Proceedings of the National Academy of Sciences of the United States of America* **101**, 16419–16424 (2004).

53. Hino, R. *et al.* Activation of DNA methyltransferase 1 by EBV latent membrane protein 2A leads to promoter hypermethylation of PTEN gene in gastric carcinoma. *Cancer Research* **69**, 2766–2774 (2009).

54. Ashfaq, U. A., Javed, T., Rehman, S., Nawaz, Z. & Riazuddin, S. An overview of HCV molecular biology, replication and immune responses. *Virology Journal* **8**, (2011).

55. Bao, W. *et al.* Loss of nuclear PTEN in HCV-infected human hepatocytes. *Infectious Agents and Cancer* **9**, article number 23 (2014).

56. Wu, Q. *et al.* The role of PTEN - HCV core interaction in hepatitis C virus replication. *Scientific Reports* **7**, 1–14 (2017).

57. Glick, D., Barth, S. & Macleod, K. F. Autophagy: Cellular and molecular mechanisms. *Journal of Pathology* vol. 221 3–12 (2010).

58. Huang, W. R. *et al.* Avian reovirus protein p17 functions as a nucleoporin Tpr suppressor leading to activation of p53, p21 and PTEN and inactivation of PI3K/AKT/mTOR and ERK signaling pathways. *PLoS ONE* **10**, (2015).

59. Berk, A. J. Adenoviridae. in *Fields Virology: Sixth Edition* vol. 1 (2013).

60. Russell, W. C. Adenoviruses: Update on structure and function. *Journal of General Virology* vol. 90 1–20 (2009).

61. Nemerow, G. R., Stewart, P. L. & Reddy, V. S. Structure of human adenovirus. *Current Opinion in Virology* vol. 2 115–121 (2012).

62. Sharma, A., Li, X., Bangari, D. S. & Mittal, S. K. Adenovirus receptors and their implications in gene delivery. *Virus Research* vol. 143 184–194 (2009).

63. Johansson, C. *et al.* Adenoviruses Use Lactoferrin as a Bridge for CAR-Independent Binding to and Infection of Epithelial Cells. *Journal of Virology* **81**, 954–963 (2007).

64. Lasswitz, L., Chandra, N., Arnberg, N. & Gerold, G. Glycomics and Proteomics Approaches to Investigate Early Adenovirus–Host Cell Interactions. *Journal of Molecular Biology* vol. 430 1863–1882 (2018).

65. Fejer, G., Freudenberg, M., Greber, U. F. & Gyory, I. Adenovirus-triggered innate signalling pathways. *European Journal of Microbiology and Immunology* **1**, 279–288 (2011).

66. Grand, R. J. The structure and functions of the adenovirus early region 1 proteins. *The Biochemical journal* vol. 241 25–38 (1987).

67. Berk, A. J. Functions of adenovirus E1A. *Cancer Surveys* **5**, 367–387 (1986).

68. Liu, H., Naismith, J. H. & Hay, R. T. Adenovirus DNA Replication. in 131–164 (2003). doi:10.1007/978-3-662-05597-7_5.

69. Mcconnell, M. J. & Imperiale, M. J. Biology of Adenovirus and Its Use as a Vector for Gene Therapy. *Human Gene Therapy* vol. 15 (2004).

70. Sundararajan, R., Cuconati, A., Nelson, D. & White, E. TNF-α Induces Bax-Bak Interaction and Apoptosis Which is Inhibited by Adenovirus E1B 19K. *Journal of Biological Chemistry* vol. 276 (48) 45120-45127 (2001).

71. Hoeben, R. C. & Uil, T. G. Adenovirus DNA replication. *Cold Spring Harbor Perspectives in Biology* **5**, (2013).

72. Lichtenstein, D. L., Toth, K., Doronin, K., Tollefson, A. E. & Wold, W. S. M. Functions and mechanisms of action of the adenovirus E3 proteins. *International Reviews of Immunology* vol. 23 75–111 (2004).

73. Täuber, B. & Dobner, T. Molecular regulation and biological function of adenovirus early genes: The E4 ORFs. *Gene* vol. 278 1–23 (2001).

74. Evans, J. D. & Hearing, P. Distinct Roles of the Adenovirus E4 ORF3 Protein in Viral DNA Replication and Inhibition of Genome Concatenation. *Journal of Virology* **77**, 5295–5304 (2003).

75. Fukuhara, H., Ino, Y. & Todo, T. Oncolytic virus therapy: A new era of cancer treatment at dawn. *Cancer Science* vol. 107 1373–1379 (2016).

76. Baker, A. T., Aguirre-Hernández, C., Halldén, G. & Parker, A. L. Designer oncolytic adenovirus: Coming of age. *Cancers* vol. 10 (2018).

77. Rein, D. T., Breidenbach, M., Hille, S. & Curiel, D. T. Current developments in adenovirus-based cancer gene therapy. *Future Oncology* vol. 2 137–144 (2006).

78. Waddington, S. N. *et al.* Adenovirus Serotype 5 Hexon Mediates Liver Gene Transfer. *Cell* **132**, 397–409 (2008).

79. Choi, J. W., Lee, Y. S., Yun, C. O. & Kim, S. W. Polymeric oncolytic adenovirus for cancer gene therapy. *Journal of Controlled Release* **219**, 181–191 (2015).

80. Perri, F., Pisconti, S. & Vittoria Scarpati, G. della. P53 mutations and cancer: A tight linkage. *Annals of Translational Medicine* **4**, (2016).

81. Dix, B. R., Edwards, S. J. & Braithwaite, A. W. Does the Antitumor Adenovirus ONYX-015/dl1520 Selectively Target Cells Defective in the p53 Pathway? *Journal of Virology* **75**, 5443–5447 (2001).

82. Thomas, S. M. & Grandis, J. R. The current state of head and neck cancer gene therapy. *Human Gene Therapy* vol. 20 1565–1575 (2009).

83. Lei, J. *et al.* The antitumor effects of oncolytic adenovirus H101 against lung cancer. *International Journal of Oncology* **47**, 555–562 (2015).

84. Harrington, K., Freeman, D. J., Kelly, B., Harper, J. & Soria, J. C. Optimizing oncolytic virotherapy in cancer treatment. *Nature Reviews Drug Discovery* vol. 18 689–706 (2019).

85. Giacinti, C. & Giordano, A. RB and cell cycle progression. *Oncogene* vol. 25 5220–5227 (2006).

86. Irving, J. *et al.* Conditionally replicative adenovirus driven by the human telomerase promoter provides broad-spectrum antitumor activity without liver toxicity. *Cancer Gene Therapy* **11**, 174–185 (2004).

87. Phoenix system. https://web.stanford.edu/group/nolan/_OldWebsite/retroviral_systems/phx.html.

88. Lee, P. Y., Costumbrado, J., Hsu, C.-Y. & Kim, Y. H. Agarose Gel Electrophoresis for the Separation of DNA Fragments. *Journal of Visualized Experiments : JoVE* 3923 (2012) doi:10.3791/3923.

89. Sur, S. *et al.* A panel of isogenic human cancer cells suggests a therapeutic approach for cancers with inactivated p53. *Proceedings of the National Academy of Sciences of the United States of America* **106**, 3964–3969 (2009).

90. Sheng, X., Koul, D., Liu, J. L., Liu, T. J. & Yung, W. K. A. Promoter analysis of tumor suppressor gene PTEN: Identification of minimum promoter region. *Biochemical and Biophysical Research Communications* **292**, 422–426 (2002).

91. Carnero, E., Sutherland, J. D. & Fortes, P. Adenovirus and miRNAs. *Biochimica et Biophysica Acta - Gene Regulatory Mechanisms* vol. 1809 660–667 (2011).

92. Piedade, D. & Azevedo-Pereira, J. M. MicroRNAs as important players in host-adenovirus interactions. *Frontiers in Microbiology* vol. 8 1324 (2017).

93. Liu, W. *et al.* Targeting miR-21 with Sophocarpine Inhibits Tumor Progression and Reverses Epithelial-Mesenchymal Transition in Head and Neck Cancer. *Molecular Therapy* **25**, 2129–2139 (2017).

94. Egawa, H. *et al.* The miR-130 family promotes cell migration and invasion in bladder cancer through FAK and Akt phosphorylation by regulating PTEN. *Scientific Reports* **6**, (2016).

95. Garofalo, M. *et al.* miR-221&222 Regulate TRAIL Resistance and Enhance Tumorigenicity through PTEN and TIMP3 Downregulation. *Cancer Cell* **16**, 498–509 (2009).

96. Ma, F. *et al.* Upregulated microRNA-301a in breast cancer promotes tumor metastasis by targeting PTEN and activating Wnt/β-catenin signaling. *Gene* **535**, 191–197 (2014).

97. Cui, L. *et al.* Expression of MicroRNA-301a and its Functional Roles in Malignant Melanoma. *Cellular Physiology and Biochemistry* **40**, 230–244 (2016).

98. Fu, X. *et al.* MicroRNA-155-5p promotes hepatocellular carcinoma progression by suppressing PTEN through the PI3K/Akt pathway. *Cancer Science* **108**, 620–631 (2017).

99. Zhao, H., Chen, M., Tellgren-Roth, C. & Pettersson, U. Fluctuating expression of microRNAs in adenovirus infected cells. *Virology* **478**, 99–111 (2015).

100. Aparicio, O. *et al.* Adenovirus VA RNA-derived miRNAs target cellular genes involved in cell growth, gene expression and DNA repair. *Nucleic Acids Research* **38**, 750–763 (2009).

101. Bellutti, F., Kauer, M., Kneidinger, D., Lion, T. & Klein, R. Identification of RISC-Associated Adenoviral MicroRNAs, a Subset of Their Direct Targets, and Global Changes in the Targetome upon Lytic Adenovirus 5 Infection. *Journal of Virology* **89**, 1608–1627 (2015).

102. Carrigan, D. R. Adenovirus infections in immunocompromised patients. *American Journal of Medicine* **102**, 71–74 (1997).

103. Pulido, R. PTEN inhibition in human disease therapy. *Molecules* vol. 23 (2018).

104. Koski, A. *et al.* Treatment of cancer patients with a serotype 5/3 chimeric oncolytic adenovirus expressing GMCSF. *Molecular Therapy* **18**, 1874–1884 (2010).

105. Chu, R. L., Post, D. E., Khuri, F. R. & van Meir, E. G. Use of replicating oncolytic adenoviruses in combination therapy for cancer. *Clinical Cancer Research* vol. 10 5299–5312 (2004).

106. van Rooij, E., Purcell, A. L. & Levin, A. A. Developing MicroRNA therapeutics. *Circulation Research* vol. 110 496–507 (2012).

9. Appendix

Table 1: Luciferase assays in A549

		Luciferase activity		Mean		Standard deviation			Mean normalised to mock	
Experiment Number	Replicate	mock	Ad5	mock	Ad5	mock	Ad5	T-test	mock	Ad5
1	1	0.035383	0.014849	0.028383	0.013273	0.00495	0.001968	0.015974	1	0.467617
	2	0.024816	0.014472							
	3	0.024951	0.010498							
2	1	0.076853	0.029346	0.074695	0.02994	0.004557	0.001282	0.000181	1	0.400827
	2	0.078875	0.031721							
	3	0.068357	0.028753							
3	1	0.011033	0.00997	0.013206	0.010615	0.001538	0.000457	0.084306	1	0.803742
	2	0.014234	0.010901							
	3	0.014352	0.010973							
4	1	0.00743	0.00625	0.006785	0.006222	0.000577	0.000237	0.27052	1	0.916978
	2	0.00603	0.006497							
	3	0.006897	0.005919							
5	1	0.003753	0.004236	0.004672	0.007117	0.000982	0.00341	0.385152	1	1.523133
	2	0.006033	0.011906							
	3	0.004231	0.005208							
6	1	0.001345	0.003094	0.001927	0.003222	0.000412	0.000519	0.050743	1	1.672256
	2	0.002177	0.002659							
	3	0.002257	0.003912							
7	1	0.007397	0.01094	0.007633	0.010817	0.00018	0.000155	4.6E-05	1	1.417087

	2	0.007667	0.010913							
	3	0.007835	0.010597							
8	1	0.008571	0.011305	0.008684	0.010945	0.000101	0.000283	0.000443	1	1.260347
	2	0.008816	0.010916							
	3	0.008665	0.010613							
9	1	0.002918	0.002842	0.003547	0.003649	0.000459	0.000611	0.859425	1	1.028744
	2	0.003997	0.004318							
	3	0.003727	0.003787							
10	1	0.003854	0.003873	0.005064	0.005497	0.00131	0.001686	0.788287	1	1.085589
	2	0.006884	0.007821							
	3	0.004454	0.004798							
11	1	0.003495	0.004181	0.002956	0.002932	0.000382	0.000885	0.973601	1	0.991881
	2	0.002719	0.002233							
	3	0.002654	0.002383							
12	1	0.005725	0.007781	0.00374	0.004559	0.001405	0.002327	0.691884	1	1.219031
	2	0.002831	0.003527							
	3	0.002664	0.002369							
13	1	0.005982	0.003306	0.003986	0.002672	0.001412	0.000451	0.278074	1	0.670334
	2	0.002968	0.002412							
	3	0.003008	0.002298							

Table 2: Luciferase assay results in H1299

Normalised to mock

		Luciferase activity		Mean		Standard deviation				
Experiment Number	Replicate	mock	Ad5	mock	Ad5	mock	Ad5	T-test	mock	Ad5
1	1	0.011149	0.021779	0.011925	0.019543	0.000632	0.001631	0.003527	1	1.638861
	2	0.011926	0.018913							
	3	0.012698	0.017936							
2	1	0.004363	0.007918	0.004415	0.008168	0.00037	0.000391	0.000592	1	1.850152
	2	0.003989	0.008719							
	3	0.004891	0.007866							
3	1	0.005662	0.001017	0.003334	0.001341	0.001652	0.00023	0.166419	1	0.402261
	2	0.001989	0.001485							
	3	0.002351	0.001522							
4	1	0.001873	0.001378	0.006027	0.006582	0.003155	0.004456	0.892715	1	1.092024
	2	0.009514	0.012262							
	3	0.006694	0.006105							
5	1	0.001878	0.001515	0.005659	0.006596	0.002987	0.004126	0.807592	1	1.165565
	2	0.009181	0.01162							
	3	0.005919	0.006653							
6	1	0.002888	0.002618	0.004325	0.003837	0.002223	0.002166	0.835104	1	0.88729
	2	0.002622	0.002014							
	3	0.007465	0.00688							
7	1	0.010439	0.003071	0.005619	0.003101	0.003418	0.000273	0.357636	1	0.551884
	2	0.003525	0.00345							
	3	0.002894	0.002783							
8	1	0.010439	0.002367	0.005619	0.003771	0.003418	0.002013	0.545875	1	0.671068

	2	0.003525	0.006617							
	3	0.002894	0.002329							
9	1	0.008767	0.004831	0.004795	0.003433	0.002813	0.000996	0.553654	1	0.715904
	2	0.002991	0.002885							
	3	0.002627	0.002583							
10	1	0.006976	0.008768	0.004221	0.004687	0.001962	0.002892	0.859463	1	1.110529
	2	0.002559	0.002892							
	3	0.003127	0.002402							
11	1	0.006052	0.010757	0.004116	0.005483	0.001373	0.003741	0.65302	1	1.332033
	2	0.003013	0.003217							
	3	0.003284	0.002476							
12	1	0.010421	0.009764	0.006928	0.005102	0.003306	0.003311	0.610381	1	0.73642
	2	0.007873	0.003152							
	3	0.00249	0.00239							
Mean n=36		0.005582	0.00597							